2023

Development of a QA plan for a 3.0T Cannon Galan MR-SIM

Nathaniel D. Teague
Virginia Commonwealth University

Development of a QA plan for a 3.0T Cannon Galan MR-SIM

A thesis submitted in partial fulfillment of the requirements for the degree of Master of Science at Virginia Commonwealth University

By

Nathaniel Teague

Bachelor of Science in Physics, Longwood University, December 2020

Advisor: Siyong Kim Ph.D.

Professor

Department of Radiation Oncology

Division of Medical Physics

Virginia Commonwealth University

March 2023

Acknowledgements

I would like to give my sincere thanks to:

Dr. Siyong Kim for serving as my mentor and thesis advisor

My committee for their time

Han Liu, Alireza Omidi and Mateb Alghamwa for their patience

My family and friends for their unending support and love

Table of contents

List of figures

List of tables

List of equations

Acronyms

ACR – American College of Radiology

ADC – Apparent diffusion coefficient

BW - Bandwidth

CF – Center frequency

CT – Computed tomography

CT-SIM – Computed tomography simulator

DQA – Daily quality assurance

DSV – Diameter spherical volume

DWI – Diffusion weighted imaging

FOV – Field of view

FSE – Fast spin echo

LCD – Low contrast detectability

MFH – Magnetic field homogeneity

MR – Magnetic resonance

MR-SIM – Magnetic resonance simulator

NAQ – Number of acquisitions

NEMA – National Electrical Manufacturers Association

NIST - National Institute of Standards and Technology

PE – Phase encoding

PIU – Percent intensity uniformity

PPM – Parts per million

PSG – Percent signal ghosting

FWHM – Full width at half maximum

RF – Radiofrequency

RG – Receiver gain

RO - Readout

ROI – Region of interest

SE – Spin Echo

SD – Standard deviation

SNR – Signal to noise ratio

TE – echo time

TG -Transmit gain

TGC – transmit gain calculation

TR – Repetition time

OAR – Organ at risk

QA – Quality Assurance

QC – Quality Control

QD – Quadrature

2D – Two dimensional

3D – Three dimensional

Abstract

Development of a QA plan for a 3.0T Cannon Galan MR-SIM

By

Nathaniel Teague

Bachelor of Science in Physics, Longwood University, December 2020

Advisor: Siyong Kim Ph.D.

Professor

Department of Radiation Oncology

Division of Medical Physics

Virginia Commonwealth University

March 2023

Purpose: To develop and incorporate a QA (quality assurance) program for a Canon Galan 3 tesla MR Simulator for applications in radiation therapy.

Methods and materials: The QA program was centered around tests performed with three separate levels of frequency. The daily QA procedure consisted of scanning a vendor provided daily QA cube phantom that measures basic performance parameters. Additionally, a series of basic safety check were performed. The monthly QA procedure consisted of several tests, including scanning the ACR MRI large accreditation phantom and manually performing its corresponding image quality tests. Scanning the MagPhan RT for its detailed geometric distortion analysis capabilities. Scanning the CaliberMR diffusion phantom for DWI QA. Performing a series of basic mechanical checks on the positional accuracy of the patient couch and external LAP laser positioning system. And outsourcing coil QA to a vendor service engineer who utilized a vendor analysis method. The annual QA tests consisted of an abbreviated version of the ACR image quality tests, along with an ACR table position accuracy test that was also performed on the ACR MRI large accreditation phantom. Further tests include a magnetic field homogeneity test, an evaluation of the complete clinical stock of RF coils, and a retroactive analysis of center frequency using results from the daily QA cube phantom. Additionally, the external laser offset from the isocenter was also verified using the AQUARIUS MRI phantom, monitor QC was performed based on the set of ACR advised SMPTE tests, and the ACR MRI accreditation visual checklist was filled out. Scanner manual and automatic transmit gain calculations were compared using the method outlined in AAPM report 100. All acquired images were examined for the presence of artifacts. Lastly, a qualified medical physicist performed a review of the facility's MR safety program.

Results: Daily QA has enabled long term tracking of basic performance parameters. Percent SNR experienced an initial drop during December 2021 before stabilizing for the remainder of project. Other basic performance parameters such RF level, helium level, and receiver gain maintained consistency with minor fluctuations occurring day to day. Center frequency remained at 123.196MHz for most of the project duration. Monthly QA and annual QA test protocols were successfully adopted and incorporated into the ongoing quality assurance effort.

Conclusions: This project has established a foundational quality assurance program that can be adjusted to meet the evolving needs of VCU's department of radiation oncology.

Keywords: Quality Assurance (QA), Magnetic Resonance Simulator (MR-SIM), Phantom

1. Introduction

1.1 Workflow

A crucial step in radiation treatment planning is the simulation process, in which patients are imaged in positions which are similar to the ones they will be in during treatment[1]. This process is generally performed using volumetric imaging modalities such as CT (Computed tomography) scanners and MR (magnetic resonance) scanners to obtain critical information such as tumor/target location, proximity to OARs (organs at risk), inhomogeneities within the patient and patient body contours[1]. Both volumetric imaging modalities offer unique advantages and disadvantages over the other. One of the most obvious advantages of MR scanners over CT scanners is that they offer a non-ionizing radiation form of imaging[2]. MR scanners image soft tissue with better contrast than CT scanners[2]. Additionally, MR scanners require longer scan times, and offer lower spatial resolution than CT scanners[2]. Lastly, the strong magnetic field of MR scanners introduces a variety of potential hazards and places limitations on which patients are eligible for a MR scan, due to potential complications from and interactions with the magnetic field. Ultimately, many modern radiation treatment facilities utilize a combination of both modalities to provide a high level of care to patients[3]. Often times MR images of soft tissue are registered with CT-SIM (CT Simulator) images in an effort to reap the benefits of both modalities[3].

1.2 MR Scanners in radiotherapy

As touched upon earlier, MR scanners fundamentally provide images with soft tissue contrast levels that are better than CT image soft tissue contrast levels[3]. Excellent soft tissue contrast is

one of the core imaging goals of the simulation process, since adequate tissue contrast is necessary for accurate delineation of tumors and OARs[3]. Given the improved soft tissue contrast of MR images, it is of no surprise that MR images allow for more accurate segmentation of OARs and targets[3]. This improved segmentation is associated with superior patient outcomes through reduced patient toxicities and dose escalation in target regions[3]. However, conventional MR scanner image co-registration with CT-SIM images can systematically introduce geometric uncertainties which could persist throughout the entire course of treatment, shift high dose regions away from targets or even potentially result in a miss of the target entirely[3]. This is due to conventional MR scanners not accurately recreating the CT-SIM position[3].

1.3 MR-SIMs

However, with the use of specially designed MR simulators or MR-SIMs, a radiation oncology department will be able to reap the benefits of improved tissue delineation of MR, without the geometric distortion that occurs during image co-registration with conventional MR scanners. MR-SIMs feature a wide bore that is generally at least 70cm in diameter to accommodate patient immobilization devices that a conventional "small" bore scanner would not be able to[3]. While the wide bore may negatively impact the image quality of certain imaging techniques such as DWI (diffusion weighted imaging), it is considered a crucial aspect of its design that makes it superior to conventional MR scanners for applications in radiation therapy[3]. Additionally, MR-SIMs include flat tabletop features that can be placed on the patient couch to more accurately recreate the position the patient will be in during the course of their CT simulation and treatment[3].

1.4 Differing QA needs

To ensure that the images produced by the MR-SIM meet and maintain a minimum (but high) level of quality, the performance of a MR-SIM scanner must be consistently and thoroughly evaluated through the incorporation of a quality assurance program. QA requirements between an MR scanner intended for diagnostic purposes may differ from MR scanners intended for applications in radiotherapy, with the latter often placing greater emphasis on evaluating geometric accuracy or spatial relationships[3]. Furthermore, advised QA test methods and or performance criteria will likely differ even when evaluating the same parameter. MFH (Magnetic field homogeneity), geometric distortion, low contrast object detectability and percent signal ghosting are some examples of this trend[3].

2. Purpose

The purpose of this project was to develop the foundations of an ongoing quality assurance program for VCU's new Canon Galon 3 tesla MR simulator, with the objective that the quality assurance program would meet the specific quality assurance requirements unique to MR-SIM applications in radiotherapy. To achieve this goal, the necessary quality assurance tests and test frequencies had to be determined. TG-284 served as the primary guiding resource for designing this quality assurance program. However, supplemental resources were also utilized during the course of this project and include materials such as the ACR MRI QC manual, AAPM TG 1 report 100 and white papers on MR-SIM QC. These white papers include the Siemen's "*Commissioning and Quality Assurance (QA) for MAGNETOM systems in radiation therapy*" paper and the Philips "*How do you commission and implement an MRI system for radiation*

therapy planning? Experience from St. Jude Children's Research Hospital, Memphis, Tennessee, USA" paper. Lastly, vendor instructional resources were also utilized to ensure a more accurate incorporation of their product.

3. Methodology

The QA program was centered around tests based on three distinct levels of frequency. Daily QA tests, monthly QA tests, and annual QA tests. To broadly summarize, the daily QA tests assured basic operational safety and gathered data on basic system performance. The monthly QA tests and annual QA tests were larger in scope and more deeply evaluated the specific capabilities of the scanner.

3.1 Daily QA

The daily QA procedure was performed every day where patients were scanned using the MR-SIM. The entirety of the daily QA procedure took approximately 10 minutes, which falls comfortably within TG-284's recommendation that daily QA take less than 30 minutes to conduct[3]. The entire list of tests performed can be seen in table 1 but can be broadly summarized as consisting of scanning a vendor provided daily QA cube phantom and performing a series of basic safety checks.

Test Name	Method	Advised under	Performance criteria	Source for Criteria
Central Frequency	Vendor cube phantom	TG-284 & Vendor	Baseline performance and track	TG-284
Transmit Gain	Vendor cube phantom	TG-284 & Vendor	±5% of Baseline	TG-284
SNR	Vendor cube phantom	TG-284 & Vendor	$50 < x < 160$	Vendor
Patient observation system	Test functionality	TG-284 & Vendor	Functional	TG-284
Patient intercom system	Test functionality	TG-284 & Vendor	Functional	TG-284
Patient call	Test functionality	TG-284 & Vendor	Functional	TG-284
Oxygen levels	Wall mounted monitor	Vendor	At least 20%	Vendor
Room temperature and humidity check	Monitor	Vendor	Scan room temperature16-24°C and Relative humidity 40-60%	Vendor

RF coil visual inspection	Visual inspection	Vendor	No signs of damages, stains, or imperfections	Vendor
Equipment visual inspection	Visual inspection	Vendor	No signs of damages, stains, or imperfections	Vendor
Bore free of foreign objects	Visual inspection	TG-284	No foreign objects in bore	TG-284
Legible Safety Signage	Visual Inspection	TG-284	Functional	TG-284
Metal Detector Tests	Test functionality	St. Jude White paper	Functional	St. Jude White paper
Emergency patient couch release	Test functionality	TG-284	Functional	TG-284

Table 1. This table lists all of the tests performed as part of the daily QA procedure, including which method of assessment is used, who advised that the test be performed, and what the passing performance criteria of that test are. A test in this table that states that it was advised by the vendor, indicates that this test is prompted to be performed after scanning the daily QA cube phantom.

3.1.A Daily QA cube phantom

A crucial component of the daily QA was the application of a vendor provided cube phantom. The phantom (shown in Figure 1) could be scanned succinctly and provide an easy-to-understand summary report of scanner performance. The phantom was scanned without the use of any receiver coils and was placed where a patient's head would naturally rest if they were to be scanned headfirst. Technicians performing the QA would position the phantom such that the onboard laser positioning system aligned with the phantom's crosshair markings (shown in Figure 2) before sending the phantom to the magnetic isocenter and acquiring necessary images. Operating the scanner to perform daily QA was streamlined. The control terminal had a "quick start" button (dubbed DQA) which allowed for technicians to simply select to perform the daily QA scan, select the correct orientation of the phantom and then begin scanning. This streamlining allowed for technicians to bypass the typically necessary step of filling out the patient information prompts, saving the technicians some time and making the DQA more efficient to perform. The Daily QA cube phantom was always scanned in the axial position.

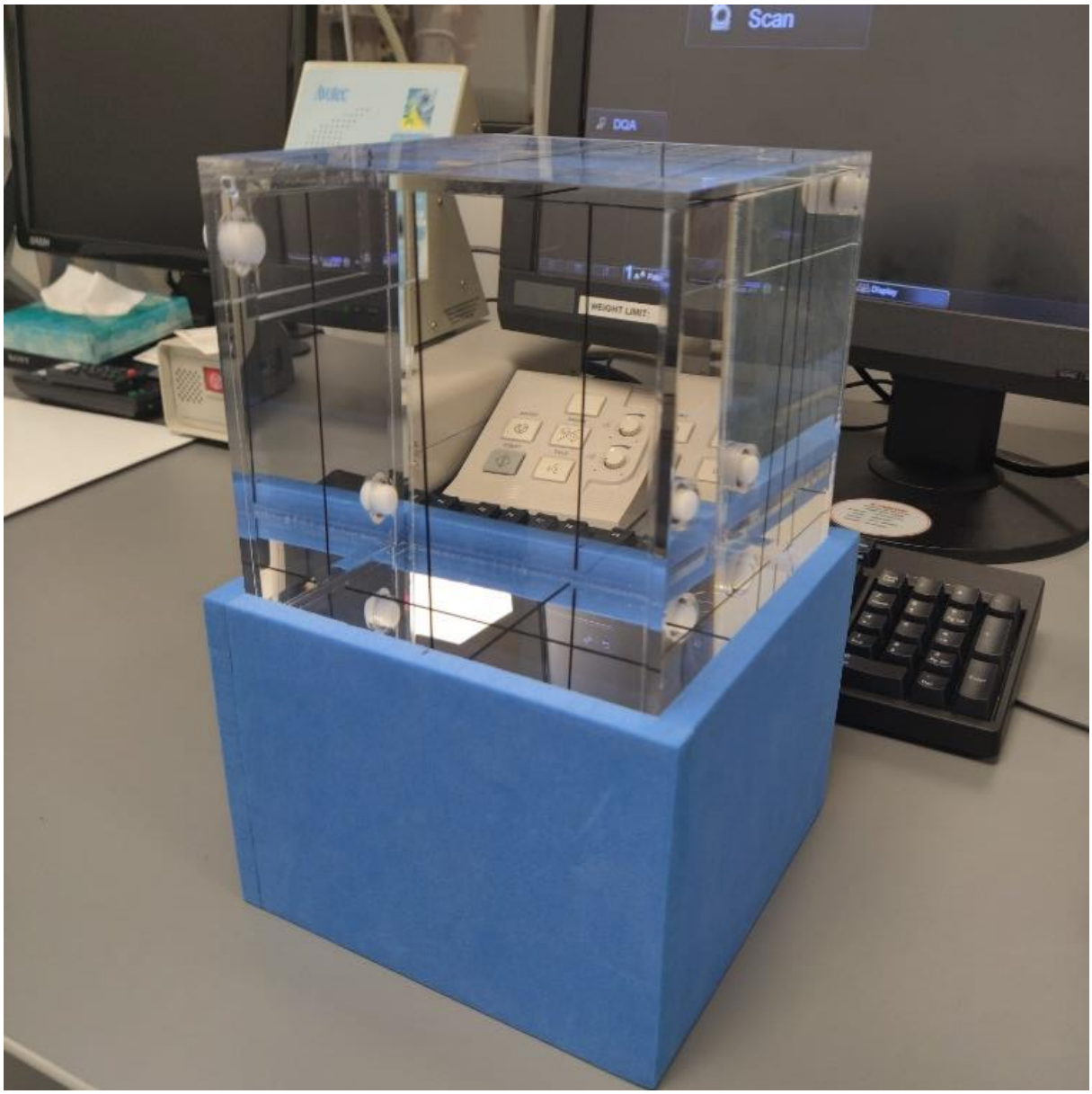

Figure 1: Photo of the daily QA cube phantom.

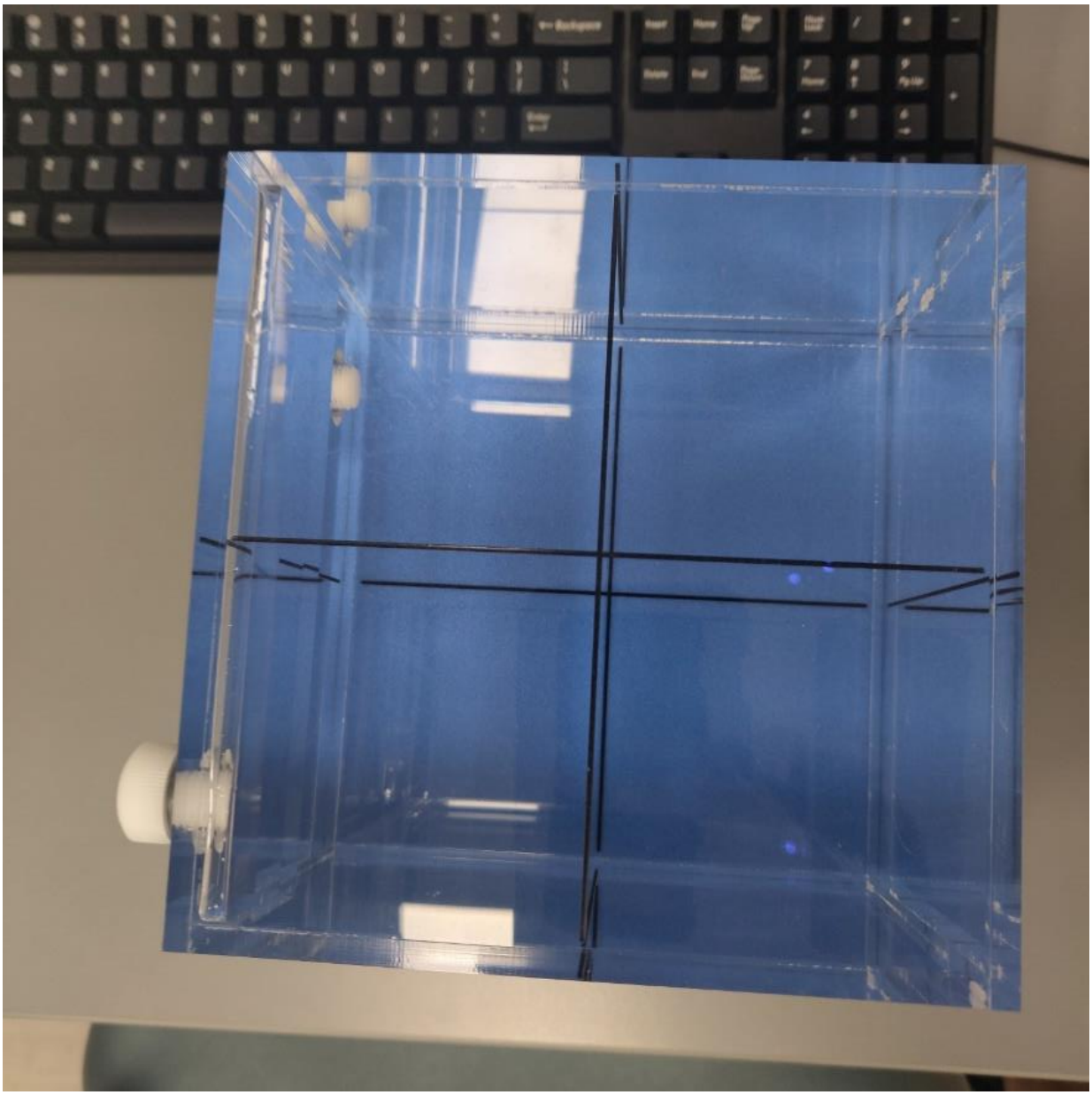

Figure 2: Overhead view of the crosshair markings along the top of the daily QA cube phantom.

Figure 3: Photo of the daily QA phantom properly oriented on the MR-SIM patient couch.

The scan time for the daily QA cube phantom was very small and took approximately one to two minutes to complete. Upon completion of the scan the phantom provided a four-tab summary report. The first tab (shown in Figure 4) was a summary tab that indicated if the daily QA passed

or failed. This tab consisted of an SNR measurement, which was compared to the acceptable range of passing SNR values which ranged from greater than 50 to less than 160.

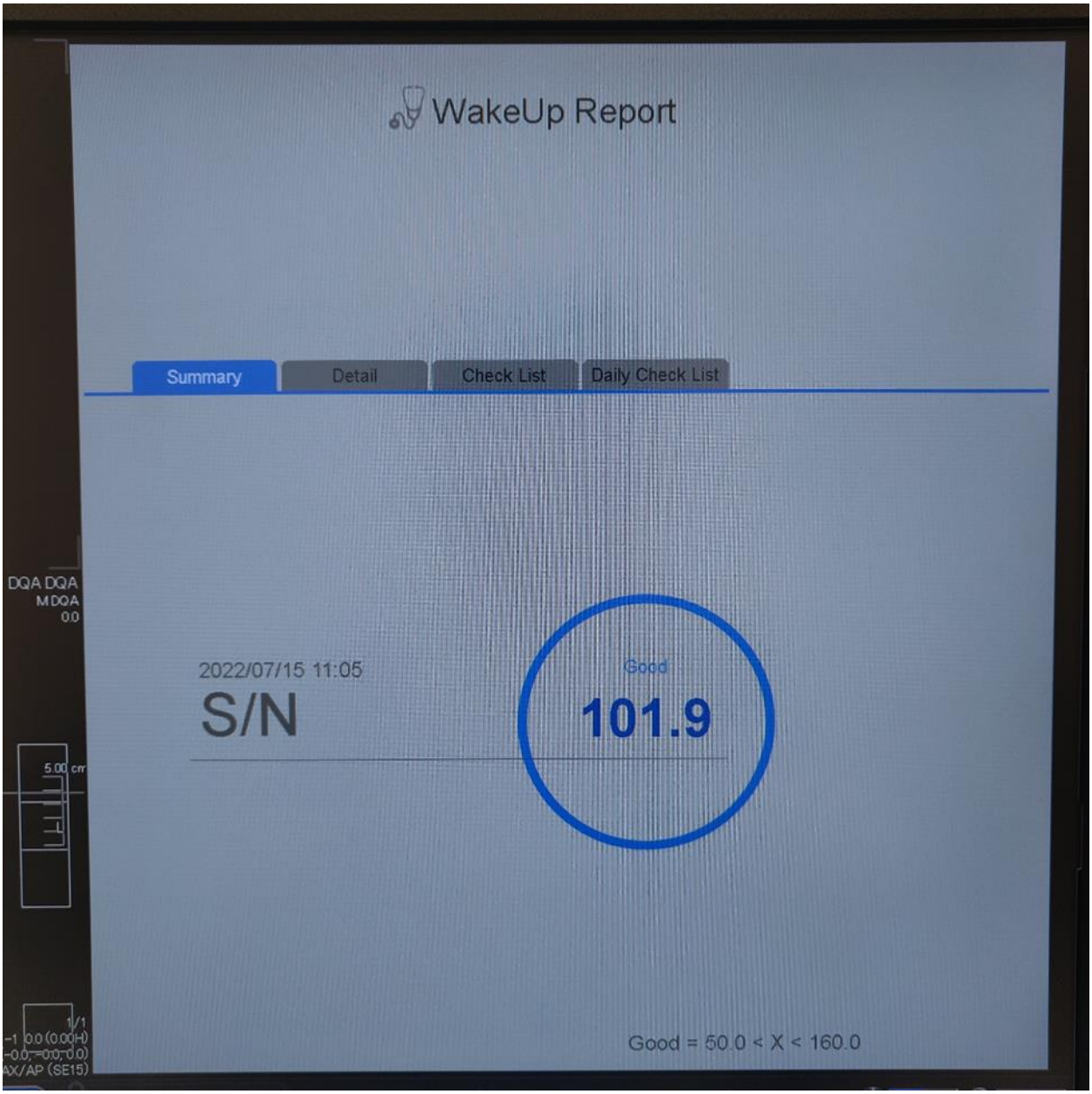

Figure 4: Photo the first tab of the four-tab daily QA report. Dubbed the “Summary” tab.

The second tab of the four-tab report (shown in figure 5) was a “detail” tab which provided a quantitative assessment of several basic system performance parameters. These parameters included percent SNR, signal, signal standard deviation, noise, noise standard deviation, DC noise, uniformity, RF, RF scale, RF power, receiver gain, center frequency, helium level and TGC. The tech who performed the daily QA would subsequently transcribe the most important of these parameters into a daily QA worksheet or logbook (shown in figure 6). The logbook was periodically transcribed into a digital record where long-term system performance tracking was performed.

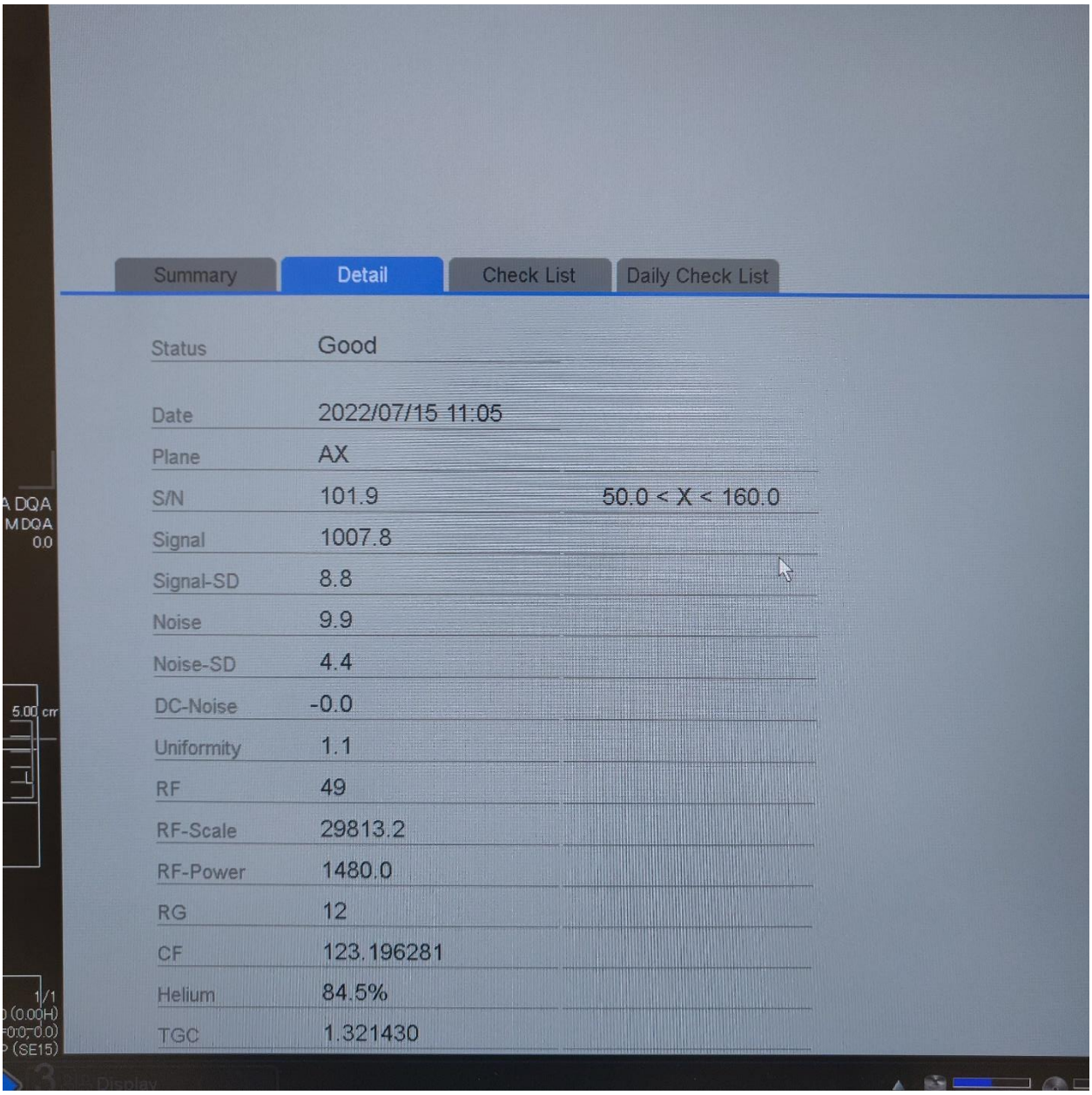

Figure 5: Photo of the second tab of the four-tab daily QA report. Dubbed the “detail” tab.

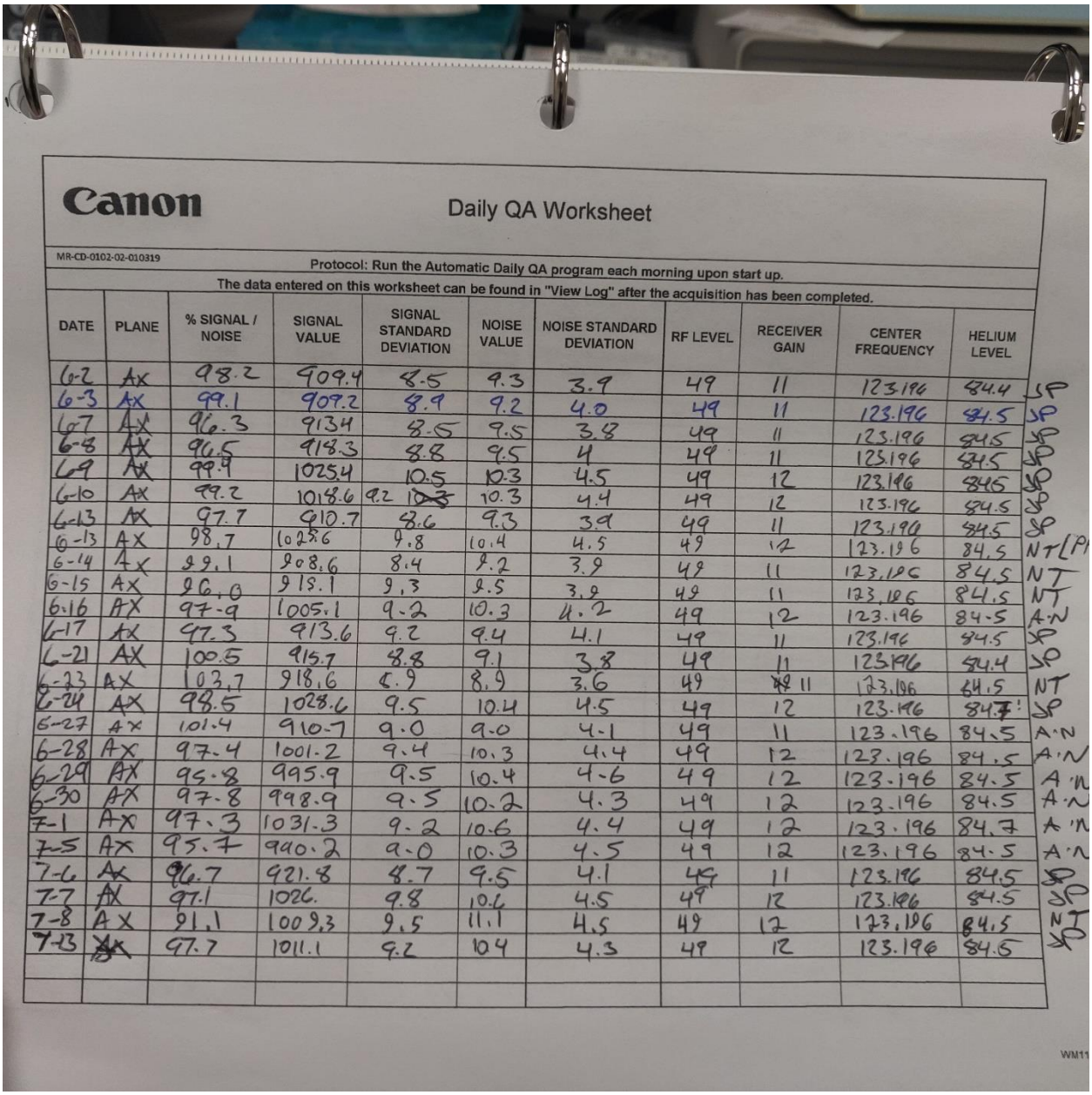

Canon

Daily QA Worksheet

MR-CD-0102-02-010319

Protocol: Run the Automatic Daily QA program each morning upon start up.

The data entered on this worksheet can be found in "View Log" after the acquisition has been completed.

DATE	PLANE	% SIGNAL / NOISE	SIGNAL VALUE	SIGNAL STANDARD DEVIATION	NOISE VALUE	NOISE STANDARD DEVIATION	RF LEVEL	RECEIVER GAIN	CENTER FREQUENCY	HELIUM LEVEL	
6-2	AX	98.2	909.4	8.5	9.3	3.9	49	11	123.196	84.4	JP
6-3	AX	99.1	907.2	8.9	9.2	4.0	49	11	123.196	84.5	JP
6-7	AX	96.3	913.4	8.5	9.5	3.8	49	11	123.196	84.5	JP
6-8	AX	96.5	918.3	8.8	9.5	4	49	11	123.196	84.5	JP
6-9	AX	99.9	1025.4	10.5	10.3	4.5	49	12	123.196	84.5	JP
6-10	AX	99.2	1018.6	9.2 10.3	10.3	4.4	49	12	123.196	84.5	JP
6-13	AX	97.7	910.7	8.6	9.3	3.9	49	11	123.196	84.5	JP
6-13	AX	98.7	1025.6	9.8	10.4	4.5	49	12	123.196	84.5	NT[P
6-14	AX	99.1	908.6	8.4	9.2	3.9	49	11	123.196	84.5	NT
6-15	AX	96.0	918.1	9.3	9.5	3.9	49	11	123.196	84.5	NT
6-16	AX	97.9	1005.1	9.2	10.3	4.2	49	12	123.196	84.5	A·N
6-17	AX	97.3	913.6	9.2	9.4	4.1	49	11	123.196	84.5	JP
6-21	AX	100.5	915.7	8.8	9.1	3.8	49	11	123.196	84.4	JP
6-23	AX	103.7	918.6	8.9	8.9	3.6	49	11	123.196	84.5	NT
6-24	AX	98.5	1028.6	9.5	10.4	4.5	49	12	123.196	84.7	JP
6-27	AX	101.4	910.7	9.0	9.0	4.1	49	11	123.196	84.5	A·N
6-28	AX	97.4	1001.2	9.4	10.3	4.4	49	12	123.196	84.5	A·N
6-29	AX	95.8	995.9	9.5	10.4	4.6	49	12	123.196	84.5	A·N
6-30	AX	97.8	998.9	9.5	10.2	4.3	49	12	123.196	84.5	A·N
7-1	AX	97.3	1031.3	9.2	10.6	4.4	49	12	123.196	84.7	A·N
7-5	AX	95.7	990.2	9.0	10.3	4.5	49	12	123.196	84.5	A·N
7-6	AX	96.7	921.8	8.7	9.5	4.1	49	11	123.196	84.5	JP
7-7	AX	97.1	1026.	9.8	10.6	4.5	49	12	123.196	84.5	JP
7-8	AX	91.1	1009.3	9.5	11.1	4.5	49	12	123.196	84.5	NT
7-13	AX	97.7	1011.1	9.2	10.4	4.3	49	12	123.196	84.5	JP

Figure 6: Photo of the daily QA worksheet that was filled out by a technologist as a part of the DQA procedure. The information filled in can all be found in the detail tab of the four-tab summary report.

The third tab of the four-tab report was the “check list” tab (shown in figure 7). This tab prompted the operator to perform a series of basic system checks. The majority of these tests

were simple visual inspection tests that are more concerned with the safe operation of the scanner instead of a quantitative assessment of system performance. The performing technician would record their observations by selecting OK, NG (for no good) or N/A (for not available). Once finished with the check list, the operator would select their initials from the reporter drop down box and submit the DQA results.

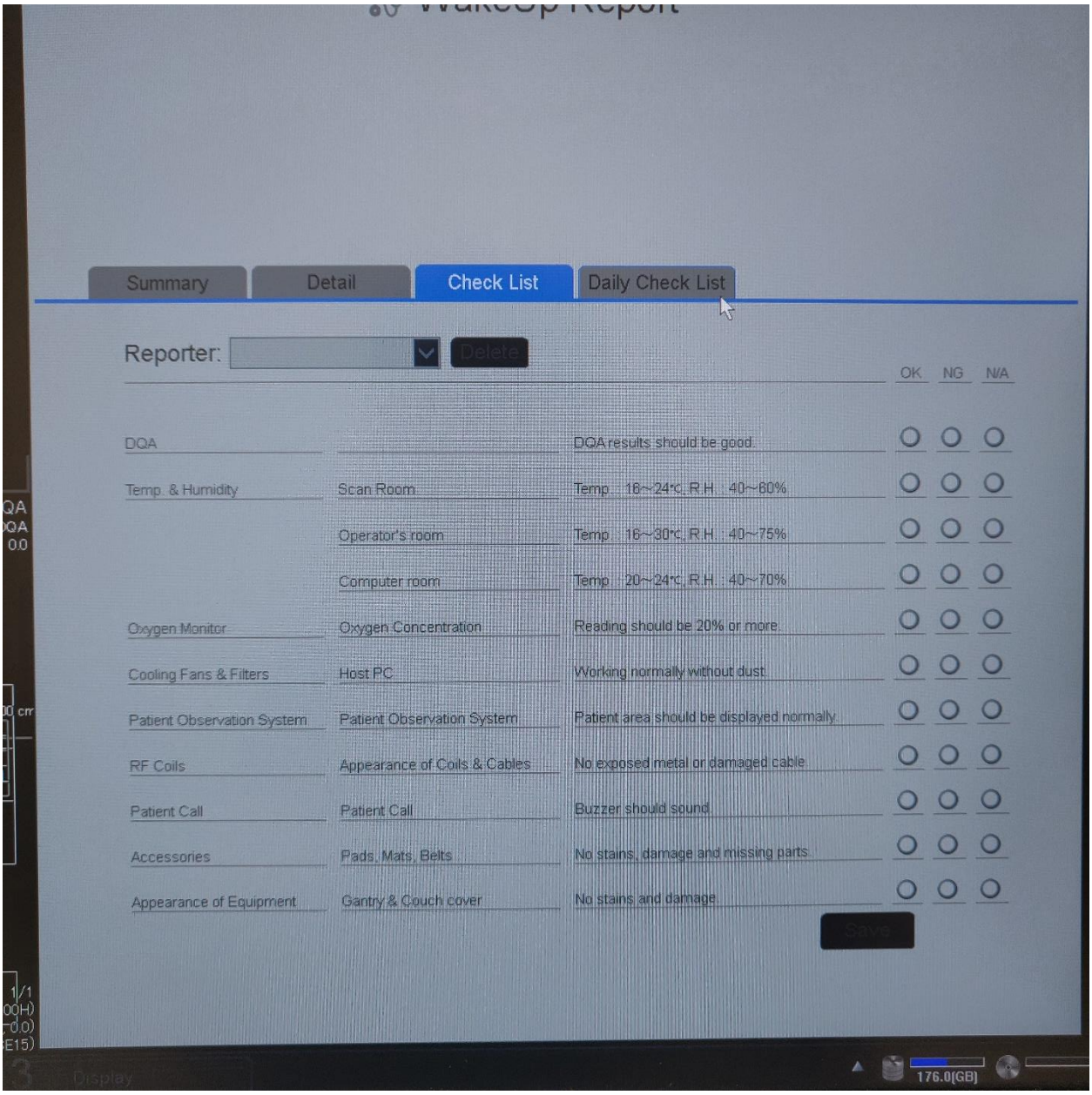

Figure 7: Photo of the third tab of the four-tab daily QA report. Dubbed the “check list” tab.

Below is a quick summary of what each of these items on the checklist were:

DQA Results – On the first tab of the report, the summary tab, the report would indicate if the DQA results passed or appeared satisfactory. As long as the summary tab indicated passing results, and there were no red flags in the detail tab, the operator could select OK.

Temperature and humidity – The operator would utilize a handheld temperature and humidity monitor placed on the window still of the scanner room to determine the temperature and humidity of the scanner room itself.

Oxygen Monitor – behind the scanner control console and nearby the door into the scanner room was a green wall mounted monitor that displayed the oxygen content of the scanner room in terms of a percentage (see figure 8). The operator would use this monitor to ensure that oxygen levels were at least 20%.

Cooling fans / filters – The operator would visually check that the host PC's fans and filters were free of any dust and that the fans were working properly.

Patient observation system – The operator would ensure that the live camera feed of the bore of the MR-Sim is functional by simply attempting to see the daily QA phantom in the bore.

RF Coils – The operator would perform a simple visual inspection of the receiver coils to check for any obvious signs of damage.

Patient Call squeeze ball – With the aid of an additional staff member who had received proper training, safety education and who had undergone the prerequisite MR safety screening, the operator would pinch the patient call squeeze ball to ensure that it is functioning properly. This was also often a good time to test the patient intercom system as well.

Accessories – The operator would perform a simple visual inspection of any pads, restraining straps, or attachable coverings and ensure that they were clean, undamaged, and present.

Equipment appearance – The operator would perform a simple visual inspection of the gantry, bore and patient couch to check for any signs of damage, or the presence of any foreign metal objects.

Figure 8: Photo of the wall mounted oxygen monitor.

Figure 9: Photo of the patient intercom system.

While a fourth tab, the “daily check list” tab (shown in figure 10) was available, this tab was not utilized as part of the QA plan. This tab was not utilized because it did not instruct the operator to perform any QA tests.

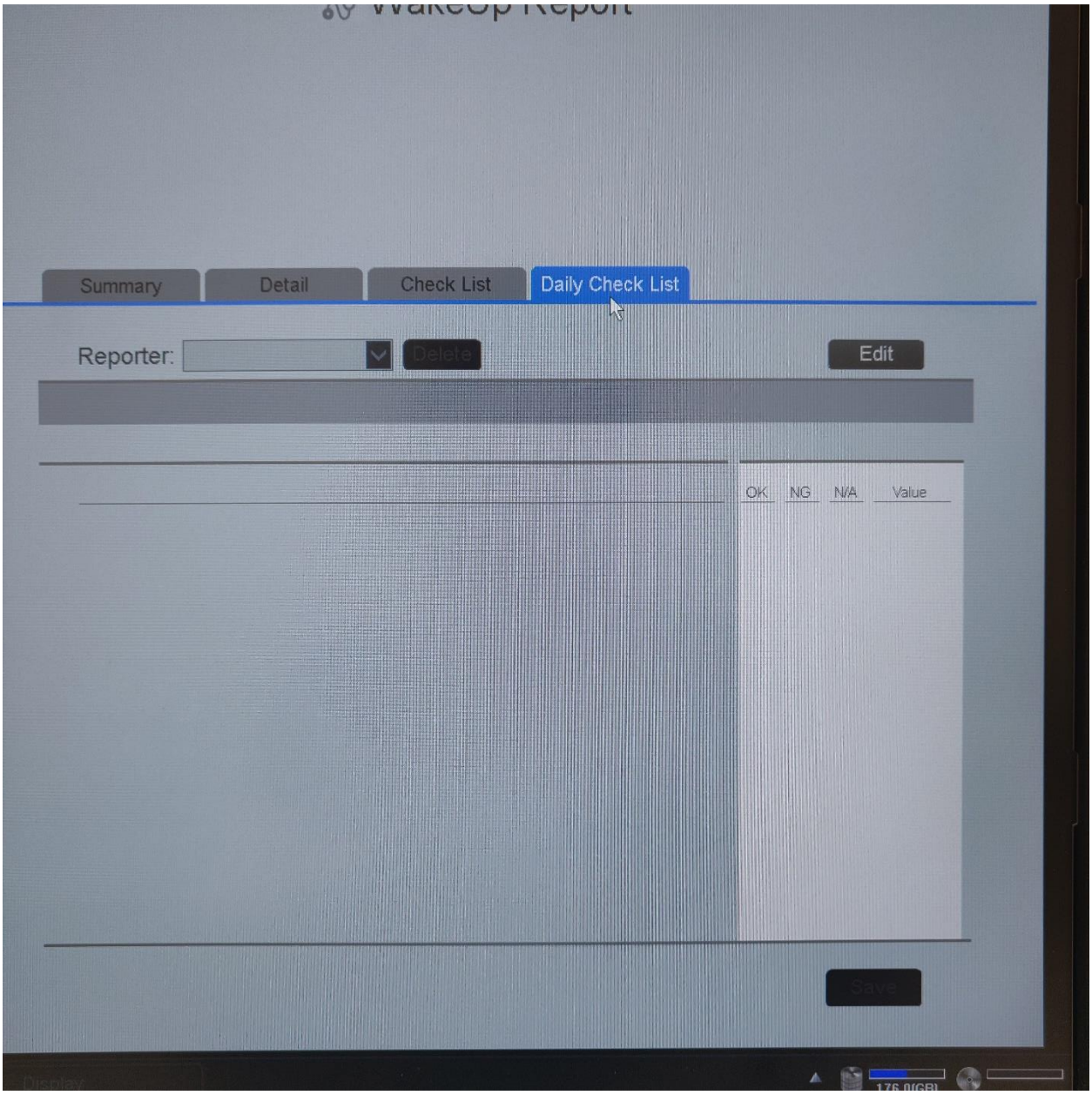

Figure 10: Photo of the fourth tab of the four-tab daily QA report. Dubbed the “daily check list” tab. This tab was not utilized as part of the DQA procedure.

3.1.B Safety Checks

There were two more basic safety checks advised by TG-284 that the daily QA cube phantom did not prompt the technologist to perform[3]. These included visually assessing and confirming the presence of safety signs that are legible and clearly communicate the potential dangers associated with MR scanners[3]. And checking that the patient couch emergency release system was fully functional by simply testing that the couch would release, was able to move and was then able to reattach[3]. Lastly, the final test performed as a part of the Daily QA procedure was testing the functionality of both the handheld metal detectors and the wall mounted ferromagnetic metal detectors by testing their functionality on a known ferromagnetic object. The metal detector test, while not advised under TG-284, had instead been adopted from the precedent set by the daily QA performed in Philip's white paper: "How do you commission and implement an MRI system for radiation therapy planning? Experience from St. Jude Children's Research Hospital, Memphis, Tennessee, USA" [4].

3.2 Monthly QA tests

The monthly QA procedure was performed on a monthly basis, with flexibility regarding when in the month the procedure was performed based on patient scheduling and the availability of staff to perform the procedure. The procedure did not have to be performed in one continuous session and could be split into as many sessions as were needed to complete the QA procedure, as long as the entirety of the procedure was completed within the month of examination. The full set of tests performed for the monthly QA procedure can be seen in table 2, but broadly consisted of five main components: the ACR image quality tests, a MagPhan RT phantom scan, a series of

basic mechanical checks, a CaliberMR diffusion phantom scan and RF coil analysis. RF coil QA is discussed in further detail in section 3.2.E, but please note that coil QA was actually performed roughly every six weeks to two months instead of monthly.

Test Name	Method	Advised under	Performance criteria	Source for Criteria
Geometric accuracy	ACR Phantom	ACR	±2mm of phantom dimensions	ACR
High contrast spatial resolution	ACR Phantom	ACR	At least 1mm resolution	ACR
Low contrast Detectability	ACR Phantom	ACR	40 spokes for 3.0T	TG-284
Slice position accuracy	ACR Phantom	ACR	within 5 mm	ACR
Slice thickness accuracy	ACR Phantom	ACR	5mm ± 0.7mm	ACR
Image intensity uniformity	ACR Phantom	ACR	PUI >82.0%	TG-284
Percent signal ghosting	ACR Phantom	ACR	Ghosting ratio ≤ 0.025	TG-284

Geometric distortion	MagPhan	TG-284	verify ≤ 2mm distortion over 25cm FOV	TG-284
External laser offset from isocenter	MagPhan	TG-284	Verify laser alignment within 2mm	TG-284
RF Coil checks	Vendor method	TG-284	Vendor performance criteria	Vendor
Longitudinal patient couch position accuracy	Ruler	TG-284	tolerance of ±1mm	TG-284
External LAPS laser position accuracy	Ruler	TG-284	tolerance of ±2mm, but within ±1mm preferred	TG-284
DWI Accuracy	CaliberMR Diffusion Phantom	Not specified	TBD	TBD

Table 2. This table lists all the tests performed as part of the monthly QA procedure, including which method of assessment was used, who advised that the test be performed, what the passing performance criteria of that test was, and where that performance criteria came from.

3.2.A – ACR Image Quality Tests

3.2.A.I - ACR Large MRI accreditation phantom Background

The ACR MRI Accreditation phantom comes in two primary versions[5]. A large and a small version[5]. However, the small variation for this phantom is predominantly used for magnets used to image extremities whereas the large phantom is used for magnets used to image bodies[5]. Due to this distinction we chose to utilize the large ACR MRI accreditation phantom. The phantom was used to examine seven separate image quality tests: geometric accuracy, high contrast spatial resolution, slice thickness accuracy, slice position accuracy, image intensity uniformity, percent signal ghosting and low contrast object detectability[5]. The large ACR phantom is a cylinder that is 148mm long and 190mm across[5]. The phantom is intended to be scanned in the institution's most utilized head coil, using the distinct "nose" and "chin" markings on the phantom to orient the phantom as a human head would be positioned[6]. The phantom is also filled with a10 mM $NiCl_2$ (nickel chloride) and 75 mM NaCl (sodium chloride) solution[5].

Figure 11. Photo of the large ACR MRI accreditation phantom.

Figure 12. Photo of the large ACR MRI accreditation in the head receiver coil.

The phantom was scanned monthly following the recommended ACR instructions. The ACR advises obtaining 5 total sets of images: a sagittal locater, and two "ACR series" (an ACR axial T1 and T2) and two "site series" (a site axial T1 and T2)[6]. The scan parameters for the sagittal

locater and the ACR axial image series are dictated by the ACR[6]. In contrast to this, the parameters for the site series should be the same as the parameters utilized in that location's most frequently used axial T1 and axial T2 brain protocols[6]. With the added exception that the site series should utilize the same number of slices, slice thickness and slice gap parameters utilized in the ACR axial image series[6]. An important distinction to raise is that we have opted to not utilize site series as a part of ACR image quality testing, and instead rely entirely upon the ACR prescribed series.

	Sagittal locater	ACR T1	ACR T2
Sequence	SE2D	SE2D	SE2D
Plane	Sagittal	Axial	Axial
Subject orientation	Head-Foot	Right-Left	Right-Left
PE FOV in cm	25	25	25
PE Matrix size	256	256	256
PE resolution in mm	0.97	0.97	0.97
PE No Wrap	1	1	1
RO FOV in cm	25	25	25
RO matrix size	256	256	256
RO resolution in mm	0.97	0.97	0.97

RO No Wrap	2	2	2
Number of slices	1	11	11
Slice thickness in mm	20	5	5
Slice gap in mm	0	5	5
NAQ	1	1	1
TR	200	500	2000
TE	20	20	80
speeder	off	off	off

Table 3: The pulse sequence parameters for the ACR series as they appeared in the 3T MR-SIM control terminal.

A quick aside, the term speeder refers to an acceleration technique supported by canon that can be utilized to reduce overall scan time.

3.2.A.II Geometric Accuracy

The ACR advises that when a medical physicist examines geometric distortion using the ACR accreditation phantoms they should evaluate image distortion and image displacement in terms of percent geometric distortion[5]. Percent geometric distortion can be calculated using equation 1[5]:

$$\text{Eqn. 1 [\%GD]} = \left(\frac{(True\ dimension)-(observed\ dimension)}{True\ dimension}\right)\text{x}100$$

For modern MR scanners it is reasonable to expect to achieve a percent geometric distortion of within 1%, which for the large MRI accreditation phantom would correspond to 2mm across the phantom and 1.5mm along the phantom[5]. In practice, this means that the ACR advises that the test should be considered passing if the observed dimensions of the large ACR phantom are within 2mm of the true dimensions when examined across a 25cm FOV[5]. The measured or observed dimensions are located along the phantom length in the superior-inferior direction for the sagittal locater[6]. In the anterior to posterior and left to right directions in slice 1 of the ACR Axial T1 image series[6]. And lastly in the anterior to posterior, left to right, and along both diagonal directions in slice 5 of the ACR Axial T1 image series[6]. For a grand total of 7 measurements. Please note that geometric distortion is not evaluated using the ACR T2 image series. While TG-284 does advise that geometric distortion be evaluated on a monthly basis, the large ACR accreditation phantom's geometric distortion test does not meet the requirements outlined by TG-284 for this test. TG-284 specifically recommends that geometric distortion be evaluated utilizing a phantom with a width or a diameter greater than 30cm [3]. The large ACR MRI accreditation phantom's largest dimension is its diameter which comes out to 19cm across[5]. Thus, the ACR phantom does not satisfy TG-284's recommendations. Instead we have implemented the MagPhan RT phantom for geometric distortion testing. This phantom is discussed in more detail in section 3.2.B.II.

3.2.A.III High contrast spatial resolution

This image quality test examines a scanner's ability to evaluate and resolve small details by having the operator examine a series of holes in a grid like pattern[6]. These grids or hole arrays come in pairs dubbed as the upper left and lower right hole arrays with one shared hole between

the two (for the upper left array this hole is the bottom most right hole and for the lower right array this hole is the upper most left hole)[6]. The upper left hole array is used to evaluate resolution along the array's rows (in the right to left direction) while the lower right hole array is used to evaluate the resolution across the array's columns (in the anterior to posterior direction)[6]. The large ACR MRI accreditation phantom has three separate hole array pairs with progressively smaller holes and hole distancing: 1.1mm, 1.0mm and 0.9mm [6]. To be considered passing, the scanner had to be able to resolve hole arrays as small as 1.0mm [5]. This test was evaluated on both the ACR T1 and ACR T2 image series and had to demonstrate adequate performance for both to be considered passing[6].

3.2.A.IV Slice thickness accuracy

This test examined the accuracy with which the scanner was able to achieve a prescribed slice thickness[5]. This test was performed by measuring the length of two signal ramps present in slice 1 of the axial image series[5]. Once measurements had been made of both the "top" and "bottom" signal ramps, their observed lengths were plugged into equation 2 to calculate an observed slice thickness[5]. In the context of equation 2 the "top" and "bottom" refer to length measurements of the top signal ramp and bottom signal ramp respectively[5]:

$$\text{Eqn. 2: Slice thickness} = 0.2\ x\ \left(\frac{top*bottom}{top+bottom}\right)$$

The calculated or observed slice thickness was then compared to the prescribed slice thickness, which in the case of the ACR axial image series was 5mm [5]. Per ACR recommendations this test was only considered passing if the observed slice thickness was ±0.7mm of 5mm [5]. This test was performed for both the ACR T1 and ACR T2 image series[5].

3.2.A.V Slice position accuracy

The slice position accuracy test compared the measured slice position to the prescribed slice position[5]. This test was performed on both the ACR T1 and ACR T2 series[5]. To perform this test the operator examined the crossed wedges present in slices 1 and 11 [5]. These crossed wedges appeared as vertical bars[5]. If the scanner was positioning slices to exactly where they had been prescribed, then the two crossed wedges should have appeared to have equal length[5]. If the left wedge was longer than the right, then the slice was placed inferior relative to the vertex of the crossed wedges[5]. And if the right wedge was longer than the left, then the slice was placed superior relative to the vertex of the crossed wedges[5]. Using control terminal image analysis software, the operator performing the test measured the difference in length between the two cross ramps in both slices 1 and 11 [5]. Differences wherein the left bar was longer should have been denoted as negative, to indicate which bar was longer[5]. In order to be considered passing, the scanner must have demonstrated a crossed wedge difference of within ±5mm in all examined slices[5].

3.2.A.VI Image intensity uniformity

This test evaluated the image intensity variation produced by the scanner when imaging a uniform, water only portion of the ACR phantom[6]. This test was performed on slice 7 of both the ACR T1 and ACR T2 image series[6]. The operator performing this test placed a 200cm^2 ROI (region of interest) on slice 7 to serve as a boundary region in which the rest of the test would be

performed in[6]. In practice the boundary ROI may vary by ±5 cm^2 of 200 cm^2 [6]. The operator would adjust the window and level of the image to determine the regions with the most and least signal[6]. A 1 cm^2 ROI was placed in both the regions with the highest signal value and lowest signal value and their observed signal values were recorded[6]. These values were then utilized along with equation 3 to calculate the PIU (percent intensity uniformity)[6]. In the context of equation 3, "high" and "low" refer to the signal value measurements of the ROI with the highest signal and lowest signal respectively[6]:

$$\text{Eqn. 3: PIU} = 100\ x\ (1 - (\frac{High-low}{high+low}))$$

To be considered passing the calculated PIU must have been greater than or equal to 82.0% for a 3T system as per the recommendations of the ACR and TG-284[3,6].

3.2.A.VII Percent signal ghosting

The percent signal ghosting test quantitatively evaluated the amount of ghosting artifact produced by the scanner during ACR image quality testing[6]. This test was performed only on the ACR T1 image series[6]. To perform this test, the operator displayed slice 7 of ACR T1, and placed five ROIs: a 195-205cm^2 large circular ROI that was placed in the center of the phantom, and four separate, approximately 10cm^2 elliptical ROIs placed above, below, to the right and to the left of the large ROI[6]. The four elliptical ROIs were placed solidly within the background noise portion of slice 7 [6]. A mean pixel value was obtained for each of the five ROIs, and the ghosting ratio was calculated using equation 4 [6]:

$$\text{Eqn. 4: ghosting ratio} = \left| \frac{(top+bottom)-(left+right)}{2(Large)} \right|$$

The ghosting ratio is expressed as a fraction of the true signal and can be converted into percent signal ghosting by multiplying the calculated ratio by 100% [6]. The percent signal ghosting is also expressed as percent of the true signal[6]. The ACR advises that this test only be considered passing if the scanner demonstrates a ghosting ratio no greater than 0.03 or in other words a percent signal ghosting value that is no greater than 3% [6]. However, we opted to apply TG-284's more stringent performance criteria recommendation of a ghosting ratio no greater than 0.025 / a percent signal ghosting value that is no greater than 2.5% [3].

3.2.A.VIII Low contrast object detectability

The low contrast object detectability test assessed the ability of a scanner to resolve objects that have low contrast[6]. This test was performed by evaluating slices 8 through 11 of the ACR T1 and ACR T2 series[6]. Each of the examined slices had 10 "spokes" radiating from the center of the slice, with each spoke consisting of 3 circular features in a line[6]. Each circle in a spoke had an identical diameter to all other circles in that given spoke[6]. Each successive spoke in a slice has progressively smaller circles[6]. At their largest, the circular features had a diameter of 7mm and at their smallest they had a diameter of 1.5mm [6]. The spokes in each slice had a set contrast value, which, in order from slice 8 to slice 11, are 1.4%, 2.5%, 3.6% and 5.1% respectively [6]. In practice, this means that the various spokes had different levels of visibility depending on their combination of feature diameter and contrast value. The operator performing this test examined the four relevant slices and tallied the number of spokes visible between them, while only counting a spoke as visible if all three circular features were discernable[6]. The operator could freely adjust the window and level of the images to increase the visibility of the spokes[6]. While a total of 40 spokes are visible in the large ACR accreditation phantom, the ACR specifically

advises that a scanner be considered passing if the operator is able to discern 37 or more spokes during this test when performed on a 3 tesla system[5]. However, TG-284 advises a more stringent performance criterion for this test wherein all 40 spokes should be visible for a 3T scanner[3]. Since TG-284 specifically advises QA protocol for MR-SIMs in radiation therapy settings, its recommendations are assumed to supersede the recommendations of the more general ACR MRI QC manual. As such we have opted to utilize the 40 spoke performance criteria for the ACR LCD test.

3.2.B - MagPhan RT

3.2.B.I MagPhan Background

The MagPhan RT is a two-piece phantom, that when assembled and scanned with adequate coverage (I.E., complete coverage) can be used to assess the performance of a wide variety of pulse sequences (see figures 13 and 14)[7]. While this phantom was predominantly incorporated into this QA program for its geometric distortion analysis capabilities, the phantom is capable of evaluating resolution, SNR, signal uniformity, laser alignment and slice thickness[7]. Since the phantom is intended for applications across a variety of scan protocols, it does not have a rerecommended set of scan protocols to utilize for QA purposes. Instead, ongoing QA efforts with the MagPhan relied upon using custom QA designated pulse sequences, determining a base level of performance, and long-term tracking of system performance relative to baseline measurements for parameters without performance criteria recommendations. Our MagPhan protocol consisted of scanning the phantom using a body coil and obtaining three sets of images. These image sets included two axial 3D T1 series and an axial T2 series. The axial 3D T1 series

were identical with the exception that one utilized a speeder whereas the other did not. All three scan protocols were designed in collaboration with scanner vendor personnel. The scan parameters for all three image sets can be seen in table 4. Upon scan completion, the obtained images were exported, and subsequently uploaded to phantom vendor proprietary analysis software, which generated a report for each set of obtained image series.

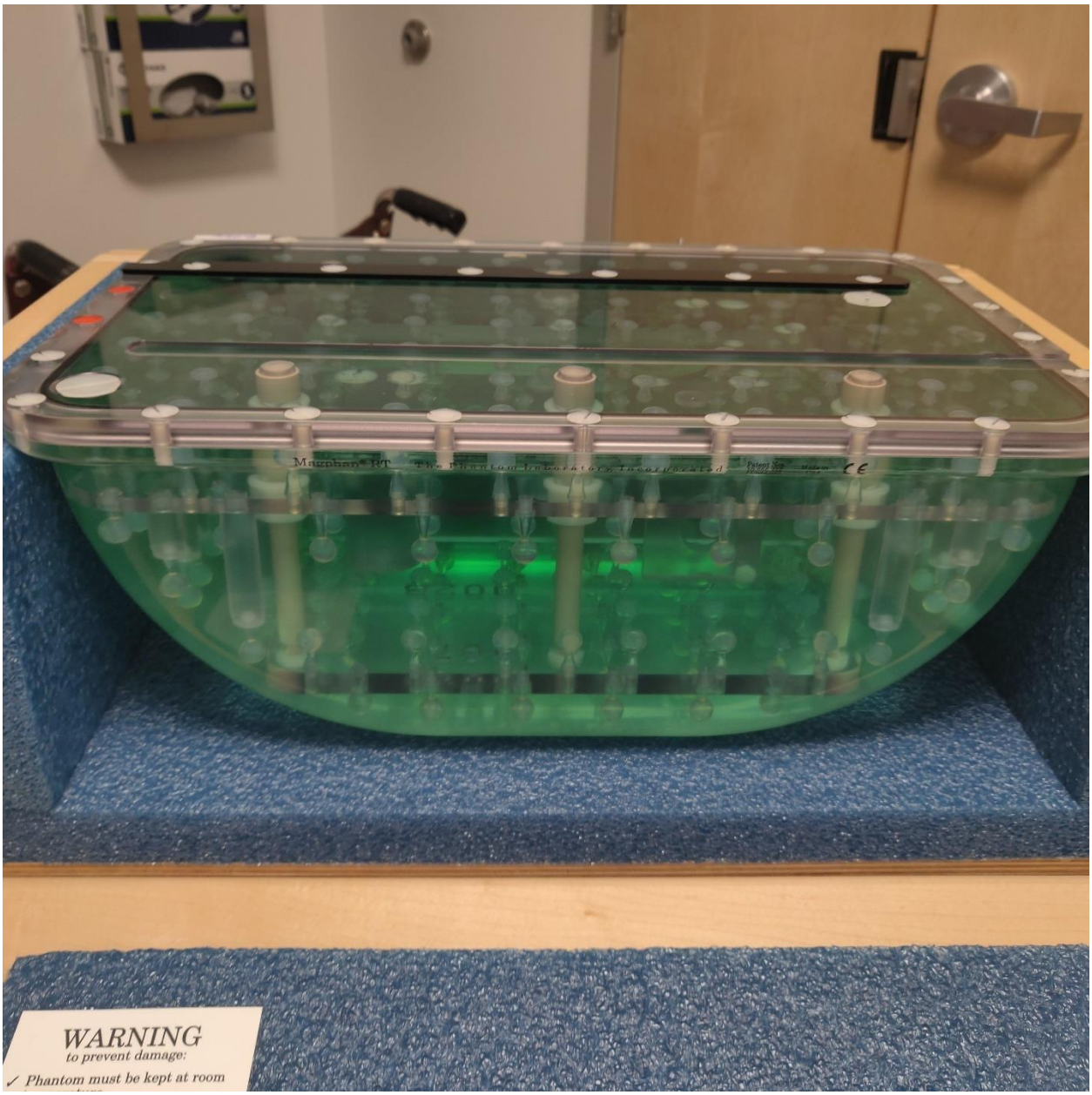

Figure 13. Photo of half of the MagPhan RT phantom in its storage container.

Figure 14. Photo of the assembled MagPhan RT on the patient couch.

	"Short" Axial 3D T1	"Long" Axial 3D T1	Axial T2
Sequence	FFE3D	FFE3D	FASE2D+10:MPV_HL

Plane	Axial	Axial	Axial
Subject orientation	Anterior-Posterior	Anterior-Posterior	Anterior-Posterior
PE FOV in cm	45	45	45
PE Matrix size	352	352	320
PE resolution in mm	1.27	1.27	1.40
PE No Wrap	1	1	1
RO FOV in cm	45	45	45
RO matrix size	352	352	320
RO resolution in mm	1.27	1.27	1.40
RO No Wrap	1	1	1
Number of slices	150	150	128
Slice thickness in mm	2	2	2
Slice gap in mm	N/A	N/A	0
NAQ	1	1	1
TR	5	5	15078
TE	2.2	2.2	80
speeder	2	1	2

Table 4. Pulse sequence information for the scanning protocols used for scanning the MagPhan RT.

3.2.B.II MagPhan RT geometric distortion tests

The geometric distortion tests performed by MagPhan RT produce four main figures[7]. The first (seen in figure 15) is a distortion magnitude plot or a distortion vs radius plot[7]. In this plot, distance from the isocenter is on the x-axis and the magnitude of the observed distortion is on the y-axis. The next figure is a fiducial location statistics diameter table (see figure 16) [7]. The automatic reports will generate two of these tables, wherein distortion is quantitatively analyzed across a prespecified, customizable diameter[7]. These tables will report the maximum observed distortion across the entire diameter, and along each axis for the evaluated diameter (x, y, z) [7]. Furthermore, these tables will state what the mean value of the largest top 10% of distortions is for each axis and across the entire observed diameter[7]. Based on the recommendations of TG-284, distortion is evaluated across a 250mm diameter and is only deemed passing if maximum distortion across the entire diameter and along each axis does not exceed 2mm [3]. The last figure generated for the geometric distortion analysis is a 3x3 distortion plot (see figure 17) [7]. While initially visually confusing, the 3x3 distortion plot consists of nine smaller figures, with each figure representing distortion that occurs in one axis, as you move across another [7]. Moving vertically across one of the smaller figures represents moving across an axis of the phantom, while moving horizontally represents the scale and direction of a distortion across another axis[7]. Since there are nine total possible combinations of distortion axis and position axis, the 3x3 plot generates a total of nine smaller figures[7].

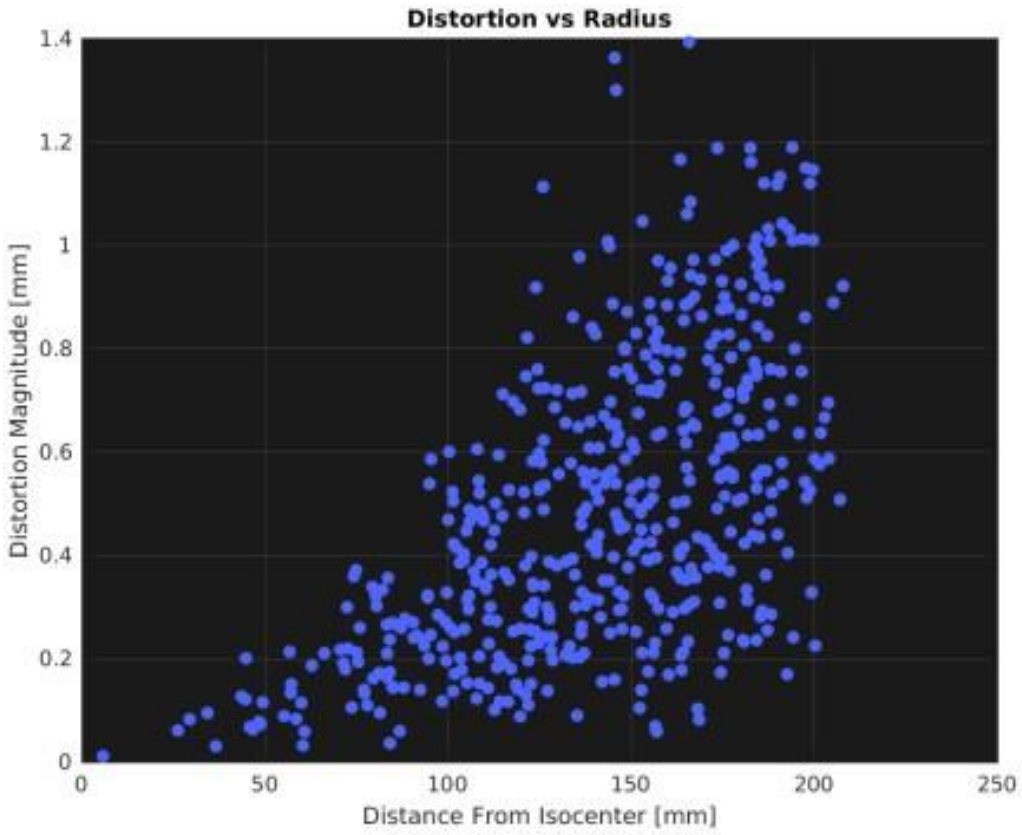

Figure 15. Example photo of the distortion magnitude plot from the November 2022 monthly QA for the "long" axial T1 pulse sequence.

Fiducial Location Statistics Diameter 1 + Add Comment

Series Description: AX 3D T1 2nd

Diameter mm	Max Distortion Magnitude mm	Mean Distortion Mag Top 10% mm	Max X Distortion mm	Max Y Distortion mm	Max Z Distortion mm	Mean X Distortion Top 10% mm	Mean Y Distortion Top 10% mm	Mean Z Distortion Top 10% mm
250	0.920	0.660	0.880	0.340	0.250	0.630	0.270	0.190

Figure 16. Example photo of one of the two fiducial location statistics figures from the November 2022 monthly QA for the "long" axial T1 pulse sequence.

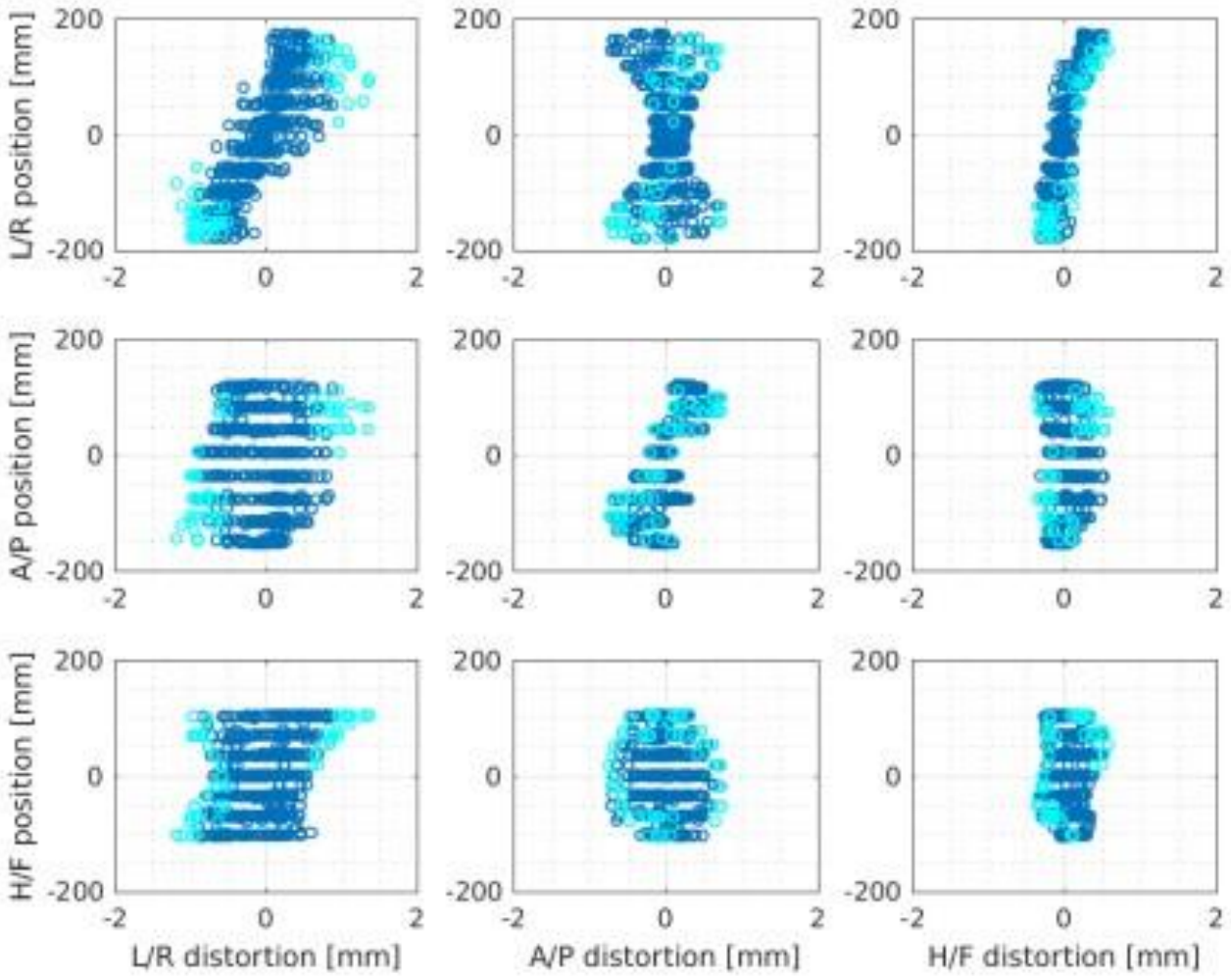

Figure 17. Example photo of the 3x3 distortion plot from the November 2022 monthly QA for the "long" axial T1 pulse sequence.

3.2.C - Basic Mechanical checks

Basic mechanical checks is an umbrella term used to describe a set of tests that evaluated the accuracy of the digital positional readout of the LAP laser external positioning system and the patient couch. TG-284 advises assessing the accuracy of both systems on a monthly basis[3]. A MR-SIM mechanical check worksheet was created to help facilitate the testing of both these

systems and a blank version is attached as appendix 1. To help facilitate ease of communication when discussing which axis is being evaluated, please consider the following. From the perspective of an observer standing at the foot of the patient couch looking into the bore, the x axis or dimension would run left to right, the y axis or dimension would run into and out of the bore, and the z axis or dimension would extend vertically from floor to ceiling.

3.2.C.I - LAP laser system testing

This test involved evaluating the positional and movement accuracy of three separate LAP laser components: two side lasers that moved vertically, and an overhead laser which moved left to right across the patient couch. Each side laser (referred to as right laser Z_A and left laser $Z_{B)}$ were evaluated independently. To evaluate these lasers, a ruler was positioned on the patient couch to run along the Z dimension, and the position of the laser on the ruler and the position of the laser according to the digital readout were recorded. The laser was then moved at least 200mm and the new positions according to the ruler and the digital readout were recorded. By subtracting the initial and final positions from each other, a ruler travel distance and a digital readout travel distance could be determined. The difference between these two travel distances was the accuracy of the laser position digital readout. To be considered passing, the difference between these two readouts could not exceed ±2mm [3]. The overhead laser component was evaluated in a similar fashion. A ruler was placed on the patient couch running right to left (or along the x dimension). The initial position of the laser on the ruler was recorded, and then the laser was moved 125mm (according to the digital readout) to the left of the initial position and then 125mm to the right relative to the initial position. The position according to the ruler was

recorded in both cases. The difference in travel distance according to the ruler and digital readout was then calculated. This test was considered passing if the difference did not exceed ±2mm [3].

3.2.C.II - Patient couch test

The patient couch test was performed in a very similar manner to the LAP tests described above. A ruler was placed on the patient running along the Y axis (aka longitudinally into the bore). The overhead LAP laser was turned on and its position on the ruler was recorded, along the position of the couch according to the couch position digital readout. The couch was then moved at least 200mm longitudinally according to the digital readout of the couch. The new ruler and readout position were then recorded. By subtracting the initial position from the final position, a ruler travel distance and digital readout travel distance could be calculated. The difference between these two travel distances is the accuracy of the patient couch digital readout system. To be considered passing, the difference between these two travel distances could not exceed ±1mm [3].

3.2.C.III - Considerations

This test has several considerations that must be discussed. The first is that none of the LAP laser components were capable of moving along the Y axis (aka towards or away from the bore). Therefore, the LAP laser positional accuracy in the Y axis did not need to be evaluated. Additionally, the patient couch could not be moved along the X axis (left to right) and likewise did not need to be evaluated along this axis. Lastly, while the patient couch could move along the Z axis (vertically), this degree of motion was only used to aid in positioning the patient on the

couch. The couch was only ever at one height when moving in or out of the bore. Because of this, it was not necessary to evaluate the accuracy of the patient couch along this axis.

3.2.D – CaliberMR Diffusion Phantom

The CaliberMR diffusion phantom was utilized for its DWI QA capabilities. The phantom contains 13 vials filled with varying concentrations of PVP ranging from 0% up to 50% (see figures 18 and 19). The phantom was scanned using a head receiver coil, and the obtained images were exported and uploaded to vendor proprietary software which automatically analyzed image data and generated summary reports. The automatic analysis software examined the uploaded image series, and utilized a phantom on board thermometer to determine what the temperature of the phantom was during the scan procedure. Note, the phantom thermometer was only functional within a range of 15 to 24°C, otherwise the analysis software assumed a temperature of 0°C. From the known PVP concentration of each vial, and the thermometer provided temperature, the vendor software was able to reference and provide a set of NIST predicted ADC values for each vial for the given scan setup. Furthermore, the software would automatically segment and analyze the supplied image data to calculate a mean ADC value for each of the 13 vials. From both the predicted NIST ADC values and the observed Mean ADC values, the software would then generate an in-depth report summarizing the scanner's DWI capabilities. DWI QA recommendations are not present in TG-284, nor are specific performance criteria recommendations provided by phantom vendors. However since the phantom was scanned on a monthly basis, regularly obtained sets of data were acquired and documented,

which will be utilized to perform baseline establishment and overall trend tracking of DWI performance over time. Enabling consistency checks of system performance.

Figure 18. Photo of the CaliberMR diffusion phantom.

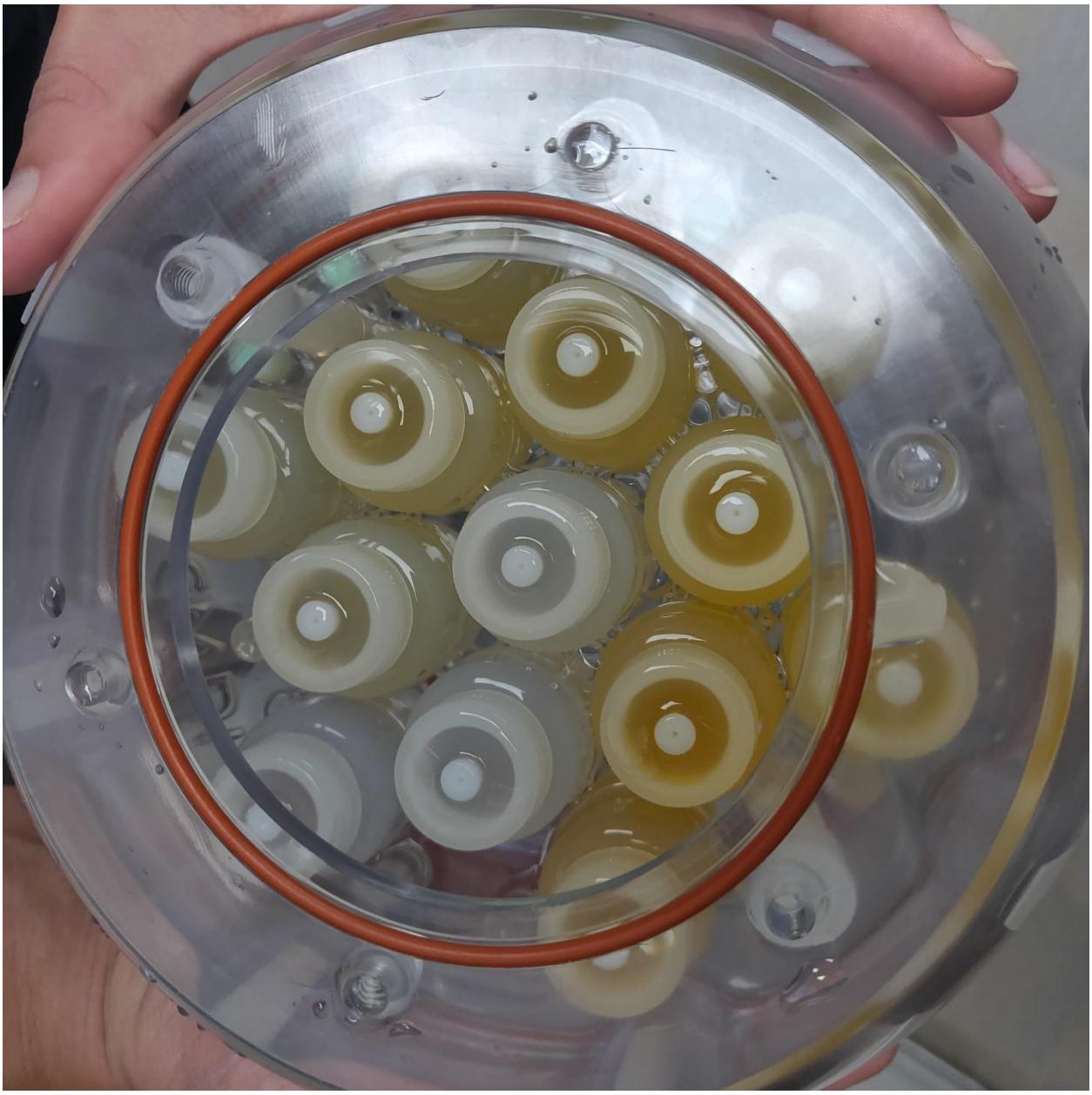

Figure 19. Photo of the 13 vials inside of the CaliberMR diffusion phantom.

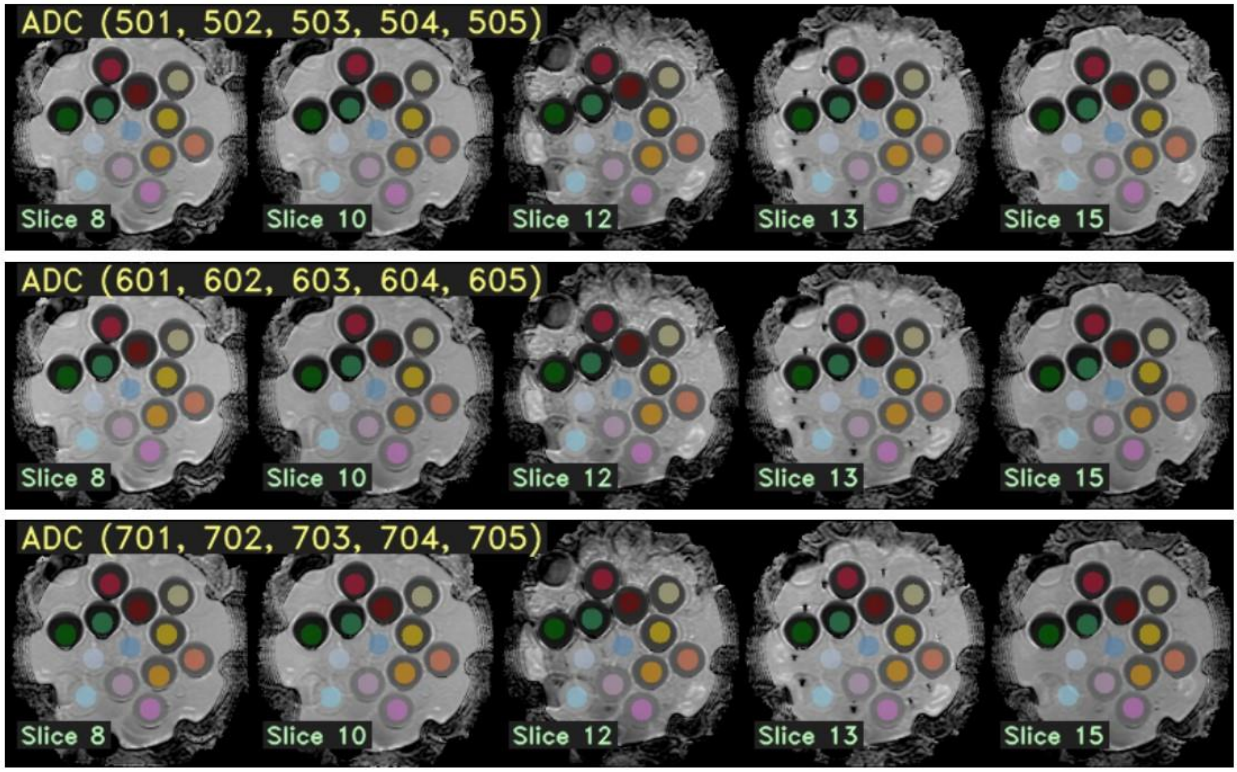

Figure 20: Example photo of automatic CaliberMR diffusion phantom vial segmentation performed by proprietary phantom vendor software. Please note that the phantom was not properly leveled during this scan and the software missed vials in several cases. Proper phantom setup and leveling is crucial for proper functioning of the analysis software.

ADC VOI Statistics

Label	Contents	# Voxels	NIST Value	Mean	Std Dev	Bias	Bias Percent	Max B-Value Dependence	SNR B0	SNR B500	SNR B1000	SNR B1500	SNR B2000	RC	Random Error	wCV
			um^2/s	um^2/s	um^2/s	um^2/s	%	% (associated b-value pair)						um^2/sec	%	%
1	water	12064	2026 +/- 57.7	2041	97.6	14.3	0.70	3.20 (500, 1500)	86.3	100	58.0	27.2	10.8	4.47	1.93	0.079
2	water	12064	2026 +/- 57.7	1998	79.2	-29.0	-1.43	3.39 (500, 2000)	81.2	110	65.0	28.1	11.0	12.3	1.96	0.22
3	PVP50	12064	274 +/- 13.6	324	24.0	50.6	18.5	13.8 (500, 2000)	29.5	39.4	38.9	40.0	40.8	2.06	3.23	0.23
4	PVP40	12064	516 +/- 20.6	566	12.3	49.6	9.61	2.00 (500, 2000)	88.3	153	157	152	136	2.59	0.78	0.16
5	PVP30	12064	846 +/- 32.4	877	13.1	31.9	3.77	0.93 (500, 1500)	66.3	93.4	102	101	85.4	1.52	0.70	0.062
6	PVP20	12064	1202 +/- 40.6	1168	16.9	-34.0	-2.83	0.28 (500, 1000)	110	147	120	83.6	52.6	1.55	0.69	0.048
7	PVP10	12064	1573 +/- 49.0	1535	35.0	-38.1	-2.42	1.47 (500, 2000)	115	154	109	58.0	28.1	6.06	0.99	0.14
8	PVP50	12064	274 +/- 13.6	329	21.7	55.1	20.2	10.6 (500, 2000)	44.5	77.6	86.2	88.7	82.3	1.46	2.47	0.16
9	PVP40	12064	516 +/- 20.6	554	13.5	37.3	7.22	2.14 (500, 2000)	65.6	113	121	123	108	2.91	1.08	0.19
10	PVP30	12064	846 +/- 32.4	861	17.3	15.1	1.78	1.30 (500, 1500)	79.3	127	143	146	113	3.86	0.64	0.16
11	PVP20	12064	1202 +/- 40.6	1232	24.9	30.4	2.53	0.36 (500, 2000)	90.2	138	132	98.4	62.5	4.16	0.62	0.12
12	PVP10	12064	1573 +/- 49.0	1506	28.9	-67.7	-4.30	1.22 (500, 2000)	77.3	84.0	75.0	58.0	30.0	4.45	0.91	0.11
13	water	12064	2026 +/- 57.7	2021	95.9	-5.74	-0.28	0.84 (500, 1500)	90.4	113	78.5	33.3	12.7	13.5	1.77	0.24

Figure 21: Example photo of ADC analysis performed by the CaliberMR diffusion phantom proprietary software.

3.2.E - Coil QA

3.2.E.I - Background

Coil QA is generally one of the most complex portions of a MR QA plan. The ACR distinguishes the parameters that must be evaluated during coil QA based on the type of coil that is evaluated[5]. For volume coils SNR, PIU and PSG must be calculated[5]. When determining SNR for volume coils the physicist may elect to use the single image method or the NEMA method[5]. For surface coils, mean and max SNR must be determined[5]. For array coils, SNR should be determined for every coil channel present in the array[5]. However, the Canon Galan 3T MR-SIM has a vendor supported method for coil QA that is simpler to perform and boasts automatic analysis. Furthermore, TG-284 advises that for coil QA the vendor method be utilized to evaluate coil

SNR and uniformity performance[3]. For both the added simplicity and per the guidelines set out by TG-284, we adopted the vendor coil analysis method.

3.2.E.II – Frequency and method

The simulation process can place additional strain on RF coils, potentially resulting in coil damage and or coil element failure, which could contribute to decreased coil performance manifesting as artifacts, lower SNR, and decreased uniformity[3]. "Rigid" coils are most resilient to simulation induced damage, with TG-284 advising that these coils undergo QA on a quarterly basis[3]. Flex coils are the most susceptible to simulation induced damage and TG-284 advises they undergo QA on a monthly basis[3]. Given these considerations, coil QA at VCU was outsourced to a vendor service engineer who evaluated coil performance roughly every six to eight weeks. However, VCU staff also learned the vendor coil QA method from the vendor service engineers so as to perform QA independently if the need arose. The method was simple to perform. The operator simply navigated to "coil QA" on the control terminal and then selected the coil that was to be evaluated. Once the coil was selected, a pop-up window would instruct the operator on which oil drum phantoms and foam phantom holders were necessary for the QA procedure. The pop-up window would also instruct the operator on how to set up the phantom and where to align the magnetic isocenter to. Once the setup was complete, the operator simply began scanning (the scan protocols were automatically selected once the desired coil had been chosen) and waited for the scanning and automatic analysis procedure to finish. The amount of time necessary for coil QA to be finished varied depending on the type of coil. The automatic analysis was performed on individual sections of the coil one at a time until all regions were evaluated. The automatic analysis was based on a vendor determined minimum passing SNR.

This minimum passing SNR was compared to the “Sum SNR Slice 2” value. The coil was considered passing if all sections of the phantom had Sum SNR slice 2 values that exceed the required minimum passing SNR unique to that section of that particular coil. During the course of this project, we had eight total receiver coils: two 16 channel flex SPEEDER medium coils, a four-channel flex SPEEDER coil, an Atlas SPEEDER Body coil, an Atlas SPEEDER Spine coil, an Atlas Head Neck coil, an Atlas Cervical coil and a QD head coil. Please note that the Atlas SPEEDER Spine coil resides under the cushioning on the patient couch.

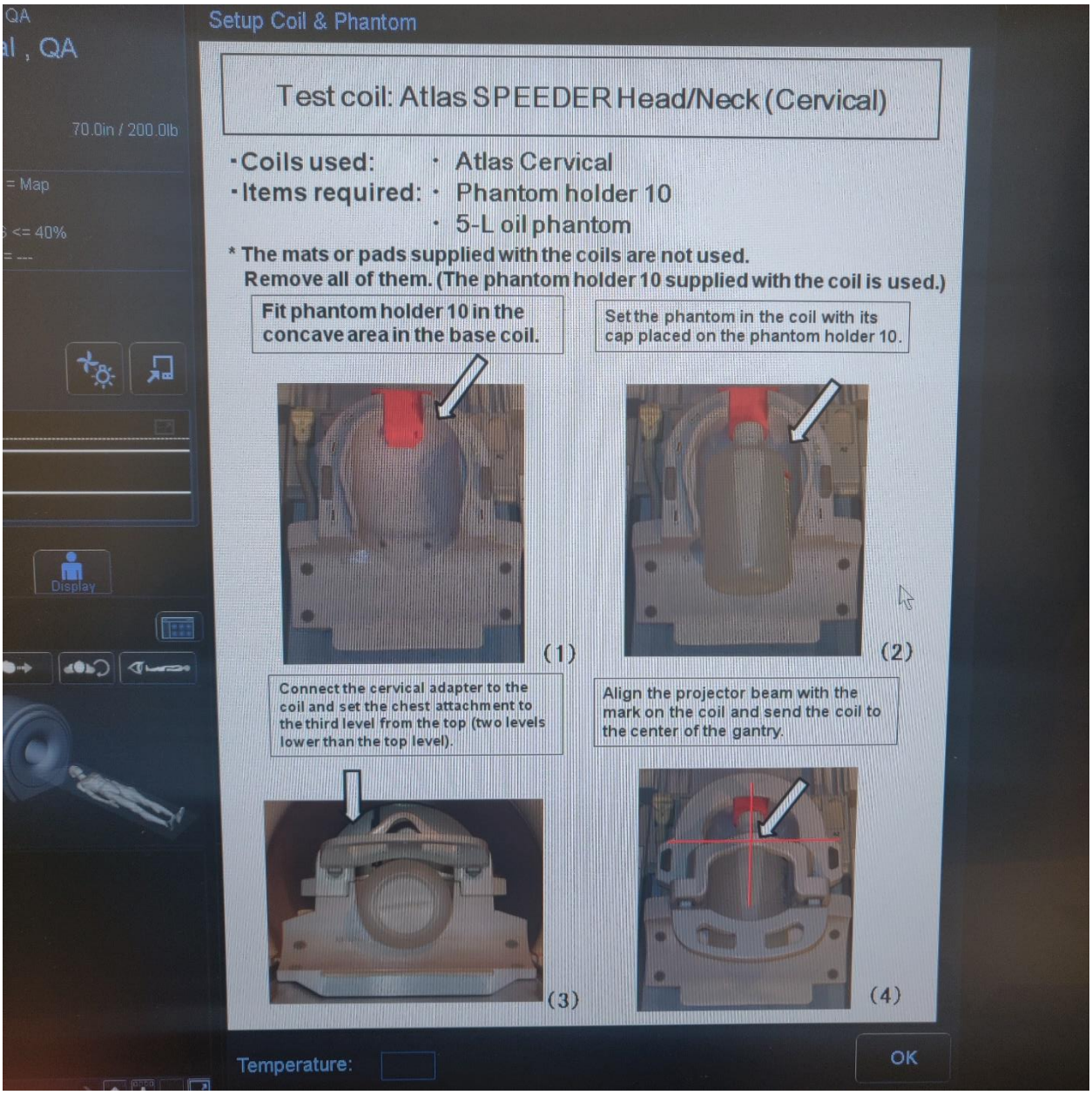

Figure 22. Example photo of the pop-up window instructions for setting up coil QA. For this example, the instructions are for an Atlas Speeder Head/Neck (cervical) receiver coil.

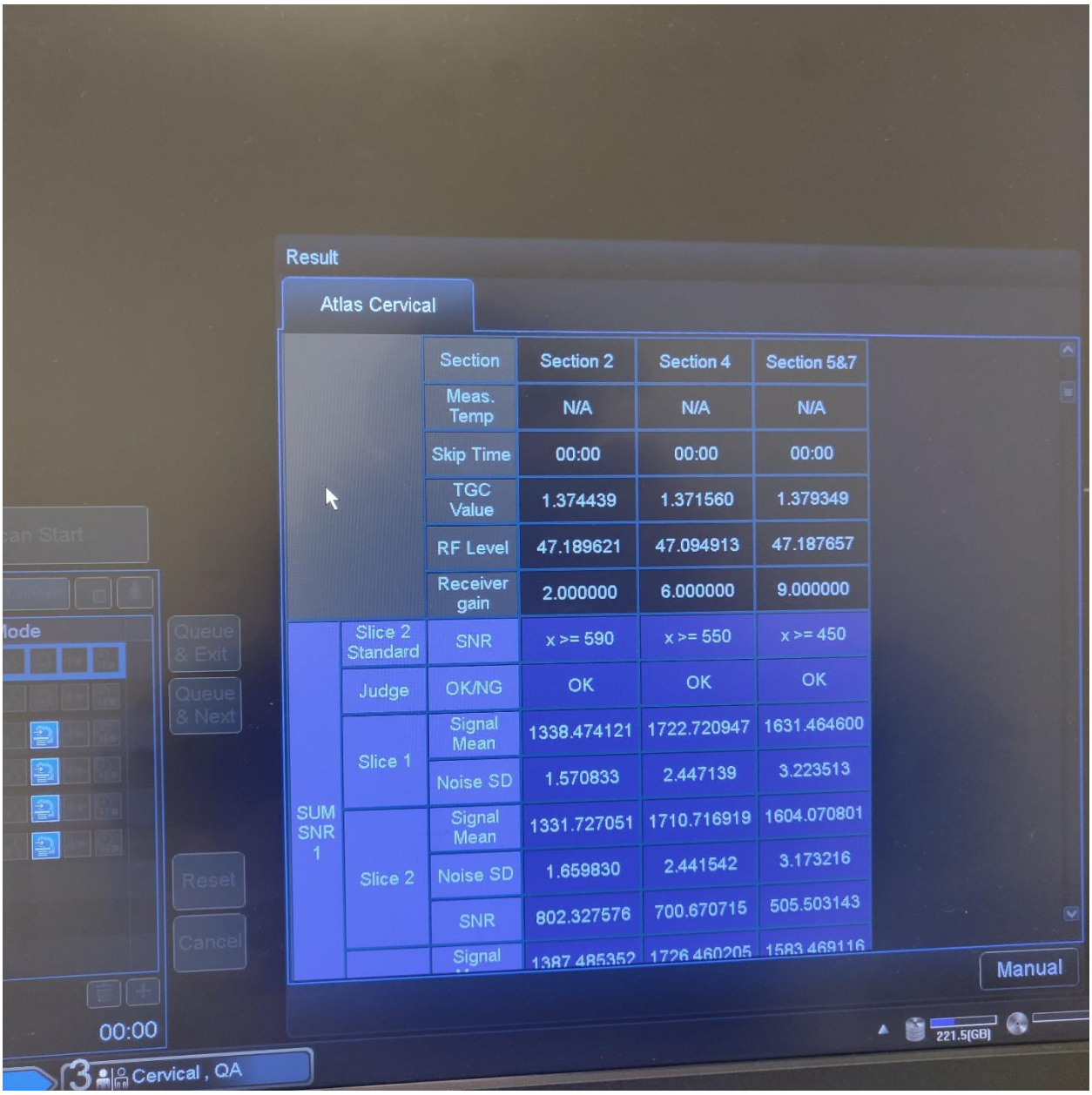

Figure 23. An example of the automatically produced results from the vendor coil QA method. For this particular example, the results are for an Atlas Speeder Head/Neck (cervical) receiver coil.

Figure 24. A photo of the base of the Atlas Head Neck coil and Atlas Cervical coil. The scanner “perceives” the coil as a different coil based on which top component is attached.

Figure 25. A photo of the top component of the Atlas Head Neck coil.

Figure 26. A photo of the top component of the Atlas Cervical coil.

Figure 27. A photo of the Atlas SPEEDER Body coil.

Figure 28. A photo of the four-channel flex SPEEDER coil.

Figure 29. A photo of one of the16 channel flex SPEEDER medium coils.

Figure 30. A photo of the QD head coil.

3.3 Annual QA procedures

The annual QA procedure (as the name implies) was performed on a yearly basis and could be spread across several days to work around patient scheduling and staff availability. The full set of tests performed for the annual QA procedure can be found in table 5 but can be broadly summarized as consisting of the following. A large ACR MRI Accreditation phantom scan which was used to complete an abbreviated version of the ACR image quality tests and table position accuracy test. Center frequency was retroactively examined based on measurements taken during the daily QA procedure. Automatic and manual transmitter gain were compared using a spherical homogenous phantom. Magnetic field homogeneity was evaluated using a spherical homogenous phantom and a provided method. The agreement between laser and magnetic isocenters was evaluated using the LAP AQUARIUS MRI phantom. The entire stock of clinically utilized RF coils was evaluated. The control terminal monitor performance was evaluated using the SMPTE set of QA tests advised by the ACR. The MRI accreditation visual checklist worksheet was filled out. All acquired images were evaluated for the presence of any artifacts. Lastly a qualified medical physicist evaluated the safety program in place at the facility.

Test Name	Method	Advised under	Performance criteria	Source of criteria
Geometric accuracy	ACR Phantom	ACR	±2mm of phantom dimensions	ACR

High contrast spatial resolution	ACR Phantom	ACR	At least 1mm resolution	ACR
Low contrast Detectability	ACR Phantom	ACR	40 spokes for 3.0T	TG-284
Slice position accuracy	ACR Phantom	ACR	within 5 mm	ACR
Slice thickness accuracy	ACR Phantom	ACR	5mm ± 0.7mm	ACR
Table position accuracy	ACR Phantom	ACR	Within 5mm	ACR
Center frequency	Check records	AAPM Report 100	< 0.25ppm/day	AAPM Report 100
Transmitter gain	AAPM Report 100 method	TG-284	±5% agreement between manual and automatic TG	TG-284
Magnetic Field homogeneity	Vendor	ACR & TG-284	Less than 0.05ppm VRMS	Vendor specified

External laser offset from isocenter	Aquarius phantom	TG-284	Equal to or less than 1mm	TG-284
RF Coil checks	Vendor method	ACR & TG-284	Vendor performance	Vendor
Artifact Evaluation	Visual inspection	ACR	Artifact free	ACR
Visual Checklist	Visual inspection	ACR	See the ACR MRI accreditation program visual checklist	ACR
Safety Program evaluation	Document review	ACR	Satisfactory safety program	ACR
Monitor QC	SMPTE method	ACR	ACR minimum criteria	ACR

Table 5: Table indicating all the tests that comprise the annual QA.

3.3.A: ACR image quality tests

The first portion of the annual QA was an abbreviated version of the large ACR MRI accreditation phantom image quality tests that were performed as a part of the monthly QA process. The tests utilize the same procedure and same performance criteria as they did under the monthly versions of these tests. The only difference was that the percent signal ghosting and the image intensity uniformity tests were not performed. The selection of tests is based on the recommendations of the ACR MRI QC Manual which specifies which tests the qualified medical

physicist should perform as part of their annual evaluation[5]. In practice this means that the percent signal ghosting and image intensity uniformity tests were entirely optional, however performing these tests would require no additional scans. It is worth noting that during the MR-SIM's first annual QA evaluation we elected to perform both of these tests. The ACR image quality tests are discussed in more detail earlier in this body of text (see section 3.2.A).

3.3.B: Setup and table Position Accuracy Test

The purpose of this test was to evaluate the scanner's ability to perform the following tasks correctly: data entry, patient poisoning and other pre-scan tasks[5]. This test can be performed using a knee coil with the small ACR MRI accreditation phantom or using a head coil with the large ACR MRI accreditation phantom[5]. We utilized the large ACR phantom when conducting the ACR image quality tests and as such elected to use the large phantom method [5]. Conveniently, the phantom setup and scan procedure necessary for this test is identical to the ACR image quality tests setup and procedure[5]. In practice, since an abbreviated version of the ACR image quality tests were already performed as a part of the annual evaluation, performing this test did not require any additional scans or phantoms. The test analysis was performed manually by the operator while examining the ACR sagittal locator image[5]. According to the ACR MRI QC manual (assuming that this test was performed properly) "…the superior edge of the grid structure should be at magnet isocenter"[5]. The operator placed a cursor or ROI tool at the edge of the grid structure (which should be at the magnetic isocenter) and assessed placement of this ROI relative to the isocenter, along the Z-axis[5]. In order to be considered passing, the edge of the grid structure had to be ±5mm of the magnetic isocenter[5].

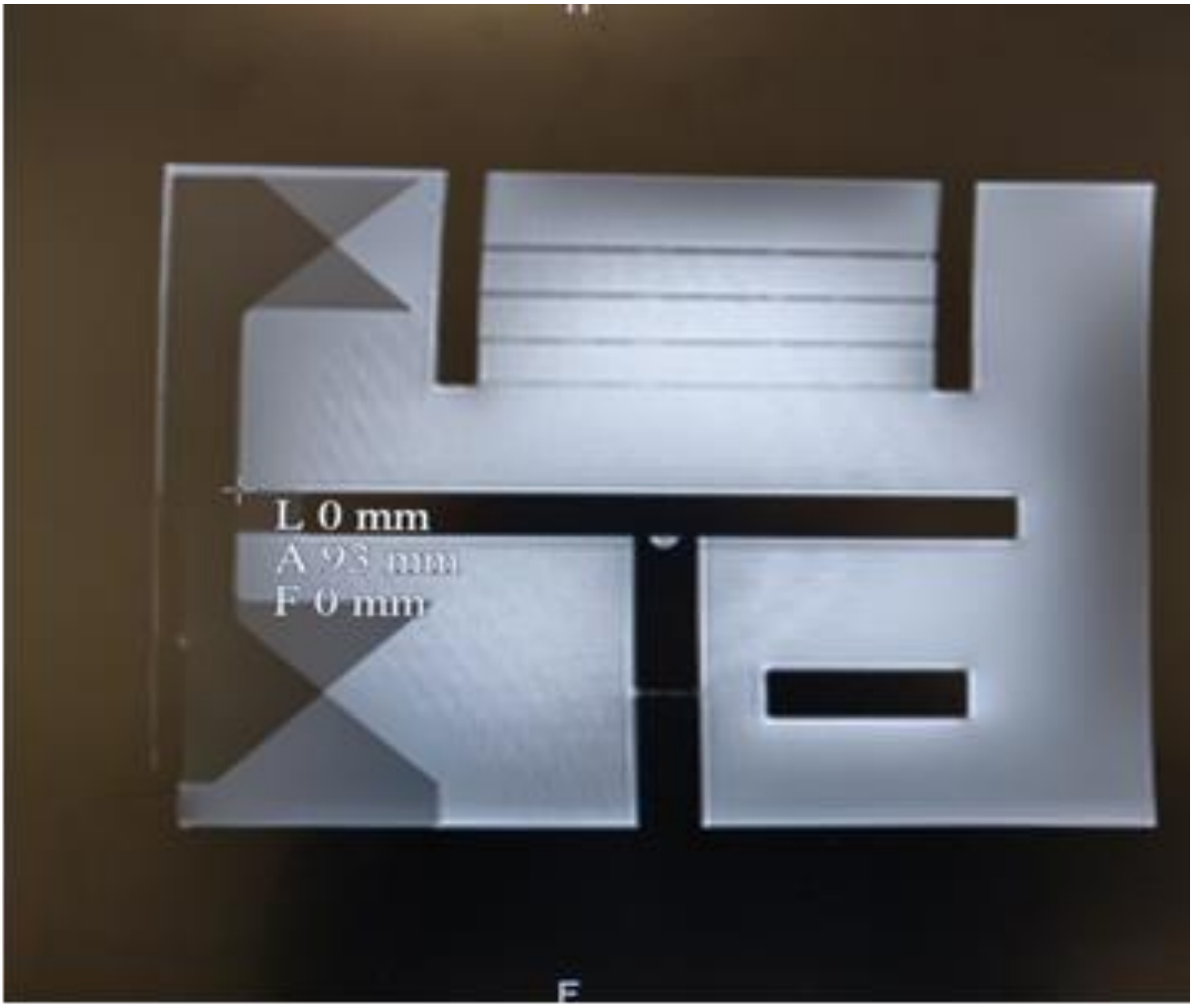

Figure 31: Photo taken of the analysis portion of the table position accuracy test during the annual QA performed in December 2022.

3.3.C: Center frequency

The annual evaluation of center frequency test can also be called the magnetic field drift test due to the relationship between center frequency and the strength of a magnetic field[8]. This relationship is explained through the Larmor equation, shown below as equation 5 [8]:

Eqn. 5: Center frequency = $(\gamma/2\pi) \times B_0$

In the context of the Larmor equation B_0 stands the strength of the magnetic field in units of tesla, and ($\gamma/2\pi$) is the gyromagnetic ratio of the nucleus of interest, which in the case of MR is the hydrogen nucleus (i.e., a proton) and will thus have a value of 42.58 MHz/T [8]. This means that tracking the center frequency of a scanner overtime can serve as an indirect method of monitoring changes in magnetic field strength over time, also known as magnetic field drift [8]. Since center frequency was measured and recorded as a part of daily QA (see section 3.1.A), we were able to retroactively examines changes in center frequency over time by plotting all center frequency measurements taken over the course of a year. The measurements were evaluated using the recommended performance criteria of TG-1 Report 100, under which center frequency should not change by more than 1ppm/day during the first few months of operation, and then no more than 0.25ppm/day following a few months of clinical operation [8].

3.3.D: Transmit and gain calibration test

The transmit and gain calibration test was used to evaluate the accuracy with which the scanner automatically determines the center frequency and transmit gain necessary to achieve the desired nutation angle for a prescribed imaging sequence[8]. To perform this test, the operator scanned a spherical homogenous phantom using the automatic pre-scan and manual pre-scan options, and recorded the observed center frequency, transmit gain, and receiver gain[8]. The test was considered passing on three conditions. The manually determined transmit gain values were within 5% of the automatically calculated values[3]. The center frequencies for the automatic and manual methods were within 10 Hz of one another[3]. The acquired images were artifact free[3]. We performed this protocol three separate times using a SE2D, FSE2D and then a FSE3D pulse sequence.

3.3.E: Magnetic field homogeneity test

Homogeneity in reference to MR scanners is used to describe the uniformity of the strength of the magnetic field[5]. A scanner that produces an inhomogeneous field may have increased geometric distortion, worsened wrapping artifacts, decreased signal uniformity, and non-uniform fat suppression[5]. Test performance is typically discussed in terms of parts per million (PPM) of the magnet's filed strength across a diameter spherical volume (DSV) [5]. There are several methods recommended by the ACR to assess the magnetic field homogeneity (MFH) of a scanner: spectral peak method, bandwidth difference method, phase map method, and phase difference map method[5]. However, TG-284 in no uncertain terms recommends the phase difference map method over the other ACR recommended methods [3]. The reason for this is because the phase difference map method evaluates inhomogeneity on a voxel wise basis across three planes and is the only method to provide spatial information [3].

3.3.E.I: Phase difference map method

The phase difference map method allows for evaluation of inhomogeneity across individual planes and on a voxel wise basis[8]. However, the ability of a site to perform this test is limited by its access to certain special analysis software that is typically blocked for end users[8]. Many locations have the vendor perform this technique and provide a summary report in leu of performing it independently[8]. This technique involves scanning a spherical homogenous phantom and obtaining two sets of gradient echo image series with slightly different echo times for each plane[8]. The obtained images are then reconstructed in phase mode instead of the typical

magnitude mode[8]. Once the images are reconstructed in phase mode, they are subtracted from one another, resulting in a final image in which the MFH can be calculated on a voxel-by-voxel basis utilizing equation 6 [8]. In the context of equation 6, $\Delta\Phi$ is the difference in phase, γ is the gyromagnetic ratio and TE_2 and TE_1 are the two slightly different echo times used [8].

$$\text{Eqn. 6: } \Delta B_0 = \frac{\Delta\Phi}{\gamma(TE2-TE1)}$$

3.3.E.II: Bandwidth difference method

The bandwidth difference method, while generally considered time consuming, has the distinct advantage of being viable as a QA procedure for almost all commercially available MR scanner systems[8]. With the stipulation that this method assumes correctly calibrated gradient fields[8]. In practice this means that the bandwidth difference method is better suited for applications in ongoing QA, and is not generally considered suitable for acceptance testing[8]. This method works by comparing distortion observed when utilizing a small and a large bandwidth when scanning a spherical homogenous phantom[8]. The conditions that define a bandwidth as small or large are predicated on equation 7 [8]. In the context of equation 7, BW stands for bandwidth in units of Hz, FOV is the field of view in units of meters, γ is the gyromagnetic ratio, and G_x is "The linear magnetic field gradient along the x-axis for conventional Fourier transform MRI… " [8].

$$\text{Eqn. 7: } G_x = (2\pi/\gamma)x(BW_x/FOV_x)$$

For a bandwidth to be considered small, it must result in a G_x that is approximately equal to $\Delta B(x,y)$, where $\Delta B(x,y)$ is the change in the main magnetic field [8]. And for a bandwidth to be considered large, it must result in a G_x that is much larger than $\Delta B(x,y)$ [8]. Once both the small

and large bandwidth images have been acquired, the MFH can be calculated utilizing equation 8 [8]. In the context of equation 8, BW1 refers to the small bandwidth used and BW2 refers to the large bandwidth used[8].

$$\text{Eqn. 8: MFH (ppm)} = \frac{BW1\ x\ BW2\ x\ (x1' - x2')}{\left(\frac{2\pi}{\gamma}\right) x B0 x (BW1 - BW2)}$$

This method can be repeated for each orientation in order to obtain an assessment of inhomogeneity across each plane [8].

3.3.E.III: Spectral peak method

The spectral peak is quick and easy to perform, but only enables a global evaluation of inhomogeneity, I.E., this method does not allow for an evaluation of inhomogeneity in a single plane [8]. For this method, an operator measures the FWHM in Hz from an MR spectrum obtained from imaging a spherical homogenous phantom scanned at the magnetic isocenter [8]. This FWHM is converted into ppm by utilizing a variation of the Larmor equation in the case of protons [8]:

$$\text{Eqn. 9: FWHM (ppm)} = \frac{FWHM\ (Hz)}{(42576000 Hz/tesla) x (B0\ tesla)}$$

3.3.E.IV: Vendor Procedure

We collaborated with scanner service engineers to create and save a scan protocol for use in annual QA evaluations of MFH. The method created was provided to us from vendor personnel and was a variation on the phase difference map method which utilized shim imaging. The test

method protocol consisted of scanning a spherical homogenous phantom using a body coil and acquiring two sets of FE-AAS images for each orientation (Axial, coronal, sagittal).

Each FE-AAS image sequence had the following parameters. A 64 by 64 matrix size, that extended 40cm in both the frequency encoding and phase encoding directions. 15 total slices with a utilized slice thickness of 5mm and a gap of 10mm. A TR of 200, a first TE of 4.8 and a second TE of 7.2.

Subsequently after scan completion, the operator adjusted shimming information from being hidden, to being shown. At this point the operator had six total FE-AAS sequences (two per each orientation), with each sequence containing four rows of data. The first row of data represented the first echo image data, the second row of data represented the second echo image data, the third row of data represented the phase image data of the first row minus the phase image data of the second row, and the fourth row of data represented the predicted phase difference map after first order shimming. Analysis for this test had to be performed for each orientation. To perform analysis, the operator navigated to the center slice of the third row of data of the second FE-AAS image series. The displayed slice was a phase difference map, that corrected for linear offsets and since it was part of the second shim image series, it also had first order shim corrections determined during the first FE-AAS applied. The operator then placed a 20cm diameter ROI and used the standard deviation tool to determine the region of the specific slice with the greatest standard deviation (RMS). This region of greatest RMS represented the area of greatest inhomogeneity. The largest observed RMS value was divided by 100 to convert it into a VRMS

value which was expressed in terms of PPM. This VRMS was compared to a very specific set of vendor provided performance criteria: for a 3T scanner, scanning a 30cm spherical phantom, utilizing a 20cm ROI, inhomogeneity should not exceed 0.05PPM. This procedure was repeated for each orientation.

3.3.F: laser offset

TG-284 advises that the agreement for offset between the external laser isocenter and true magnetic isocenter be quantitatively evaluated and that these two isocenters differ in position from one another by no more than 1mm [3]. In short, this method should involve leveling and aligning a phantom to the laser prescribed isocenter, before translating the phantom the known distance to the magnetic isocenter [3]. The requirements of this test were met by utilizing the LAP AQUARIUS MRI phantom and its corresponding procedure as a part of annual QA testing.

3.3.G: RF Coil

As advised by both the ACR and TG-284, all receiver coils underwent performance evaluation as a part of the annual QA survey[3,5]. The vendor method (discussed in detail in section 3.2.E) was employed to evaluate the performance of all clinically utilized RF coils. The operator recorded the coil being evaluated (including the serial number), and the QA results of each evaluated region of that coil. This included the SNR necessary to be deemed passing, the measured SNR,

the pass or fail status of that region, and several other performance parameters: TGC, RF level, receiver gain, the signal value and noise SD. The only exception for this procedure is the QD head coil which could not be evaluated using the vendor supported method. Instead, the QD head coil QA was outsourced to vendor service engineers.

3.3.H: artifacts

While the ACR MRI QC Manual advises evaluating the obtained images for any noticeable artifacts during an annual evaluation, this does not mean that artifacts that occur outside of the annual QA procedure should be ignored[5]. It is highly advised that any observed artifacts be thoroughly documented (including saving raw data, noting any unusual conditions, the frequency of occurrence, etc.) and that this information be provided to a qualified medical physicist[5]. Artifacts are often times impermanent, and by providing a qualified physicist with ample background information regarding the artifact, the physicist should be able to determine the severity of a given artifact, and whether or not a given artifact is cause for concern [5]. The ACR MRI QC Manual denotes that some of the most encountered artifacts in phantoms include geometric distortion, ghost imaging, lines/pixels with unusually high/low intensities, receiver saturation errors, blurring, and truncation [5]. While a detailed examination of all possible MR artifacts is beyond the scope of this text, the following section will examine some of the most common artifacts encountered when using MRI, with the underlying assumption that in order to accurately identify artifacts, that the physicist must first be familiar with the artifacts that can occur.

3.3.H.I: Aliasing artifact / wrap around artifact

Appearance: Aliasing appears as anatomy that extends outside of the image's FOV "wrapping around" or superimposing on top of the opposite side of the image. See figure 32.

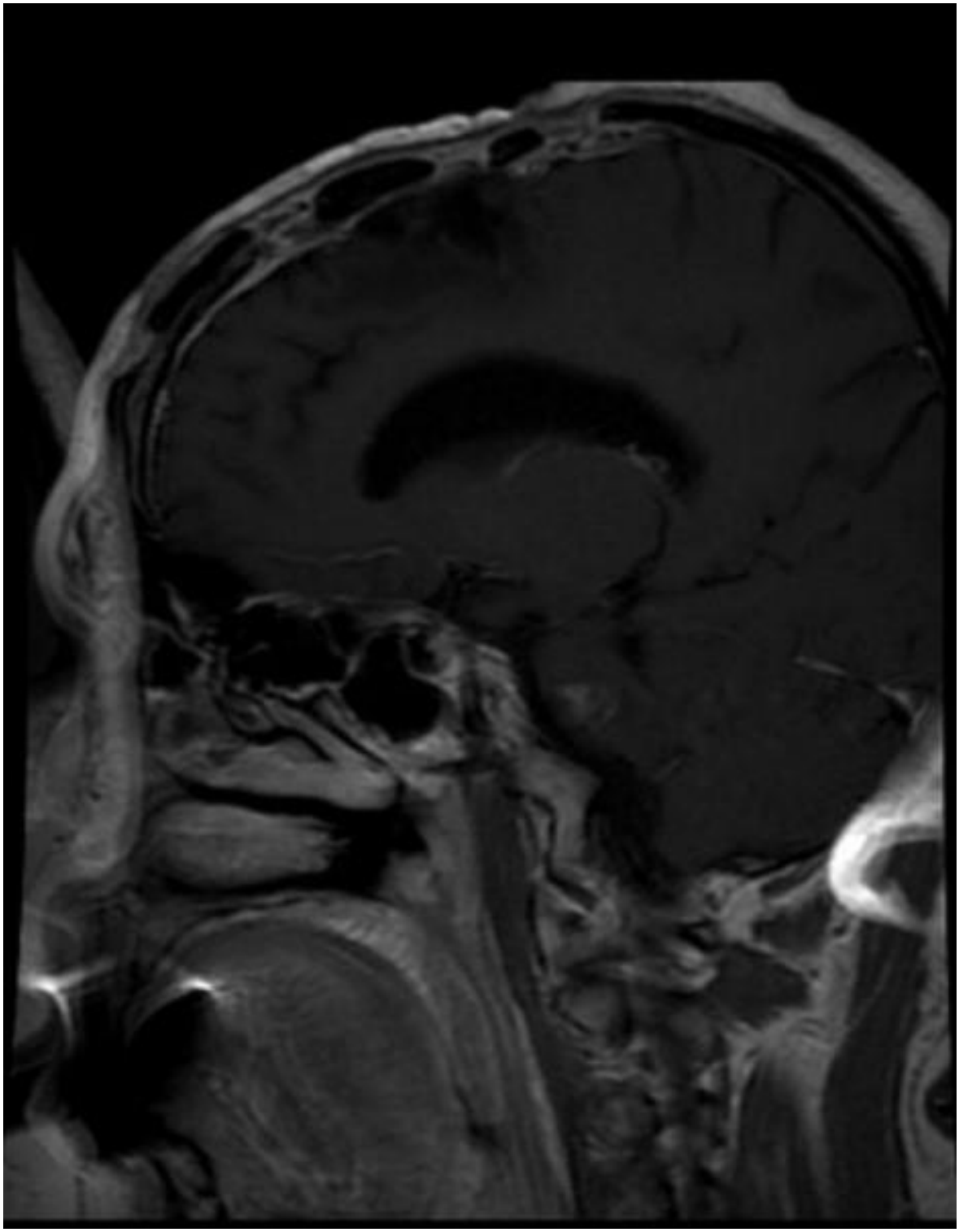

Figure 32: An example photo of an aliasing artifact from Katarzyna Krupa and Monika Bekiesińska-Figatowska's article on artifacts in MRI [9].

Cause: Aliasing artifacts can occur when the signal that is being digitized has a frequency that is greater than that of the f_N (Nyquist frequency)[10]. With the f_N being equal to half of the f_S (sampling frequency) being used (see equation 10) [10]:

Eqn. 10: $f_N = ½ \times f_S$

This means that every sampling frequency used has a corresponding Nyquist frequency that serves as an upper limit to what signals can be accurately digitized[10]. In other words, the Nyquist frequency is the maximum signal frequency that can be imaged properly before the MR system begins to misinterpret the signal as lower frequencies, resulting in an aliased image [10]. Aliasing is most often seen in the phase encoding direction but can also be seen in the slice direction, in cases where 3D images are acquired [11]. Aliasing, or wraparound artifacts as it can alternatively be known as, can also occur when the image study subject extends beyond the periphery of the FOV used, but is still contained within the slice volume and is misassigned a location in the image that is generally on the opposite end of the image that the anatomy extends out from[12].

Solutions:

1.) One the simplest and most reliable methods to address aliasing is known as the phase oversampling technique[11]. In this technique the operator doubles the FOV used in the phase encoding direction and doubles the number of phase encoding steps, which results in the pixel size remaining unchanged[11]. This typically covers the anatomy of interest that was previously outside of the FOV, preventing aliasing from occurring [11]. The additional FOV that extends beyond the anatomy of interest is simply truncated once imaging is

complete, leaving only relevant image regions[11]. Increasing the FOV in the phase encoding direction also has the effect of increasing the necessary scan time and can also result in a slight increase to SNR[11].

2.) Another (although less effective) technique used to address aliasing is to use sat bands in the anatomy outside of the FOV[11]. The sat bands, also known as spatial saturation bands, can be oriented in any direction, and set to have any thickness[11]. These sat bands work by applying a 90° excitation pulse in the anatomy outside of the FOV just before the main imaging occurs, in an attempt to suppress the signal generated in these regions[11]. However, the technique is not entirely effective as the signal is not fully suppressed[11].

3.) Depending on the coil selection available to the MR operator, switching to a surface coil is another potential aliasing solution[13]. This solution takes advantage of the fact that surface coils do not receive signals from outside of their radius[13]. By centering the region of interest with the center of the surface coil, the operator can ensure imaging of the relevant regions and prevent aliasing[13]. This technique is limited in its capacity however, since it relies upon the site having relevant surface coils of an adequate radius in order to work properly. Additionally, the operator will have to repeat the entire setup process to switch to a surface coil.

4.) Aliasing generally doesn't occur in the frequency encoding direction, due to the use of frequency filters which remove signals that are outside the region of interest, and or

signals that are outside a certain frequency range[13]. Aliasing in the frequency encoding direction is also prevented by oversampling in the frequency encoding direction, which can be done without any associated scan time penalty[13]. In certain cases, the directions for phase and frequency encoding can be switched to better image the region of anatomical interest[13].

3.3.H.II: Cross talk / cross excitation / cross relaxation

Appearance: Appears in multi-slice images as decreased signal intensity in all the slices except for the very first one[11]. This artifact can often be difficult to detect if comparing slices located in the center of the multi slice image study[11]. This artifact can be more easily detected by comparing the signal produced by center slices, to those at either end of the slice series[11].

Cause: Due to limitations in the slice selecting pulses, slice edges are not straight, but instead are curved[11]. These curved edges mean that in certain protocols that use very small slice gaps, slice overlap can occur[11]. Slice overlap means that material residing in the interstice between the two slices is excited by each slice's pulse[11]. The result of this dual excitation is that the material experiences an effective TR or repetition time that is far shorter than what was intended for the selected protocol, which leaves the material not enough time to fully relax before the next subsequent pulse arrives, reducing the signal produced by the unlucky material[11]. For T1 weighted imaging, cross talk causes lowered image contrast[12]. For T2 weighted imaging, cross

talk causes a reduction in SNR[12]. IR or inversion recovery pulse sequences are more sensitive to cross talk artifacts[11].

Solutions:

1. Increasing the size of slice gaps can reduce the size of slice overlap regions, thereby reducing the amount of cross talk that occurs, at the expense of decreased spatial resolution and the lack of image information for anatomical regions that reside in the slice gap[11].

2. If image study requirements wholesale prevents the use of large slice gaps (I.E., the subject needs to be imaged with either small slice gaps or even contiguous slices) then acquisitions utilizing interleaving or 3D imaging may help reduce or prevent crosstalk artifacts[11]. Interleaving functions by collecting slices in two groups or sets of alternating slices [12]. In other words, if an image series consisted of 10 slices, labeled as slices 1 through 10 in sequential order, an interleaved acquisition would mean that the first set of slices acquired would consist of slices 1, 3, 5, 7, 9 and the second set of slices acquired would consist of slices 2, 4, 6, 8, 10 [12].

3.3.H.III: Gibbs artifact / truncation artifact / Ringing Artifact

Appearance: The Gibbs artifact appears as series of alternating high and low intensity strips or bands around regions that serve as a boundary between bright and dark regions i.e., a high

contrast boundary[11]. This means that the Gibbs artifact can most commonly be seen in anatomical regions of sudden signal intensity change, such as can be seen between bone cortex and marrow [13]. The artifact can also cause distortion around tissues that are close to the high contrast boundary[13]. The distortion can contribute to a false pathology diagnosis, with one of the most well-known examples occurring in the T1 weighted images of the cervical spine, where the Gibbs artifact can be mistaken for syringomyelia [11].

Cause: Gibbs and truncation artifacts are often discussed together and are often described as having similar appearances, some sources describe the two interchangeably, while other sources differentiate them, citing differences in what causes them and differences in the ability of an operator resolve them[13]. The most consequential difference cited between the two, is that truncation artifacts can be resolved, but that Gibbs artifacts are an inherent consequence of using Fourier transformations to create images[13].

Truncation artifacts are generally caused by an acquisition matrix size that is too small and or having a pixel size that is too large[11]. The inappropriate sizing of these elements can inhibit the ability of the MRI to accurately interpret high contrast boundaries[11]. Truncation artifacts generally are seen in the phase encoding direction, which are typically made smaller than the frequency encoding direction to reduce the necessary scan time of a procedure[11].

Alternatively, Gibbs artifacts are a consequence of using Fourier transformations where there is a sudden change in signal intensity[13]. The sine and cosine waves used during the Fourier

transformation are unable to accurately process the sudden change in intensity, resulting in a series of over and under estimations of the true signal intensity, resulting in the distinctive low and high intensity bands[13]. Specifically, the first peak following a high contrast barrier will always overestimate signal intensity, and all subsequent peaks following this first initial peak will more accurately describe the change in signal intensity[13]. This is generally denoted as the Gibbs phenomenon[13]. More gradual changes in signal intensity can be more accurately processed by Fourier transformations, thus explaining why Gibbs artifacts do not occur in all MR images[13]. The consequences of this for MR imaging in practice, is that Gibbs artifacts are a fact of life and cannot be corrected, since typically high contrast boundaries in a phantom or patient cannot be removed, and since the MRI fundamentally relies on Fourier transformations to generate images[13]. Gibb's artifacts are sometimes known as ringing artifacts[12].

Solutions:

1.) Increasing the acquisition matrix size can help reduce the severity of truncation artifacts by decreasing the measured signal difference between different rows of data[13]. A good rule of thumb to follow, is to ensure that the phase encoding matrix is never less than half of the frequency encoding matrix[11]. This solution will have no impact on Gibbs artifacts however, since the above-described Gibbs phenomenon will occur at high contrast boundaries, regardless of the acquisition matrix size used[13].

2.) Decreasing pixel size is another potential solution to truncation artifacts, since smaller pixels will have a greater ability to resolving signal intensity differences[13].

3.) Reconstruction algorithms work to smooth the edges of interfaces, decreasing the severity of both truncation and Gibbs artifacts[13]. However, in cases where a small or reduced acquisition matrix is used, image quality can suffer, as images begin to appear blurry and lose resolution[13].

4.) Another potential solution to truncation artifacts is compensatory low pass filters, which work by removing signal above a certain frequency[13]. However, these filters are unable to correct for the Gibbs phenomenon meaning that they are unable to fix Gibbs artifacts[13]. In certain situations, the use of low pass filters may even increase the severity of Gibbs artifacts[13].

3.3.H.IV: Magnetic field inhomogeneity artifact

Appearance: Tissue/material appears distorted and or appears in the wrong regions of a generated image[12]. These artifacts can also exhibit regions with no signal, or a signal void, with the immediate boundary of these signal voids consisting of high signal bands[12].

Cause: As implied by the name of the artifact, inhomogeneity artifacts arise when the magnetic field is nonhomogeneous, with the underlying complexity of the artifact residing in what causes the inhomogeneity in the first place[12]. Sources of inhomogeneity could be as subtle as makeup on a patient or as fundamental as improper site planning[12]. A non-comprehensive list of potential

sources includes metal implants, dentures, makeup, surgical clips, improper shimming, a magnet with insufficient shielding, and even non ferromagnetic materials[12]. These inhomogeneities induce artifacts by shifting the processional frequencies of protons away from the Larmor frequency[12]. Although this shift only occurs in the immediate area of the inhomogeneity itself[12]. This causes mis mapping, signal voids, distortion, displacement, and a decrease in the amount of time needed for T2 relaxation to occur[12].

Solutions:

1. Proper site planning and the inclusion of features such as automatic shimming, adequate shielding and ongoing maintenance can decrease the overall occurrence of these artifacts[12].

2. Proper screening of patients and any equipment that is present during the scanning procedure can help prevent the introduction of unnecessary and or removable inhomogeneity causing objects.

3. Gradient echo pulse sequences are more sensitive to inhomogeneity artifacts due to protons always orienting themselves in the direction of the inhomogeneities resulting in more severe geometric distortion[12]. However, the use of spin echo pulse sequences can help mitigate these artifacts[12].

3.3.H.V: Magnetic susceptibility artifact and Metal Artifacts

Appearance: These artifacts can take on several different appearances based on the magnetic properties of the artifact causing substance, the quantity of said substance, and the type of pulse sequence employed[13]. Less severe magnetic susceptibility artifacts may have image distortion and a decrease in overall image quality, whereas more severe cases may have regions of no signal around the source of the susceptibility[13]. These signal voids are often bordered with high signal boundaries, which in combination with the void can cause truncation artifacts to occur, due to image misregistration[13]. Pulse sequences that rely on gradient echoes are particularly acute to and suffer from magnetic field distortions, which can result in T2 dephasing[13].

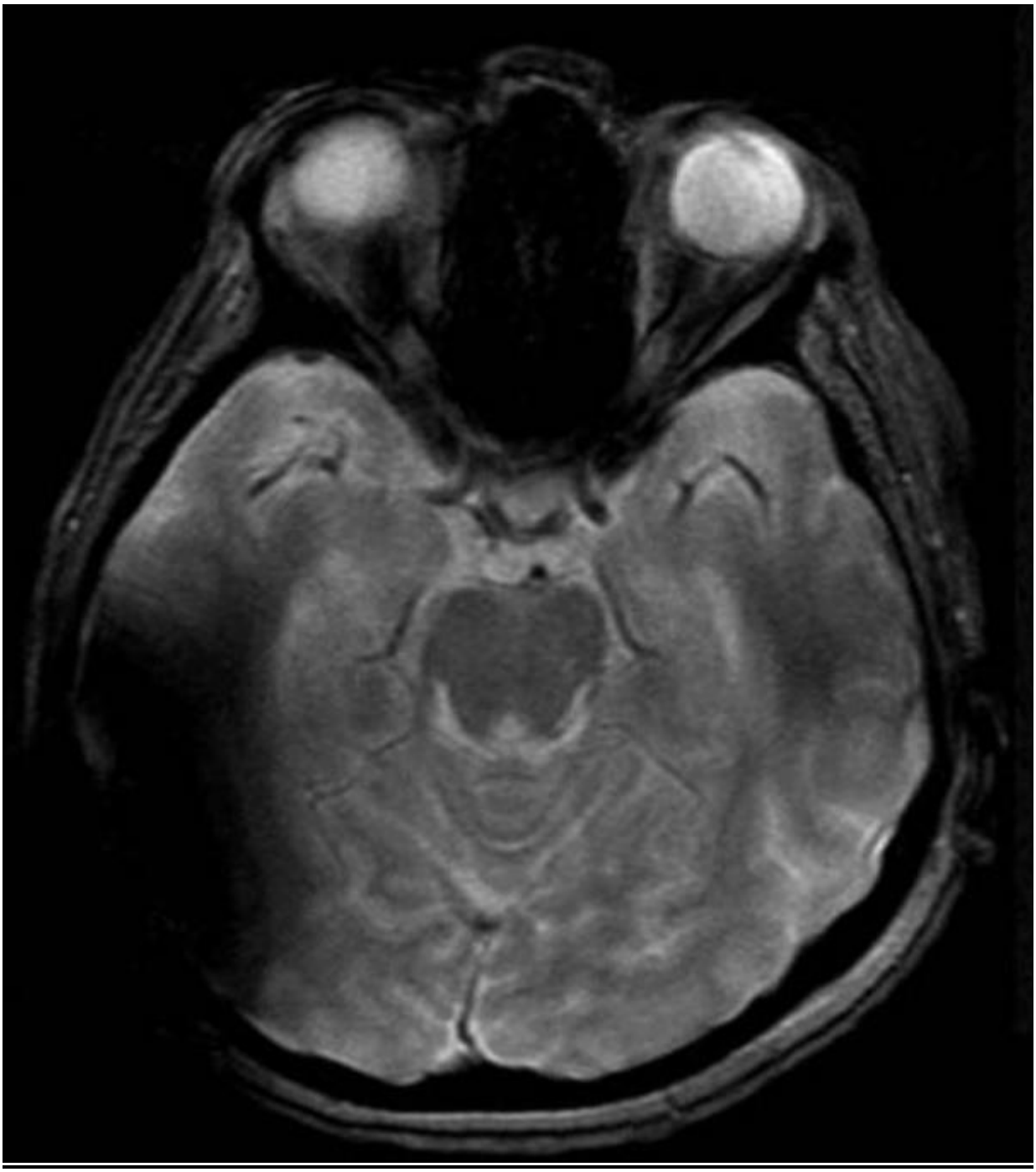

Figure 33: An example photo of a magnetic susceptibility artifact from Katarzyna Krupa and Monika Bekiesińska-Figatowska's article on artifacts in MRI [9].

Causes: Magnetic susceptibility can be thought of as a catchall term that refers to the magnetization experienced by an object within the confines of an external magnetic field[13]. Or alternatively can be thought of in terms of a ratio between an induced internal magnetic field, to an applied external magnetic field[12]. As long as the ratio between the two fields remains reasonably consistent, (I.E., as long as the magnetization experienced by an object within the external magnetic field remains reasonably consistent), then the magnetic field will maintain enough uniformity to prevent artifacts[12]. Simply put, drastic changes in magnetic susceptibility can generate artifacts[12]. Different substances will have varying degrees of induced magnetization / magnetic susceptibility, resulting in different outcomes to exposure to a magnetic field[13]. Some sources differentiate metal and magnetic susceptibility artifacts. Generally speaking, metal induced susceptibility artifacts are more severe, causing signal voids, high signal edges and greater geometric distortion than non-metal susceptibility artifacts which may have just a reduced signal region instead of a signal void[11]. Metal can further be differentiated by the fact that it serves as an efficient conductor of RF energy, creating a potential hazard to patients as the metal heats up during conduction[11]. Another layer of added complexity is that gradient magnetic fields can generate an electrical current, which in turn can generate an internal magnetic field that distorts the applied external magnetic field[13]. This effect can even be observed in materials with no magnetic properties at all[13].

Solutions:

1. Proper screening of patients and staff is paramount, not just for patient and staff safety, but also to ensure that magnetically susceptible material is not introduced into the MR environment[13]. Make sure that patients are in MR compatible clothing that does not have

any susceptibility properties that could generate an artifact[13]. Check for any cosmetics that could be potentially dangerous in the high field environment or that could degrade image quality such as jewelry, self-tanning lotion, make up, and hair accessories[13].

2. While not a foolproof solution, using a very short TE can reduce but not remove susceptibility artifacts from a generated image[11].

3. Some patients may have metal implants or magnetically susceptible objects that cannot be removed for a scan[13]. If this is the case, and if the objects will not cause any harm to the patient, staff or equipment, then modifications should be made to the pulse sequences used to generate images[13]. Gradient echo-based pulse sequences and pulse sequences that utilize a narrow bandwidth are more sensitive to magnetic susceptibility and can worsen susceptibility artifacts[13]. Spin echo-based pulse sequences are less sensitive to susceptibility artifacts and are better suited for this type of imaging[13]. This solution is also advised in cases of severe metal artifacts[11].

3.3.H.VI: Zipper artifact / Radio-frequency artifact

Appearance: The zipper artifact appears as a distinct line, a couple of pixels wide, with alternating high and low signals, creating a "zipper" like appearance[11]. The zipper runs in the

phase encoding direction, typically in the center of the FOV [11]. Occasionally, there may be more than one zipper placed at regular intervals across the image [11].

Causes: Zipper artifacts are caused by some form of radiofrequency radiation making its way into the MR scanner room, and subsequently being detected by the receiver imaging coils of the scanner[11]. More specifically the RF radiation that is detected must be within the operational frequency used by the MR system[12]. But since some of the most common RF signals generated (TV, radio, computers) occupy that same frequency, a MR system left shielded would almost undoubtedly be riddled with artifacts[12]. To prevent this, the vast majority of scanner rooms use metal shielding to create a faraday cage around the scanner, preventing device external RF radiation from reaching the scanner [13]. The presence of a zipper artifact implies that the faraday cage has, in some form, been bypassed, by either a breach in the cage itself, or by an object that produces RF radiation being brought into the scanner room [11]. Zipper artifacts are often credited with being the result of a narrow band RF pattern, whereas a board band RF pattern is often credited with causing a herringbone artifact [12].

Solutions:

1. The first potential solution is the most obvious, but also the vaguest. The operator should check for any RF sources. The first thing to check is that the door leading into the scanner room was fully closed during scanning[13]. Assuming that the door was closed, then check for other potential sources such as electronics that have been bought into the scanner room, or electronics in the room that haven't been turned off[13]. A common culprit is

anesthetic monitoring equipment, which utilizes metallic leads that go through waveguides into the scanner room[11]. These leads can sometimes pick up and transmit RF signals they are exposed to outside of the faraday cage, through the waveguide and into the scanner room[11]. The operator should check to ensure that all the electronic equipment being utilized is MR compatible[11]. If any electrical equipment must stay in the room during imaging, it should be verified to have adequate RF shielding[13]. Additionally, if a patient is being scanned, it should be ensured that the patient is in clothing that is incapable of producing RF artifacts[13]. 100% cotton clothing would be ideal for reducing the likelihood of zipper artifacts[13].

2. If the first solution is not successful in resolving the artifact, then the operator should next verify that all the electronic equipment in the scanner room uses direct current, and not alternating current[13]. Alternating current fluctuations can create RF artifacts[13]. Note that this check should also include the types of lightbulbs used[13].

3. If no solutions are resolving the problem, or if it is suspected that the RF shielding of the room itself is compromised (if this is the case zipper artifacts should appear consistently in every obtained image) then a service engineer should be called in[11]. The service engineer will be able to perform more extensive testing to determine what the potential source of the RF artifact is[13].

3.3.I: visual checklist

The ACR MRI QC Manual advises that the qualified medical physicist performing the annual evaluation of the scanner go through and fill out the ACR MR Accreditation visual checklist[5]. The visual checklist (which is attached as appendix 2) consists of 16 separate visual assessments of the scanner, scanner equipment and scanner facility design. To summarize, the 16 tests are: table position displays/electronic readouts, alignment light functionality, horizontal and vertical gantry transportation smoothness and stability[14]. Laser camera and light box functionality[14.] The presence of undamaged RF door contacts and RF window screens[14]. Functionality of a patient monitor, patient intercom, a room temperature and humidity readout system, and operator control console[14]. A functional emergency cart (or patient couch release system) [14]. The presence of a cryogen level indicator[14]. The presence of safety warning signs and a door indicator switch[14]. A few notes must be made in regard to how this visual checklist was performed in the course of this project. There are two entrances to the scanner room itself. A main entrance accessible through the scanner control room and a "back" entrance which attaches to the brachytherapy suite. Both entrances were evaluated according to the visual checklist guidelines. Additionally, the MR-SIM utilized an emergency couch release instead of an emergency cart. Lastly, the scanner had no light boxes, laser cameras, or door indicator switch and as such these items were ignored when conducting this QA procedure.

3.3.J: Monitor

As outlined in TG-18, the performance evaluation of any monitor used to display medical images falls within the range of responsibilities of the medical physicist[15]. Monitor (sometimes referred

to as soft copy) QC is extensively explored in TG-18 and in DICOM part 14, and minimum recommendations regarding MR monitor QC as a part of annual evaluation is explored in the ACR MRI QC manual[5]. If the performance of a monitor is not properly evaluated and sources of error determined and corrected for, image quality may suffer even on a well-functioning MR scanner[15]. Therefore, the set of monitor QC tests advised as a minimum standard of monitor evaluation under the ACR MRI QC manual were adopted and incorporated into the annual evaluation procedure[5]. To perform this test, the operator displayed the SMPTE pattern image on the monitor (this image was already saved on the control terminal and could be found by searching through the scan history) and utilized a NIST traceable luminance meter to obtain luminance measurements[5].

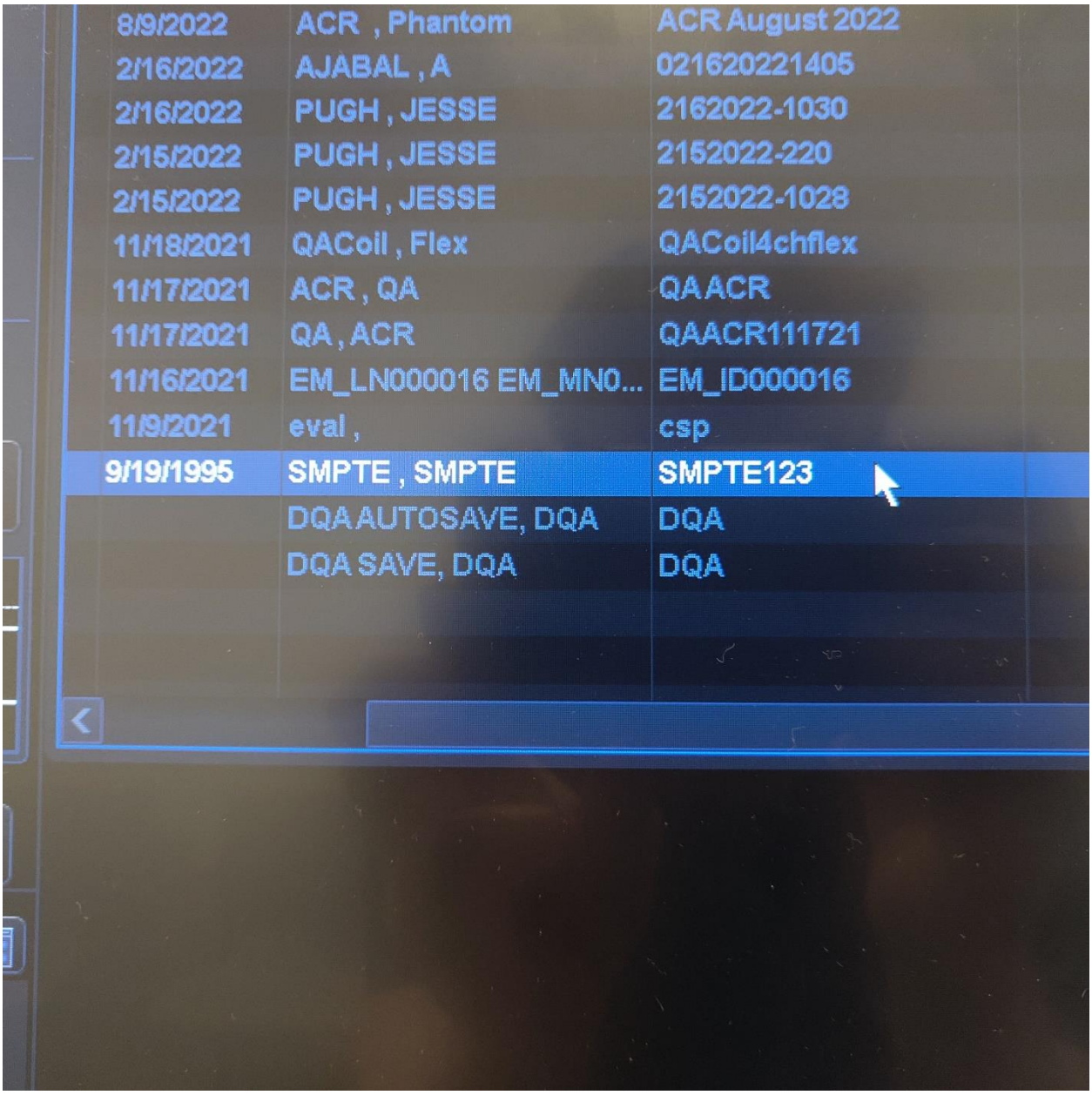

Figure 34. Photo of the scanner terminal with the patient name of the SMPTE pattern selected. Please note that the "patient date" for the SMPTE pattern "occurred" decades before the scanner was even installed. This allowed for the pattern to be located quickly since no other scans were listed as having occurred during 1995.

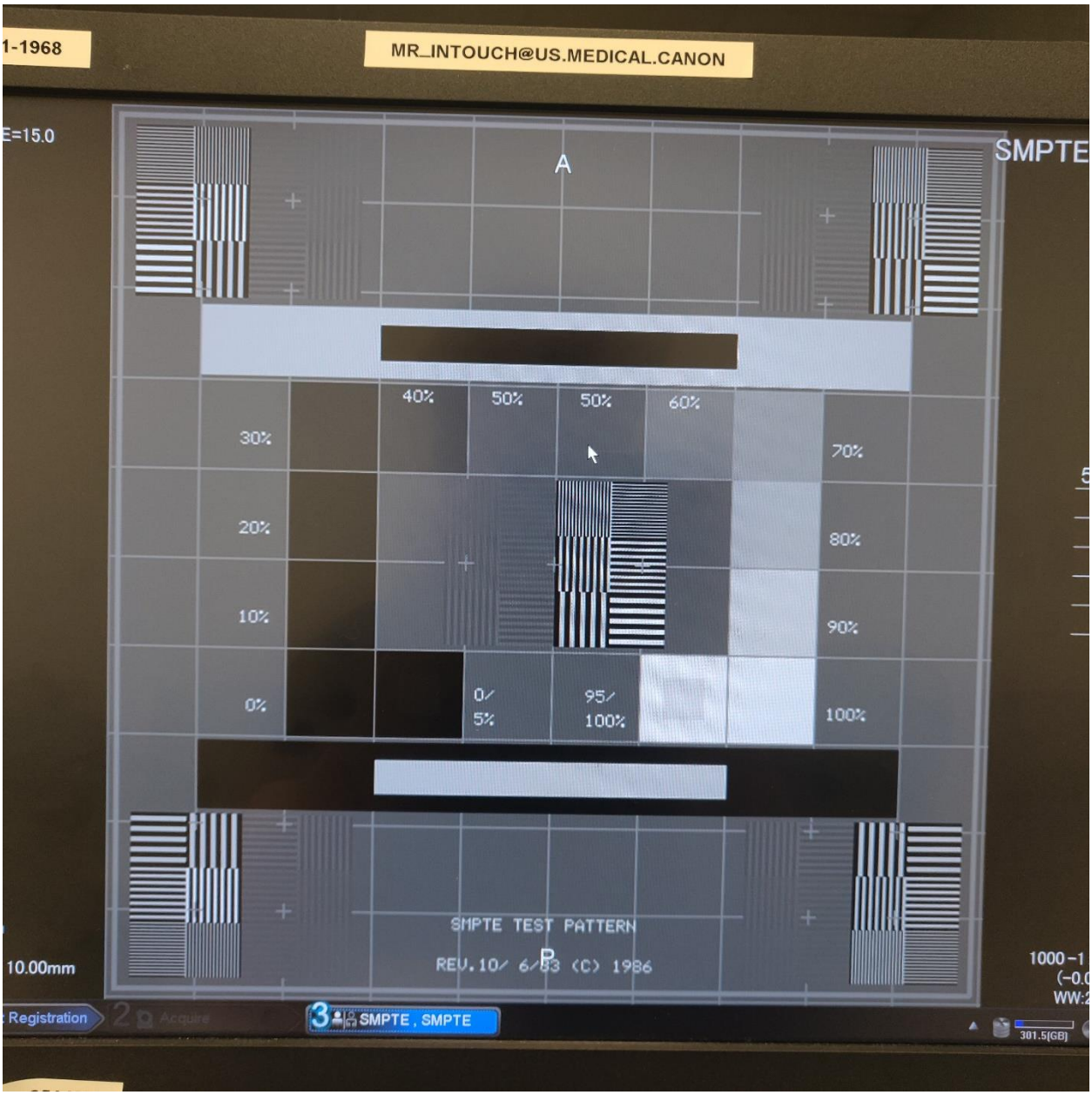

Figure 35. A photo of the scanner control terminal with the SMPTE pattern on display.

3.3.J.I: Maximum luminance

The maximum luminance of the monitor was measured utilizing the NIST traceable luminance meter[5]. Maximum luminance measurements were all expected to exceed 90 cd/m^2 in order to be considered passing [5].

3.3.J.II: Minimum luminance

The minimum luminance of the monitor was likewise measured with the NIST Traceable luminance meter [5]. Minimum luminance measurements were only considered passing if they all fell under 1.2 cd/m^2 [5].

3.3.J.III: Luminance uniformity

The luminance uniformity of the monitor was calculated using equation 11 [5]. In the context of equation 11, L_{max} was the brightest measurement obtained when measuring maximum luminance, and L_{min} was the dimmest measurement obtained when measuring maximum luminance [5].

$$\text{Eqn. 11: \% difference} = 200 \text{ x } \frac{Lmax-Lmin}{Lmax+Lmin}$$

To be considered passing the % difference could not exceed 30% [5].

3.3.J.IV: Visual assessment tests

The last portion of the monitor QC procedure was to perform a series of visual inspections of the SMPTE pattern [5]. The visual inspections were as follows [5]. Both the 0-5% and the 95-100% contrast patterns were visible [5]. Additionally, each of the steps from 0% to 100% for the gray level step pattern were discernible from the last and the next in the pattern [5]. There were no distortions of the grid in the SMPTE pattern, and the lines and borders of the pattern were all straight [5]. All of the line pairs in the pattern were distinct without any magnification applied [5]. The white and black rectangles present in the pattern were streak free [5]. And lastly the alphanumeric characters present in the pattern were clear and legible [5]. These visual assessment tests are sometimes referred to as the resolution, linearity, contrast, and distortion tests [5].

3.3.K: Safety program

As a part of the annual evaluation of the MR-SIM, the safety program of the facility was evaluated by a qualified medical physicist or MRI scientist as per the recommendations of the ACR [5]. The physicist examined the safety program and ensured that they met the satisfactory standards set out by the ACR. These standards include that the safety policies and procedures of the facility are written out, are available to staff, are reviewed on a regular basis and that they are updated [5]. Furthermore, that MR personnel receive regular training and that this training is documented [5]. The physicist also confirmed that the facility has adequate safety signs and warnings around the facility, and that access across the facility was monitored and controlled [5]. The ACR specifically advises that the written safety policies and procedures address all of the following concerns: “Designated MR medical director, site access restrictions (MR zones),

documented MR safety education/training for all personnel, patient and non-MR personnel screening, pediatric patients, magnet quench, cryogen safety, acoustic noise, pregnant patients and staff, contrast agent safety, sedations, thermal burns, emergency code procedures, device and object screening, designation of MR safe/MR conditional status, reporting of MR safety incidents or adverse incidents, patient communication, infection control and medical waste" [5].

4. Results

4.1 Daily QA Results

As discussed earlier in the daily QA cube phantom portion of this text (section 3.1.A), the basic parameters recorded as a part of the daily QA procedure were periodically transcribed to a digital record for long term performance trend tracking. For the purposes of this project, only the measurements obtained from December 1st, 2021 up until March 3rd, 2023 were considered. Many parameters such as RF level (see figure 36) and Receiver gain (see figure 37) demonstrated overall stability over time with minor fluctuations seen occurring day to day. Center frequency (see figure 38) has remained remarkably consistent, predominantly holding at a value of 123.196 MHz.

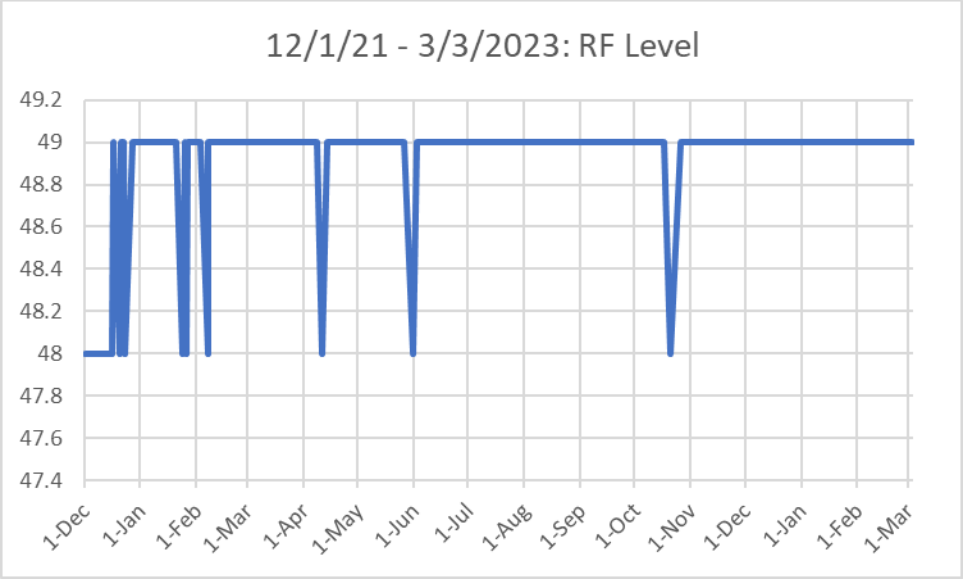

Figure 36: Plot of the RF level results for the DQA from 12/1/21 to 3/3/2023.

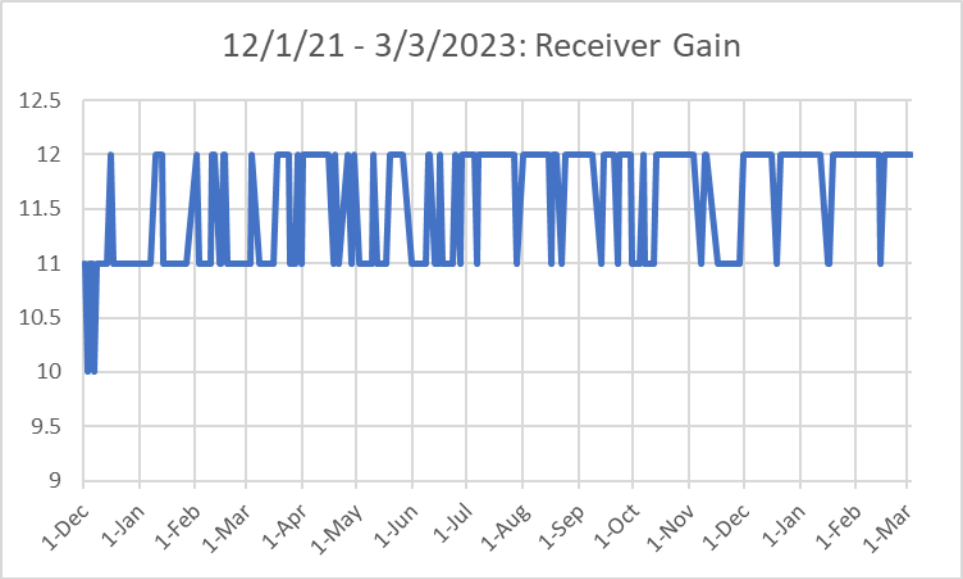

Figure 37: Plot of the receiver gain results for the DQA from 12/1/21 to 3/3/2023.

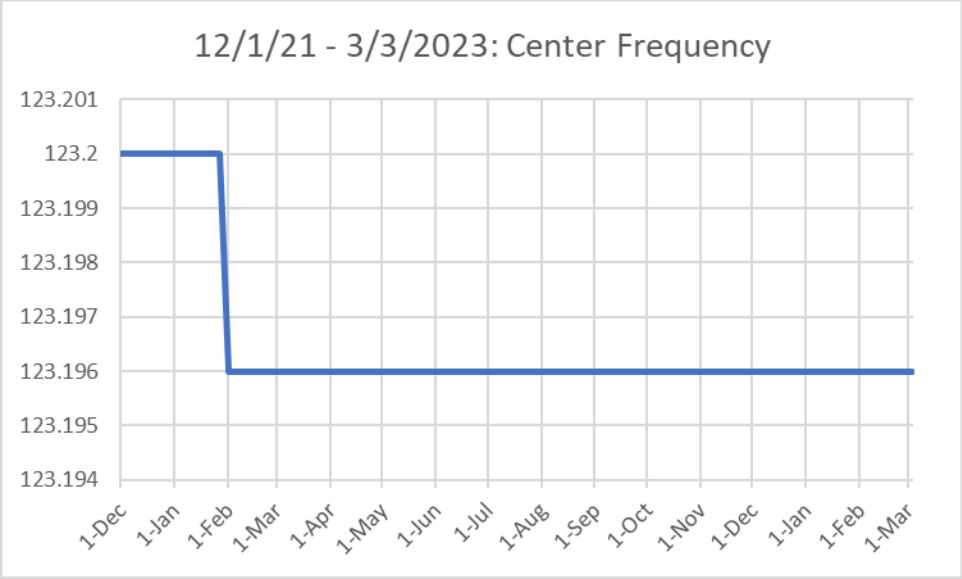

Figure 38: Plot of the center frequency results for the DQA from 12/1/21 to 3/3/2023.

Helium levels, likewise, demonstrated overall stability, with the notable exception of the January 25th, 2023, measurement, which shot upwards to a value of nearly 95% (see figure 39). However, if the January 25th measurement is considered an outlier and is removed from the data pool, helium levels demonstrate much more stable behavior, fluctuating within the range of 84.4% - 84.7% (see figure 40).

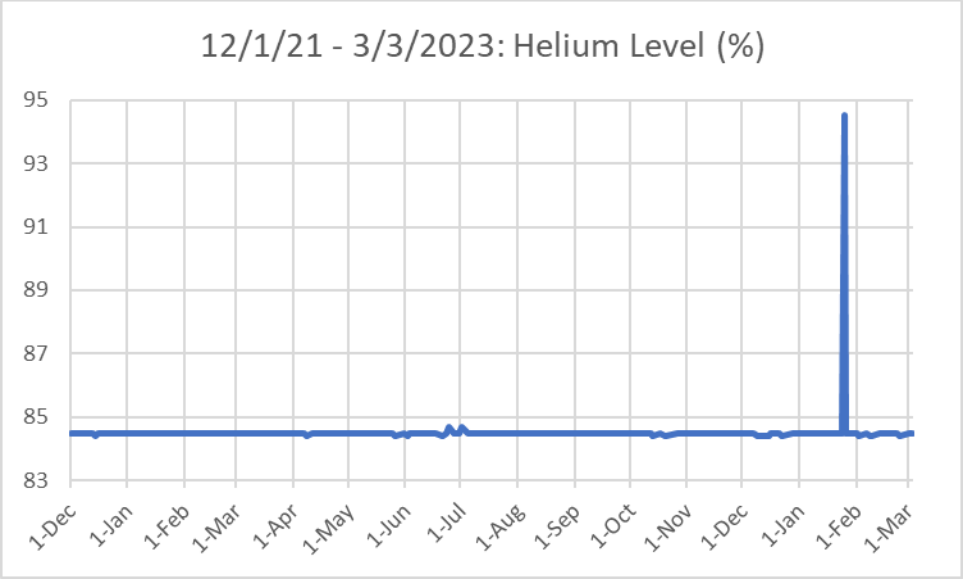

Figure 39: Plot of the helium level results for the DQA from 12/1/21 to 3/3/2023.

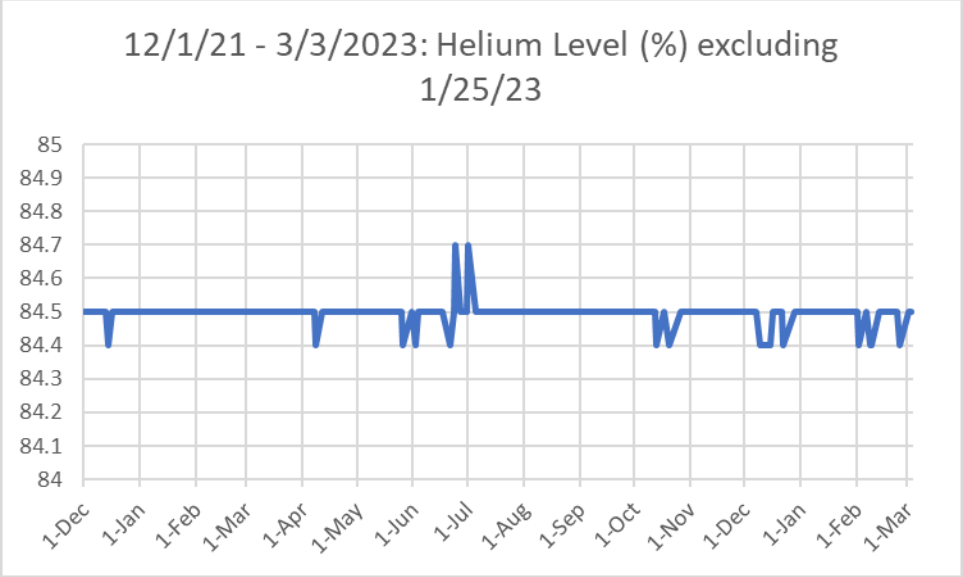

Figure 40: Plot of the helium level results for the DQA from 12/1/21 to 3/3/2023, excluding the large outlier value from 1/25/23.

The overall trend of the daily percent SNR measurements can be seen in figure 41 and is further broken down into its constituent components with the trend for signal value in figure 42, the trend for signal standard deviation in figure 43, the trend for noise value in figure 44, and the trend for noise standard deviation in figure 45. While figure 41 indicates an overall decrease in system percent SNR overtime, it also includes data from the outlier measurement that occurred on January 25th, 2023. If this measurement is removed (see figure 46) the downward trend becomes less severe. Furthermore, figure 41 and figure 46 demonstrate that percent SNR decreases during December 2021 before stabilizing in the following months. If the December 2021 measurements and the outlier measurement are both removed, the percent SNR of the scanner is seen to be much more stable over the examined period of time, suggesting an initial period of percent SNR decrease, before performance stabilized (see figure 47). Lastly, a month-by-month breakdown of percent SNR can be seen in figures 48 to 62.

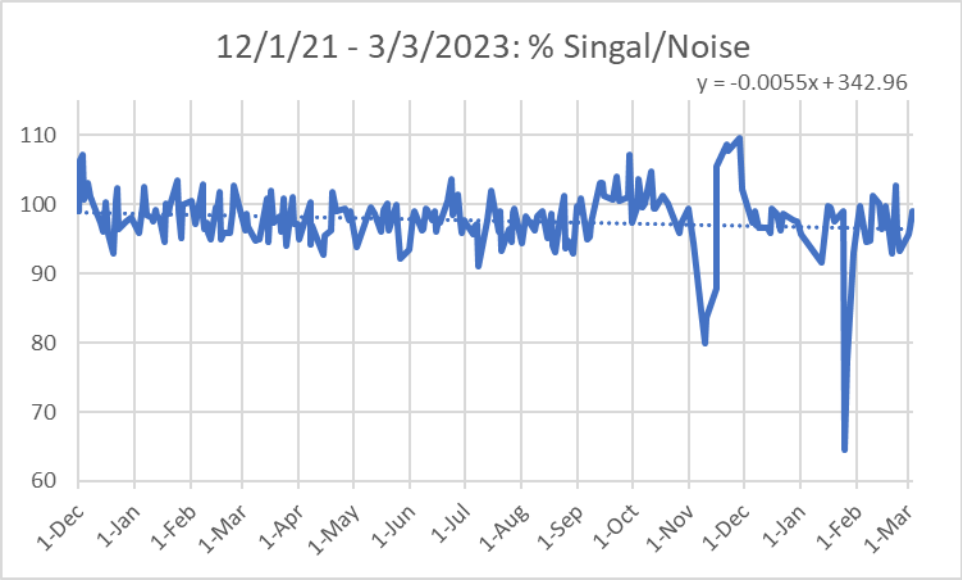

Figure 41: Plot of the % SNR results for the DQA from 12/1/21 to 3/3/2023. Note the downward trendline.

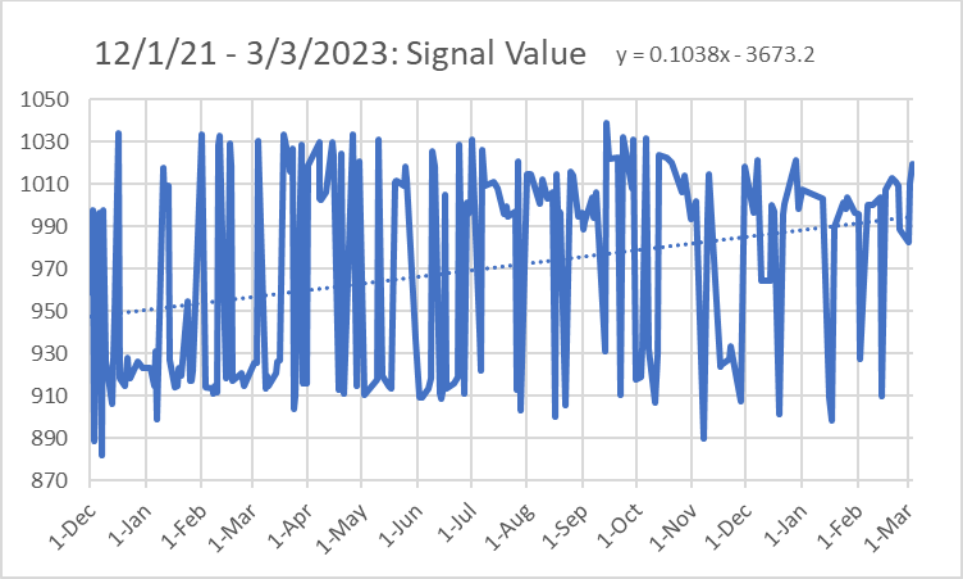

Figure 42: Plot of the signal value results for the DQA from 12/1/21 to 3/3/2023.

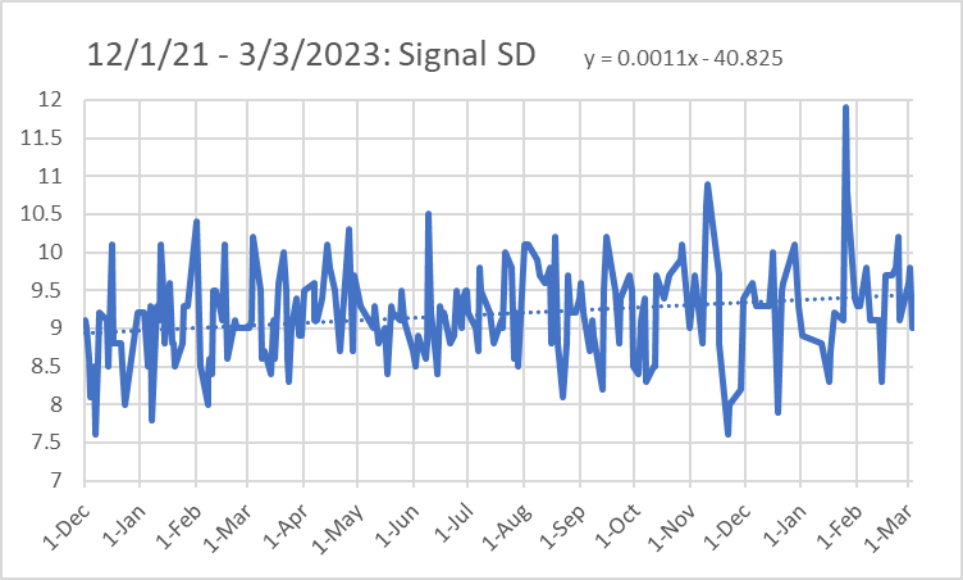

Figure 43: Plot of the signal standard deviation results for the DQA from 12/1/21 to 3/3/2023.

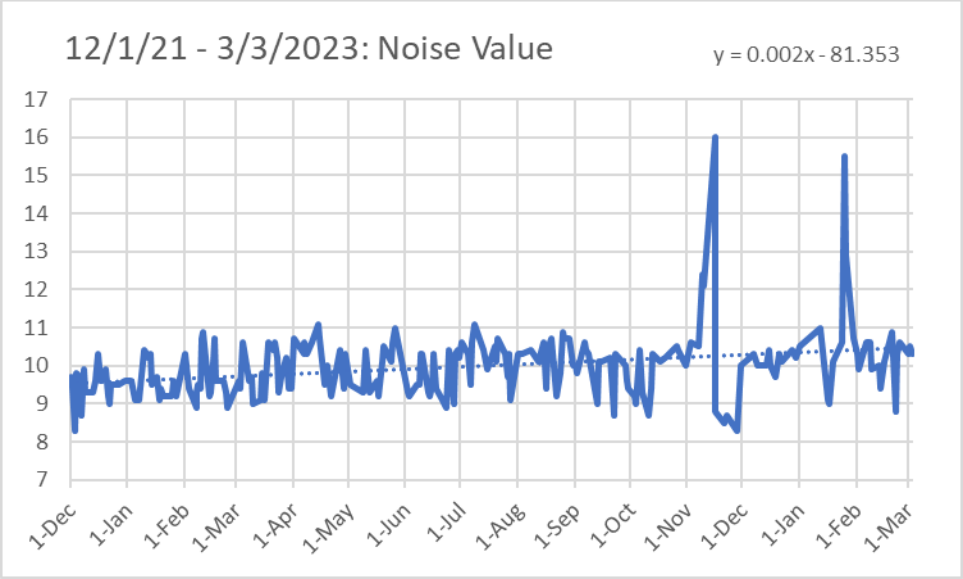

Figure 44: Plot of the noise value results for the DQA from 12/1/21 to 3/3/2023.

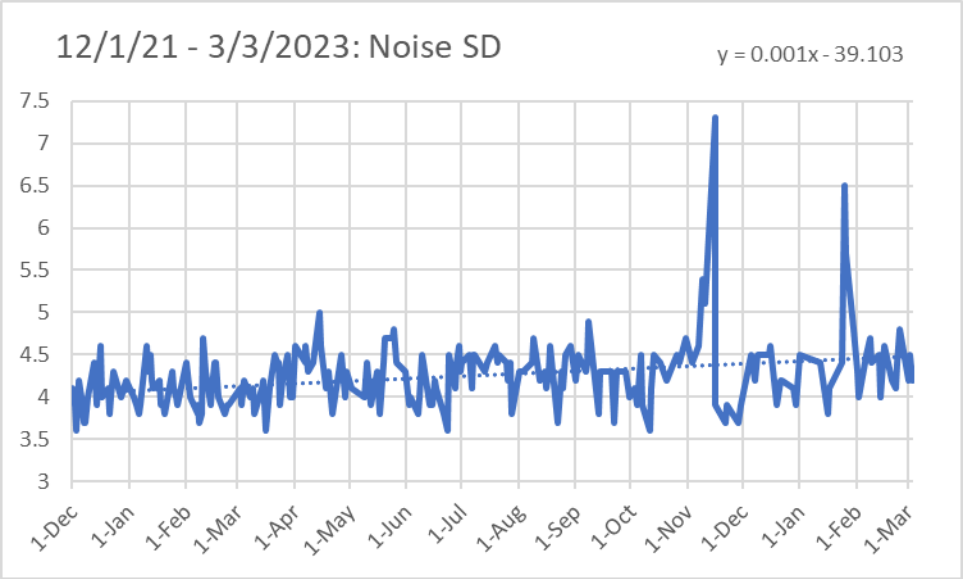

Figure 45: Plot of the noise standard deviation results for the DQA from 12/1/21 to 3/3/2023.

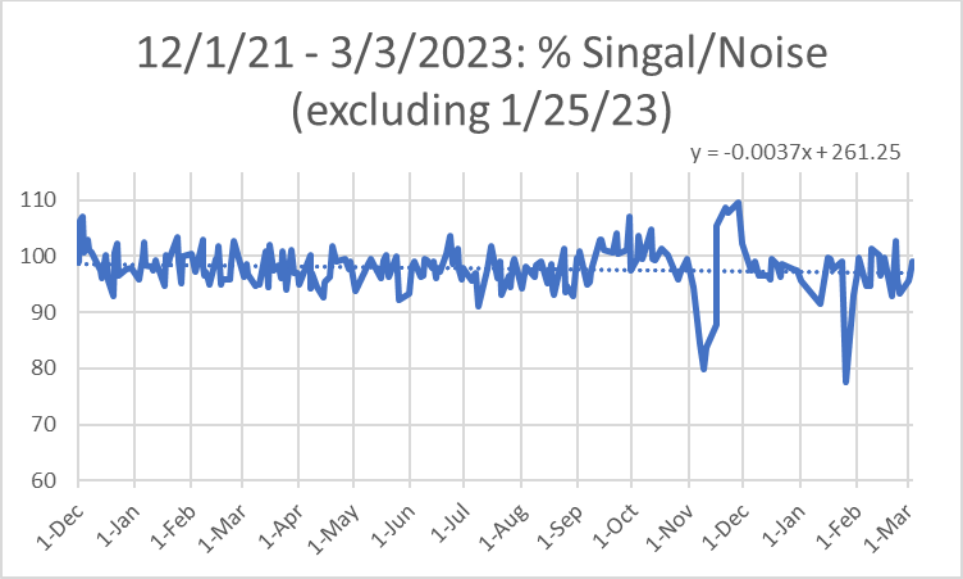

Figure 46: Plot of the % SNR results for the DQA from 12/1/21 to 3/3/2023, excluding the most extreme outlier point of data of 1/25/23. Note that the downward trendline / slope is less severe than in figure 41.

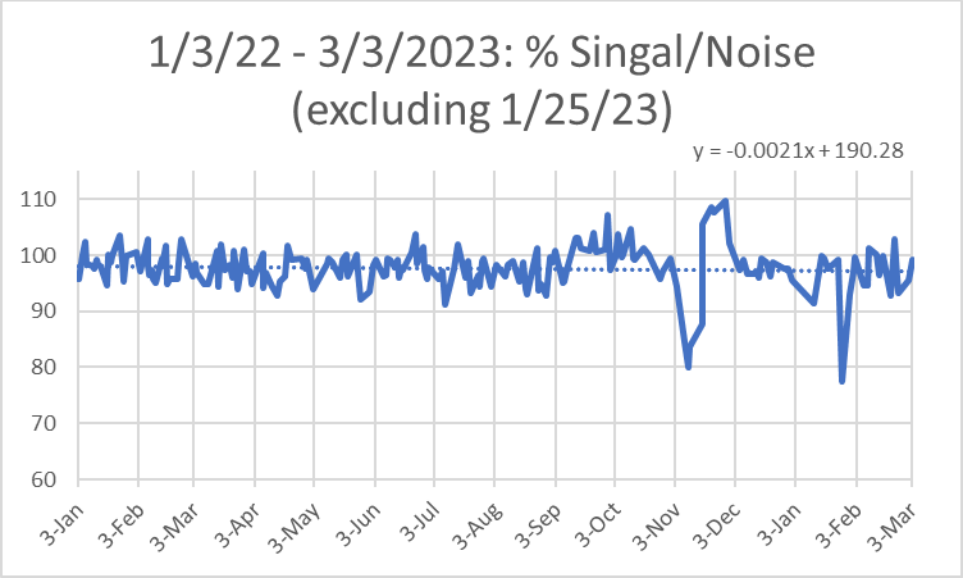

Figure 47: Plot of the % SNR results for the DQA from 1/3/22 to 3/3/2023 (I.E, excluding the first month of operation), excluding the most extreme outlier point of data of 1/25/23. Note that the downward trendline / slope is less severe than in figure 41 and 46.

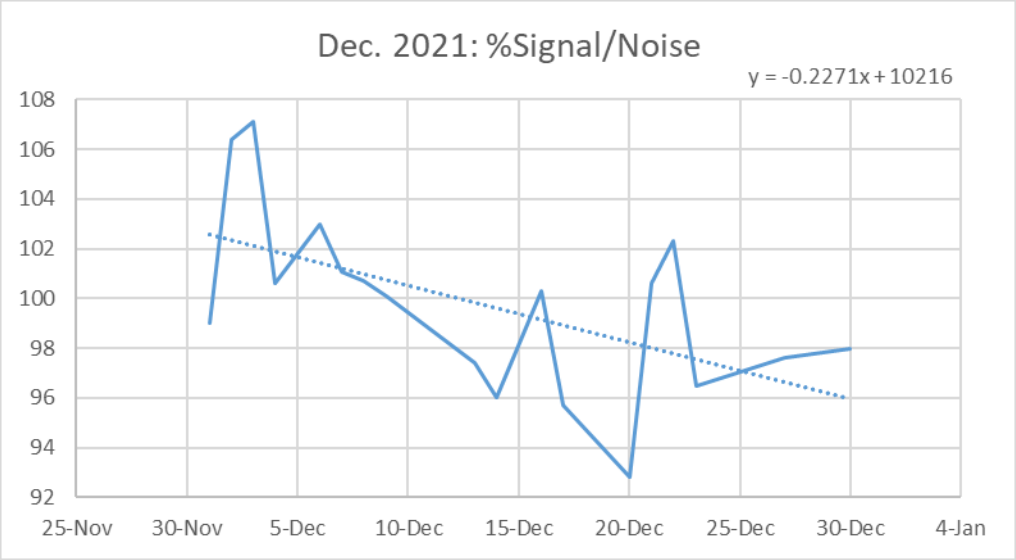

Figure 48: Plot of the percent SNR results for the DQA for December 2021.

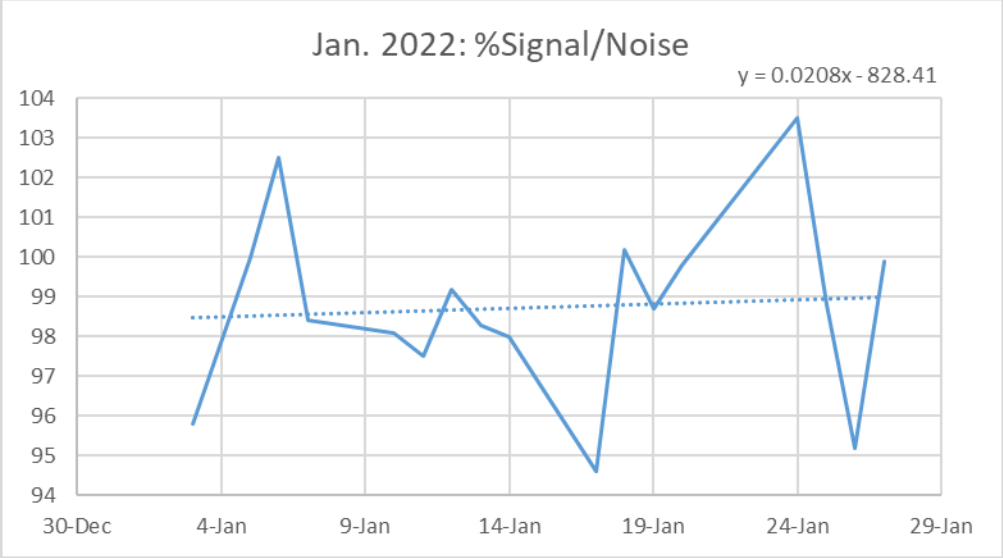

Figure 49: Plot of the percent SNR results for the DQA for January 2022.

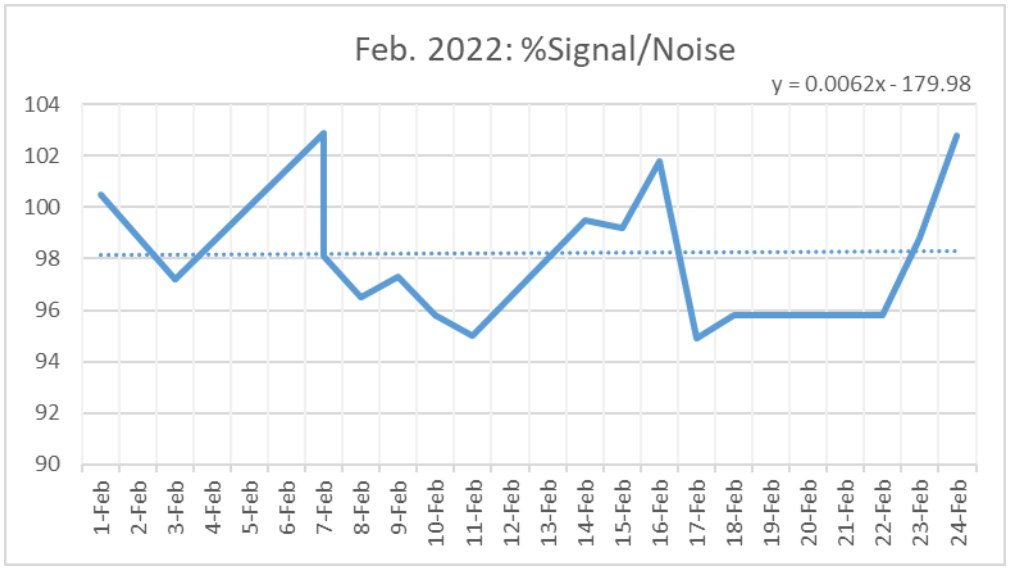

Figure 50: Plot of the percent SNR results for the DQA for February 2022.

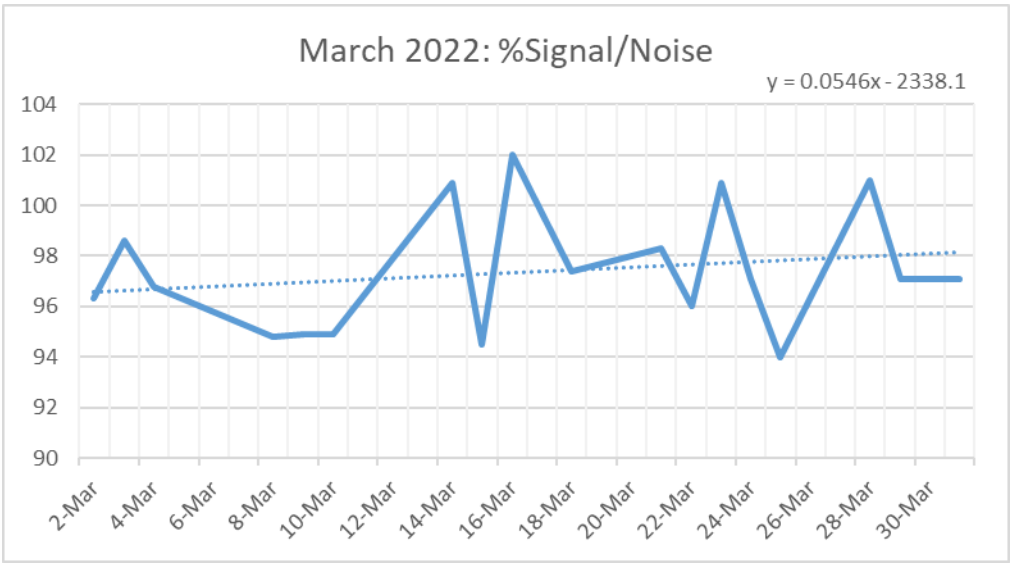

Figure 51: Plot of the percent SNR results for the DQA for March 2022.

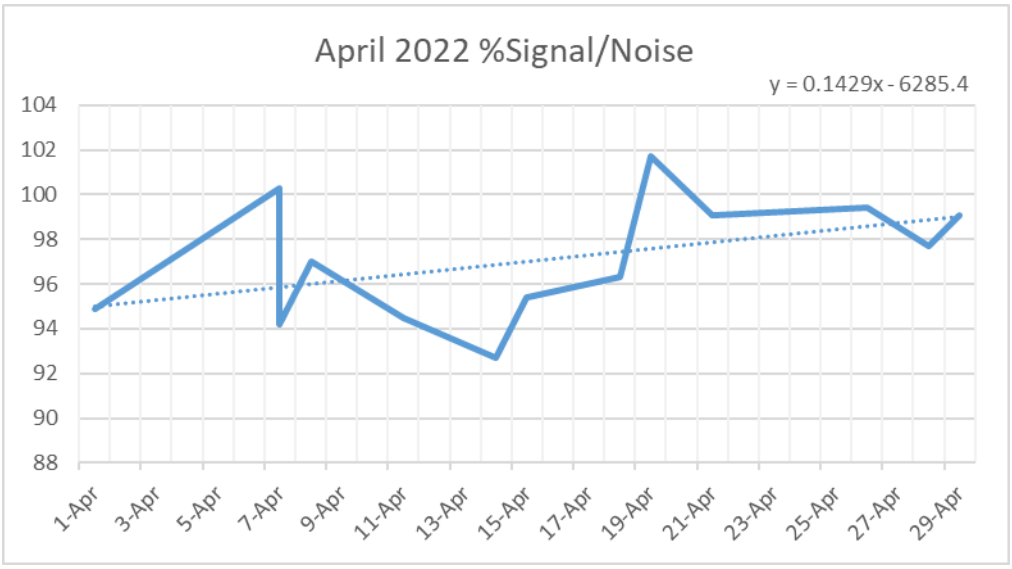

Figure 52: Plot of the percent SNR results for the DQA for April 2022.

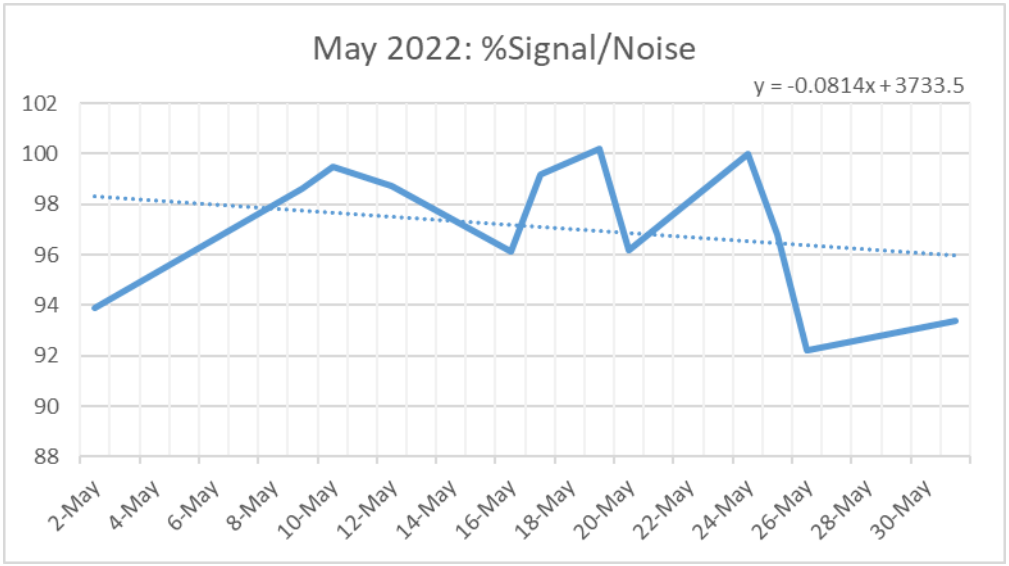

Figure 53: Plot of the percent SNR results for the DQA for May 2022.

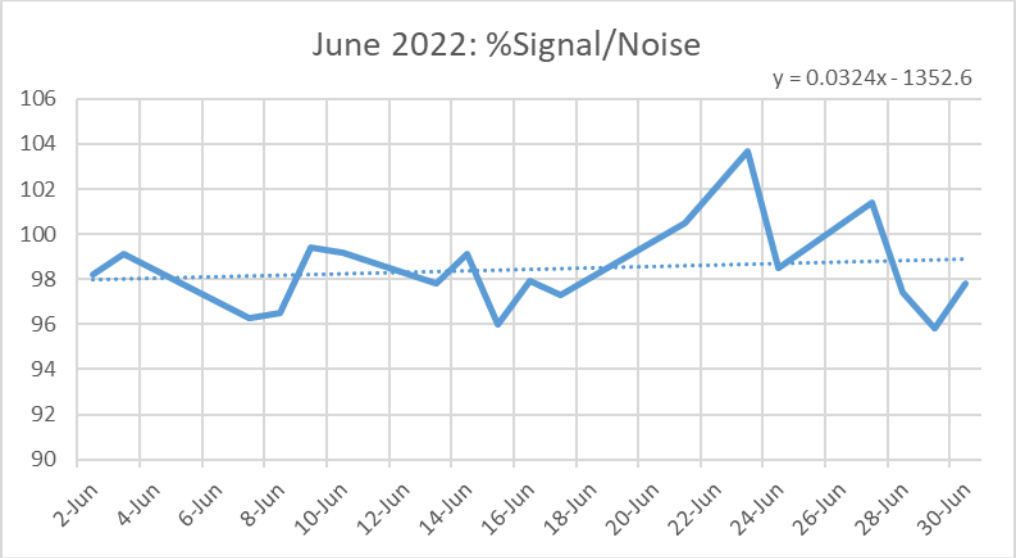

Figure 54: Plot of the percent SNR results for the DQA for June 2022.

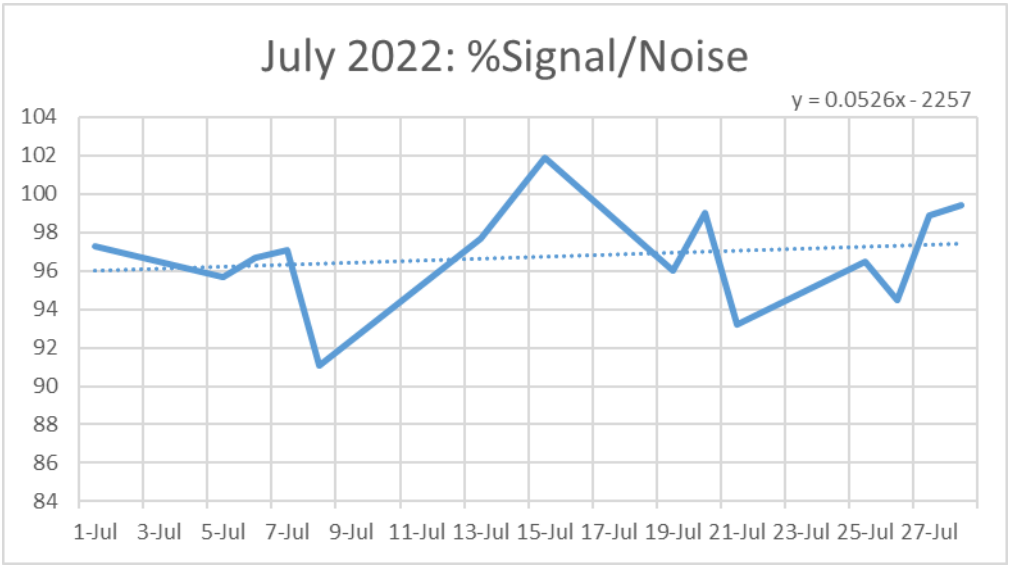

Figure 55: Plot of the percent SNR results for the DQA for July 2022.

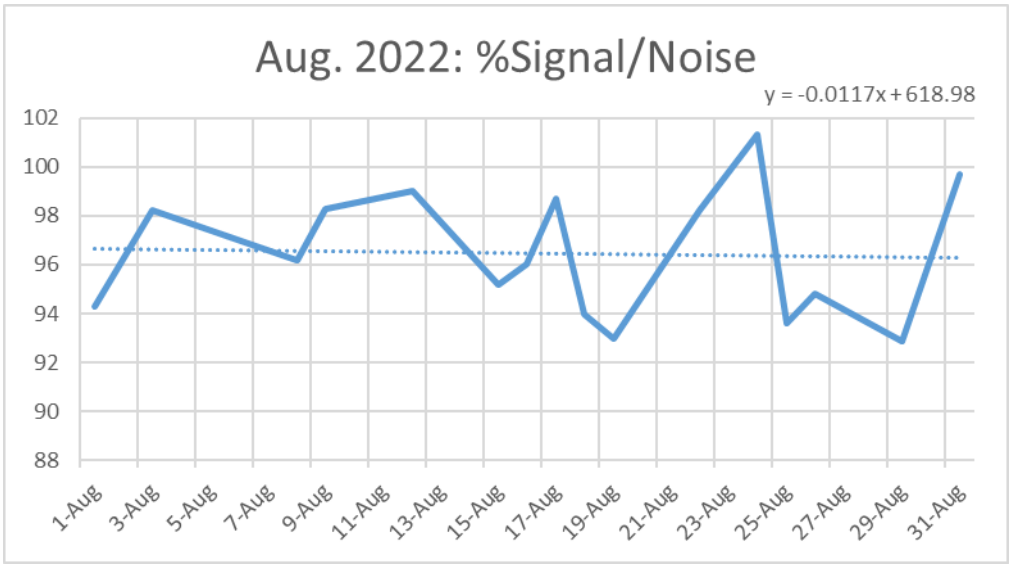

Figure 56: Plot of the percent SNR results for the DQA for August 2022.

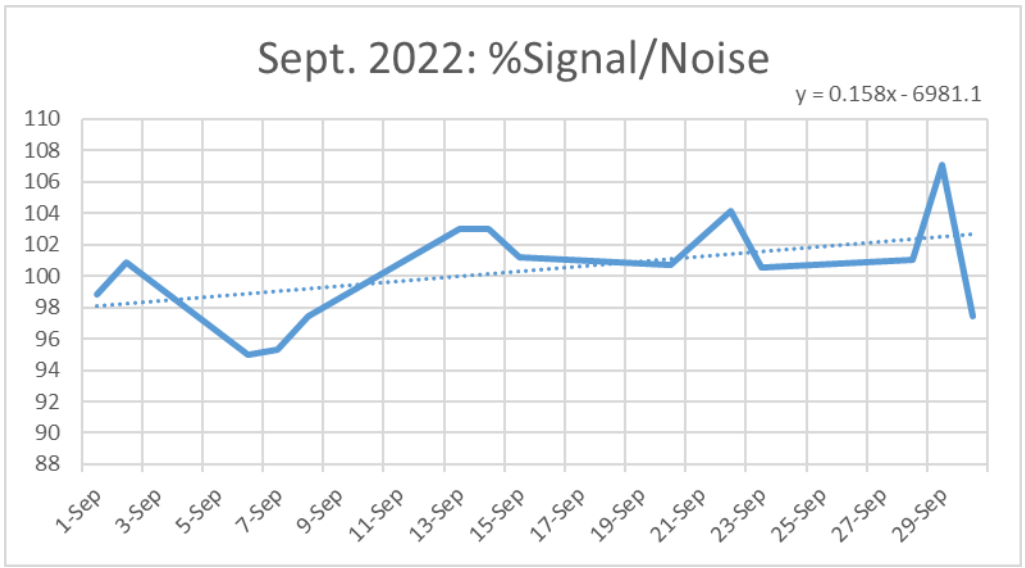

Figure 57: Plot of the percent SNR results for the DQA for September 2022.

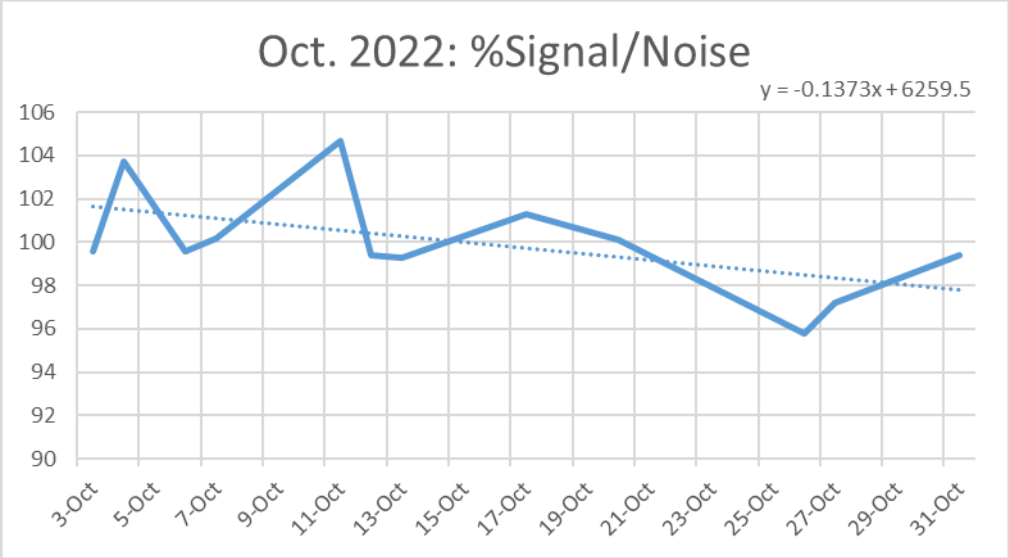

Figure 58: Plot of the percent SNR results for the DQA for October 2022.

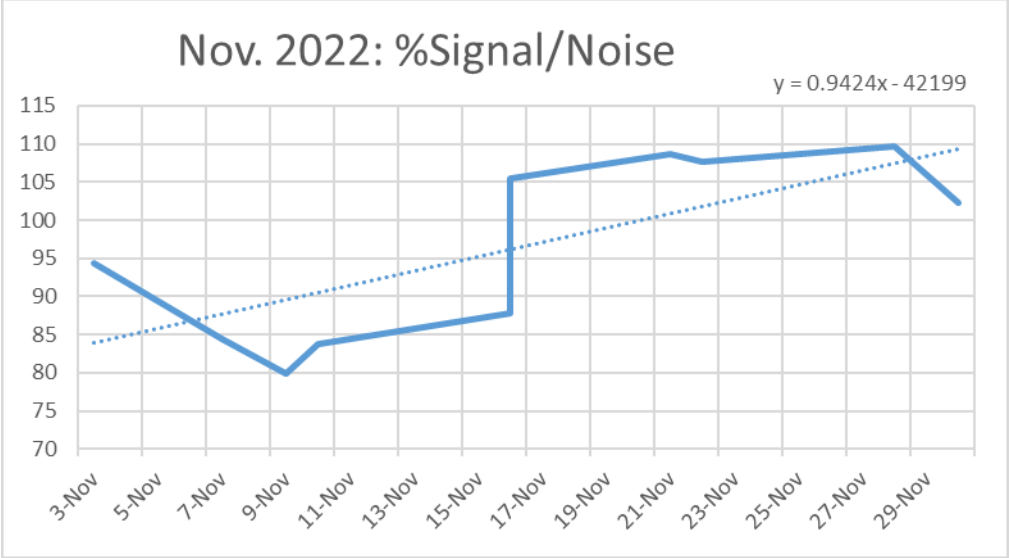

Figure 59: Plot of the percent SNR results for the DQA for November 2022.

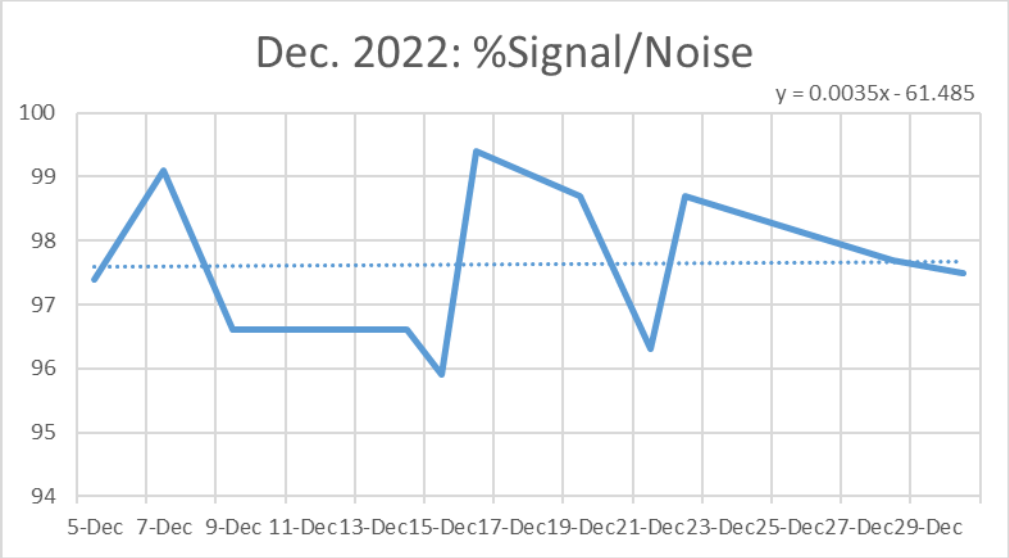

Figure 60: Plot of the percent SNR results for the DQA for December 2022.

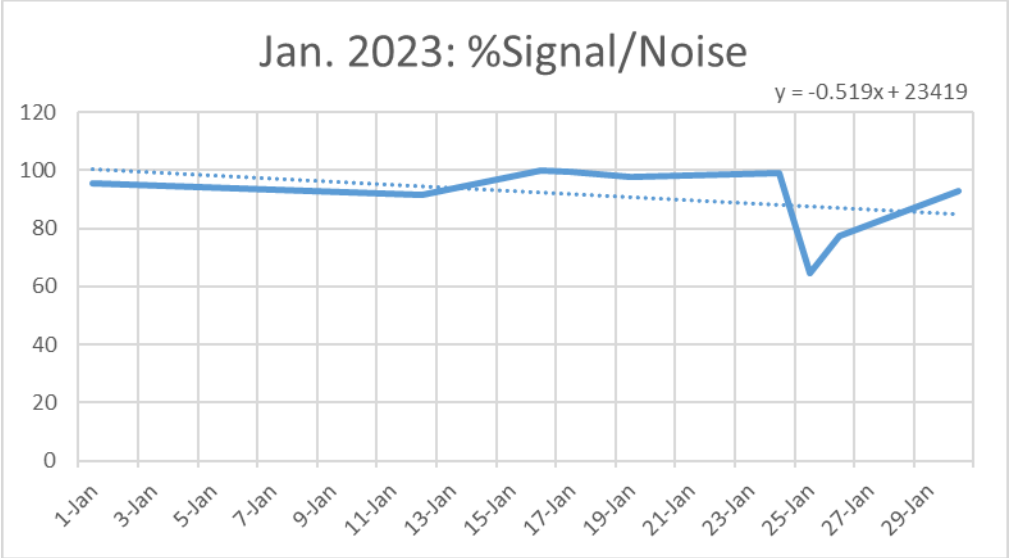

Figure 61: Plot of the percent SNR results for the DQA for January 2023.

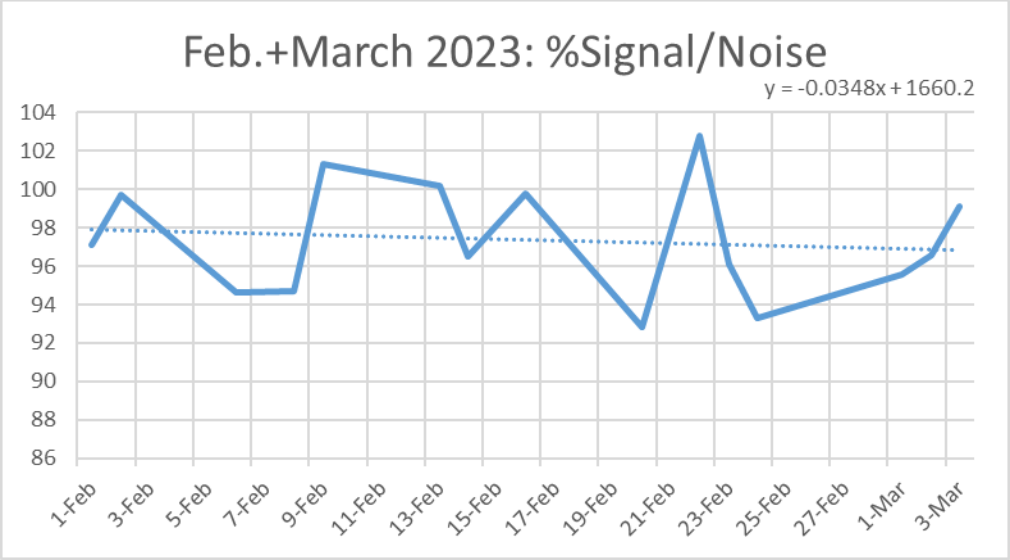

Figure 62: Plot of the percent SNR results for the DQA for February and March 2023. These two months are combined because only the first three days of march are considered in this data set, which is too small an amount of data to meaningfully examine on its own.

4.2 Monthly QA results

The incorporation of the ACR image quality tests, basic mechanical checks and vendor support coil QA has gone smoothly and demonstrated consistent and satisfactory results. However, the incorporation of the MagPhan RT phantom is more nuanced, with test results varying drastically depending on the pulse sequence utilized and the orientation of the phantom.

4.3 Annual QA results

As of the time of this writing, the MR-SIM has only undergone a single annual evaluation. While the scanner demonstrated satisfactory results, it is difficult to draw meaningful conclusions regarding the long-term performance of the scanner based on such limited data.

5. Discussion

The incorporation of daily QA procedures has enabled long term tracking of system performance parameters. From the daily QA data examined in the results section (section 4.1) it can be seen that after an initial drop in percent SNR during December 2021, basic system performance parameters remained relatively stable throughout the duration of this project with the noted exception of an outlier measurement on January 25th, 2023. The large variation in MagPhan results depending on the pulse sequence and orientation of the phantom can often be confusing, as each combination of sequence and orientation has its own performance results that would be deemed "normal." This inherent variability in results does not negate the usefulness of the MagPhan phantom but does require additional special care when analyzing QA results.

6. Future directions

Incorporating additional recommended QA tests could potentially create a program that is more effective at detecting shortcomings in the imaging chain. Furthermore, a quality assurance program should not be static, but adjust based on the evolving needs of the site. One of the tests that could be incorporated into the QA program in the future is a daily geometric distortion test. TG-284 advises a daily geometric distortion test / basic spatial fidelity test that assesses distortion across a 25cm FOV and verifies that distortion does not exceed 2mm [3]. This test cannot be performed on the daily QA cube phantom due to it being an inadequate size. I.E., too small. This test could potentially be performed utilizing the MagPhan RT phantom, but would require training technicians to scan the phantom and generate reports using MagPhan vendor

propriety analysis software. An alternative solution for the daily distortion check could be to coordinate with the MR scanner vendor to determine if a vendor phantom exists to perform the test. Another future direction that should be incorporated into the QA program is further refining the DWI QA procedures by determining a range of results that constitute action performance criteria. Lastly, additional geometric distortion analysis techniques and performance criteria should be considered if the images obtained are to be used for stereotactic radiosurgery treatment planning, as the geometric distortion requirements necessary for planning such a procedure are often times more stringent than the ≤2mm across 25cm requirements in place in this program [3].

7. Conclusions

In the course of this project a foundational set of daily, monthly and annual QA tests and procedures have been identified and incorporated into an ongoing quality assurance program. These tests have aided in meeting the unique set of QA needs for an MR scanner used for radiotherapy. Additionally, this QA program enables long term monitoring and performance tracking of the scanner. The inclusion of this program into the clinical workflow has assisted in maintaining an MR imaging chain that is able to deliver high quality images for use in radiation therapy treatment planning.

8. Appendixes

8.1 Appendix 1 – Basic Mechanical checks worksheet

MR-SIM Mechanical Checks

The MR-SIM unit has a patient couch and a LAP external laser system which are capable of moving in three orthogonal dimensions: X, Y and Z. When standing at the foot of the patient couch, staring into the bore, these dimensions can be expressed as: X running left to right, Y running into and out of the bore, and Z running up and down Using this document as a guide, and the provided MR safe rulers, the positional accuracy of these systems can be verified.

I. LAP laser Digital Accuracy

Tolerance: ±2mm [but ±1mm is preferable]

Instructions to evaluate the Z dimension: Securely place a ruler a ruler running vertically / along the Z dimension. Obtain an initial mechanical position using the LAP laser system and the rulers. Then, using the LAP control console, move the LAP laser along the examined dimension. Record this prescribed digital travel distance. Record the second mechanical position using the ruler and laser. Calculate the mechanical travel distance. Compare and find the difference between the digital and mechanical travel distance and compare the difference to the tolerance criteria. Repeat for the left and right vertical components of the LAP system. Note: the couch should not move during this test. Additionally, the LAP system is not able to move in the Y dimension, and as such cannot be tested in this dimension.

Dimension	Initial Mechanical position [mm]	Second Mechanical position [mm]	Digital Travel distance [mm]	Mechanical travel distance* [mm]	Travel distance difference** [mm]	Pass/ Fail [±2mm]
Right Laser (Dimension Z_A right side)						
Left laser (Dimension Z_B left side)						

*Subtract the initial mechanical position from the second mechanical position to obtain.

**Subtract mechanical travel distance from the digital travel distance to obtain. This value should agree with the tolerance limits and determines if the system passes or fails.

Instructions to evaluate the X dimension: Securely place a ruler running left to right / along the X dimension. Make sure the LAP control console indicates that the laser positioning is at zero along the X dimension, and record where the laser

is along the ruler. Using the control console first move the laser 125 mm to the left (-125mm) and then 125 mm to the right (+125mm) recording where the laser falls on the ruler.

Laser position Dimension X	-125mm	0mm	+125mm
Ruler position / Mechanical position Dimension X			
(Free space to calculate travel distance according to ruler)		N/A	
Pass / Fail [±2mm]		N/A	

I. Patient Couch Digital Accuracy

Tolerance: ±1mm

Instructions to evaluate the Y dimension: Securely place a ruler running along the Y dimension (which runs into and out of the bore). Using the LAP external laser system and rulers, obtain an initial position measurement. Next move the patient couch and record and compare what the digitally reported travel distance is to the mechanical (i.e. ruler) travel distance. The difference between these reported values should fall within the above tolerance limits. Note: the LAP system should stay entirely stationary during this test. Dimensions X is not tested since the couch can't move left to right, and dimension Y is not tested since imaging can only be performed at a set couch height.

Dimension	Initial Mechanical position [mm]	Second Mechanical position [mm]	Digital Travel distance [mm]	Mechanical travel distance* [mm]	Travel distance difference** [mm]	Pass/ Fail [±1mm]
Dimension Y						

*Subtract the initial mechanical position from the second mechanical position to obtain.

**Subtract mechanical travel distance from the digital travel distance to obtain. This value should agree with the tolerance limits and determines if the system passes or fails.

Note: TG-284 is the source of the performance criteria for these tests.

Additional comments and concerns:

Appendix 1: Screenshots of both pages of the MR-SIM basic mechanical checks worksheet.

8.2 Appendix 2 – ACR MRI Accreditation program visual Checklist

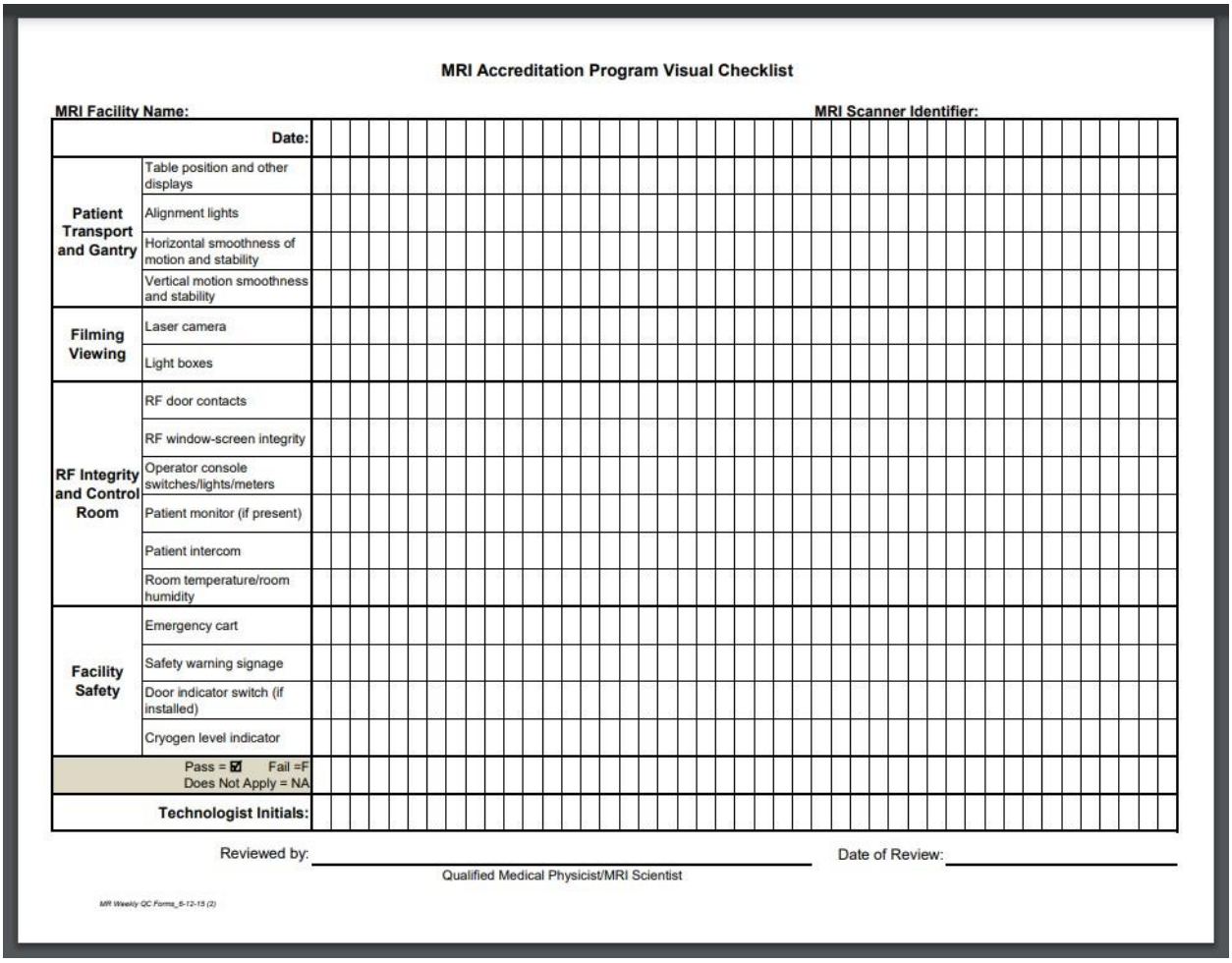

MRI Accreditation Program Visual Checklist

MRI Facility Name: **MRI Scanner Identifier:**

	Date:	
Patient Transport and Gantry	Table position and other displays	
	Alignment lights	
	Horizontal smoothness of motion and stability	
	Vertical motion smoothness and stability	
Filming Viewing	Laser camera	
	Light boxes	
RF Integrity and Control Room	RF door contacts	
	RF window-screen integrity	
	Operator console switches/lights/meters	
	Patient monitor (if present)	
	Patient intercom	
	Room temperature/room humidity	
Facility Safety	Emergency cart	
	Safety warning signage	
	Door indicator switch (if installed)	
	Cryogen level indicator	
	Pass = ☑ Fail =F Does Not Apply = NA	
	Technologist Initials:	

Reviewed by: _____ Date of Review: _____

Qualified Medical Physicist/MRI Scientist

MR Weekly QC Forms_8-12-15 (2)

Appendix 2: A screenshot of the MRI Accreditation program visual checklist. This checklist is filled out as a part of annual QA. The checklist can be found on ACRaccreditation.org: https://www.acraccreditation.org/-/media/ACRAccreditation/Documents/MRI/MR-Visual-Checklist-11614.pdf

9. References

1. Gibbons, John P., et al. *Khan's The Physics of Radiation therapy*. Wolters Kluwer Health, 2020, pp. 203-204.

2. Gibbons, John P., et al. *Khan's The Physics of Radiation therapy*. Wolters Kluwer Health, 2020, pp. 207.

3. Glide-Hurst, C.K., Paulson, E.S., McGee, K., Tyagi, N., Hu, Y., Balter, J. and Bayouth, J. (2021), Task group 284 report: magnetic resonance imaging simulation in radiotherapy: considerations for clinical implementation, optimization, and quality assurance. Med. Phys., 48: e636-e670. https://doi.org/10.1002/mp.14695

4. Hua, Chia-ho., Uh, Jinsoo. and Merchant, Thomas. (2019). How do you commission and implement an MRI system for radiation therapy planning? Experience from St. Jude Children's Research Hospital, Memphis, Tennessee, USA. Available at https://philipsproductcontent.blob.core.windows.net/assets/20191119/a6fa1f759b434b83b68cab0a00f1905c.pdf

5. Price, Ron & Allison, Jerry & Clarke, Geoffrey & Dennis, Michael & Hendrick, R. Edward & Keener, Carl & Masten, Jeff & Ness-Avier, Moriel & Och, Joe & Reeve, Donna. (2015). 2015 ACR MR QC Manual. Available at https://www.acr.org/-/media/ACR/Files/Clinical-Resources/QC-Manuals/MR_QCManual.pdf

6. American College of Radiology. Large and medium phantom test guidance for the ACR MRI Accreditation program. Available at: https://www.acraccreditation.org/-/media/ACRAccreditation/Documents/MRI/ACR-Large--Med-Phantom-GuidanceFinal.pdf. Accessed March 13, 2023.

7. Kirkaldie, David. “Magphan RT.” ImageOwl, August 2022, https://help.imageowl.com/hc/en-us/articles/360017634973-Magphan-RT

8. Jackson EF, Bronskill MJ, Drost DJ, et al. Acceptance Testing and Quality Assurance Procedures for Magnetic Resonance Imaging Facilities. Report of MR Subcommittee Task Group I. AAPM Report No. 100. 2010. Available at https://www.aapm.org/pubs/reports/RPT_100.pdf

9. Krupa K, Bekiesińska-Figatowska M. Artifacts in magnetic resonance imaging. Pol J Radiol. 2015 Feb 23;80:93-106. doi: 10.12659/PJR.892628. PMID: 25745524; PMCID: PMC4340093.

10. McRobbie, Donald W., et al. *MRI from Picture to Proton*. Cambridge University Press, 2005, pp. 48-49.

11. McRobbie, Donald W., et al. *MRI from Picture to Proton*. Cambridge University Press, 2005, pp. 86-103.

12. Bushberg, Jerrold T., et al. “13.6 MR Artifacts.” *The Essential Physics of Medical Imaging*, Lippincott Williams & Wilkins, Philadelphia, 2021, pp. 526–538.

13. Woodward, Peggy, and William W. Orrison. *MRI Optimization: A Hands-on Approach*. McGraw-Hill, Health Professions Division, 1997, pp. 37-47.

14. American College of Radiology. MRI Acreddiation program visual checklist. Available at https://www.acraccreditation.org/-/media/ACRAccreditation/Documents/MRI/MR-Visual-Checklist-11614.pdf. Accessed March 13th, 2023.

15. Samei, E., Badano, A., Chakraborty, D., Compton, K., Cornelius, C., Corrigan, K., Flynn, M.J., Hemminger, B., Hangiandreou, N., Johnson, J., Moxley-Stevens, D.M., Pavlicek, W., Roehrig, H., Rutz, L., Samei, E., Shepard, J., Uzenoff, R.A., Wang, J. and Willis, C.E. (2005), Assessment of display performance for medical imaging systems: Executive summary of AAPM TG18 report. Med. Phys., 32: 1205-1225. https://doi.org/10.1118/1.1861159